Classifying mental and cardiovascular illness from real world sensor data

Erik Reinertsen, PhD

Georgia Tech

Wallace H. Coulter Department of Biomedical Engineering
Georgia Tech College of Engineering and Emory School of Medicine

Emory University School of Medicine | MD/PhD Program

Outline

1. HR and accelerometer data contain disease-relevant information.
2. Simple statistical measures do not address complexity, time scales, or interactions.
3. My work explores these limitations using data from different patient cohorts.
4. Entrepreneurship & venture capital are important to translation.
5. Future direction.

How can we make clinical use of data from smartphones & wearables?

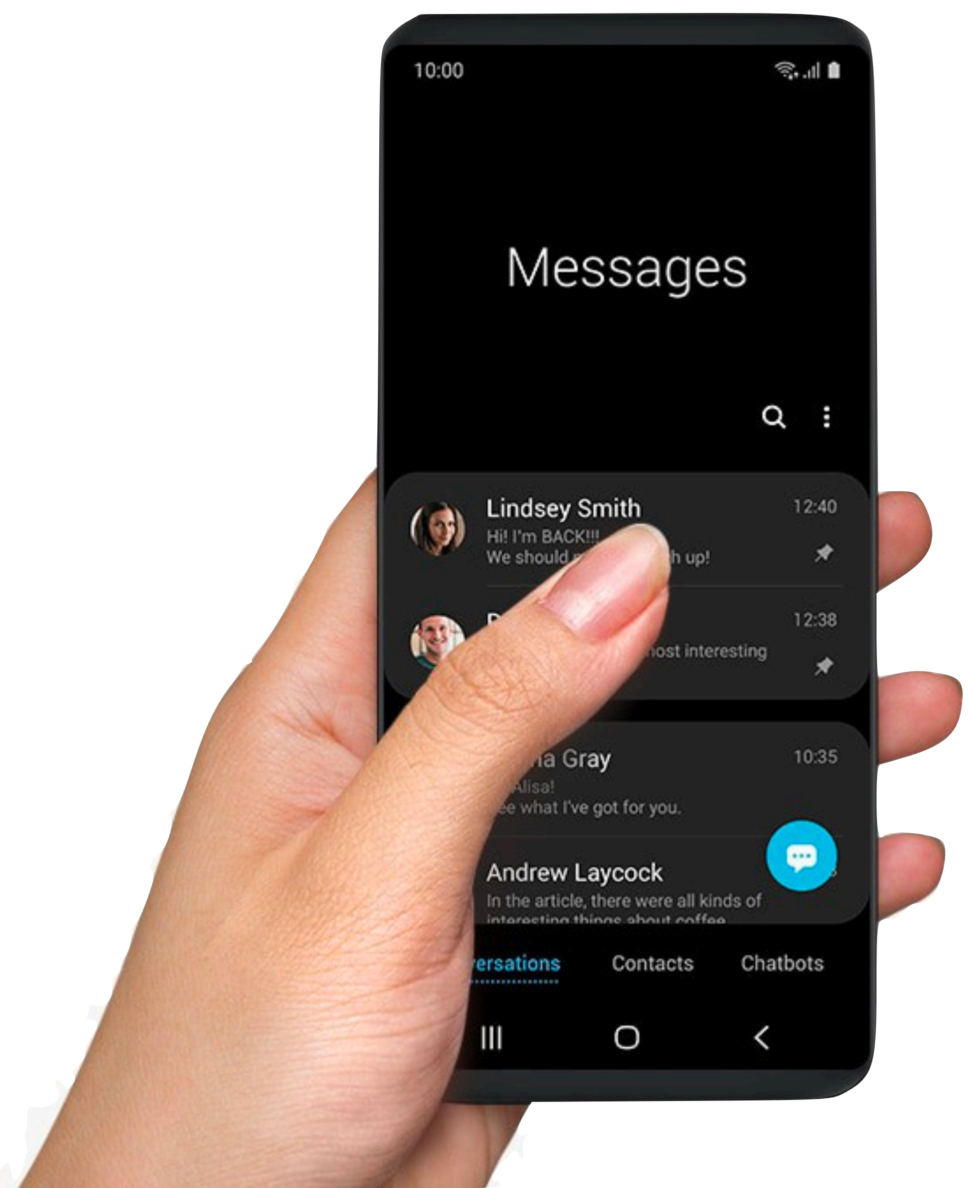

Example heart rate (RR intervals) and activity (accelerometry) time series from phone & watch

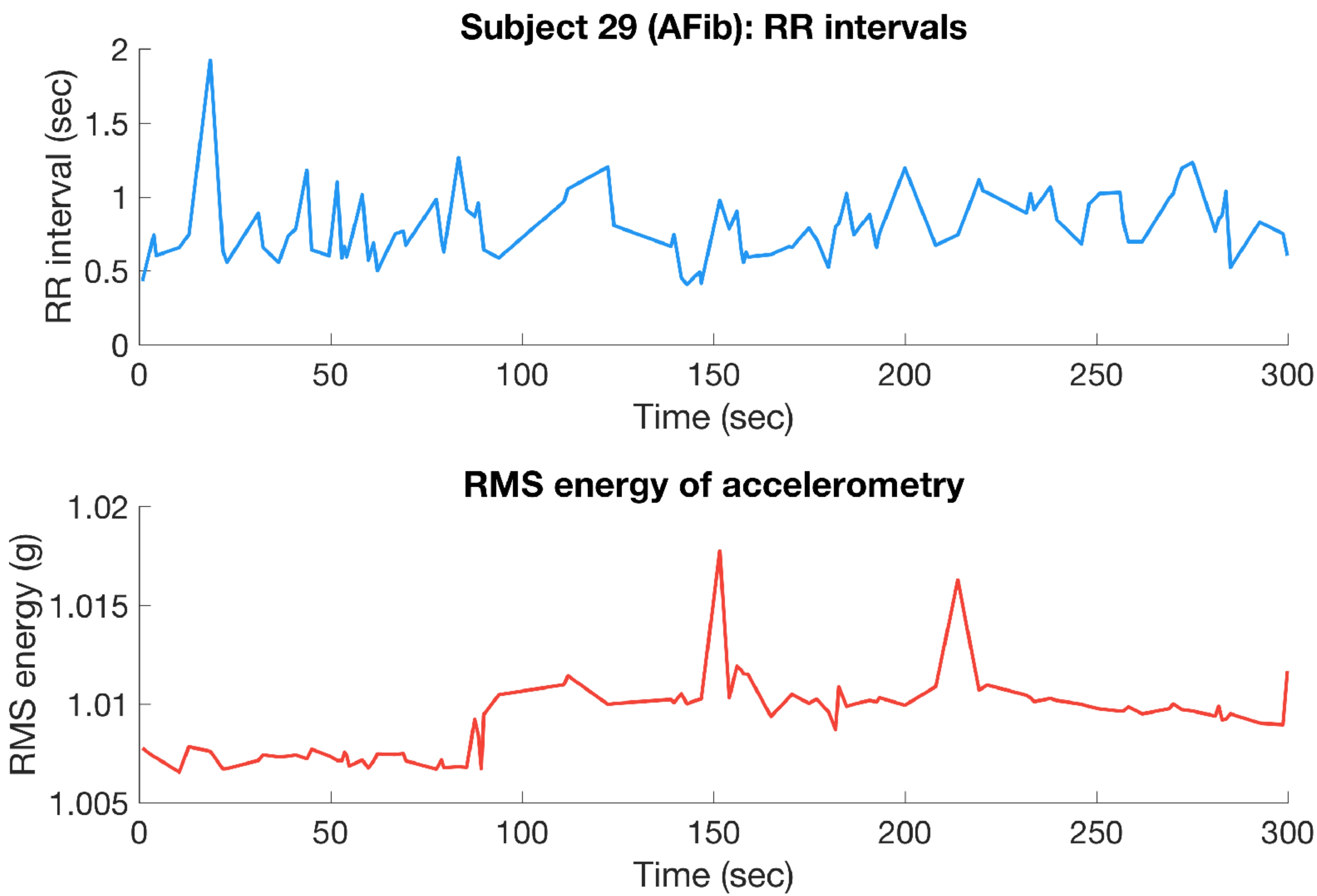

Unpublished data from Reinertsen, Cakmak, and Clifford.

These devices generate trillions of data points from billions of people, yet we use little of it

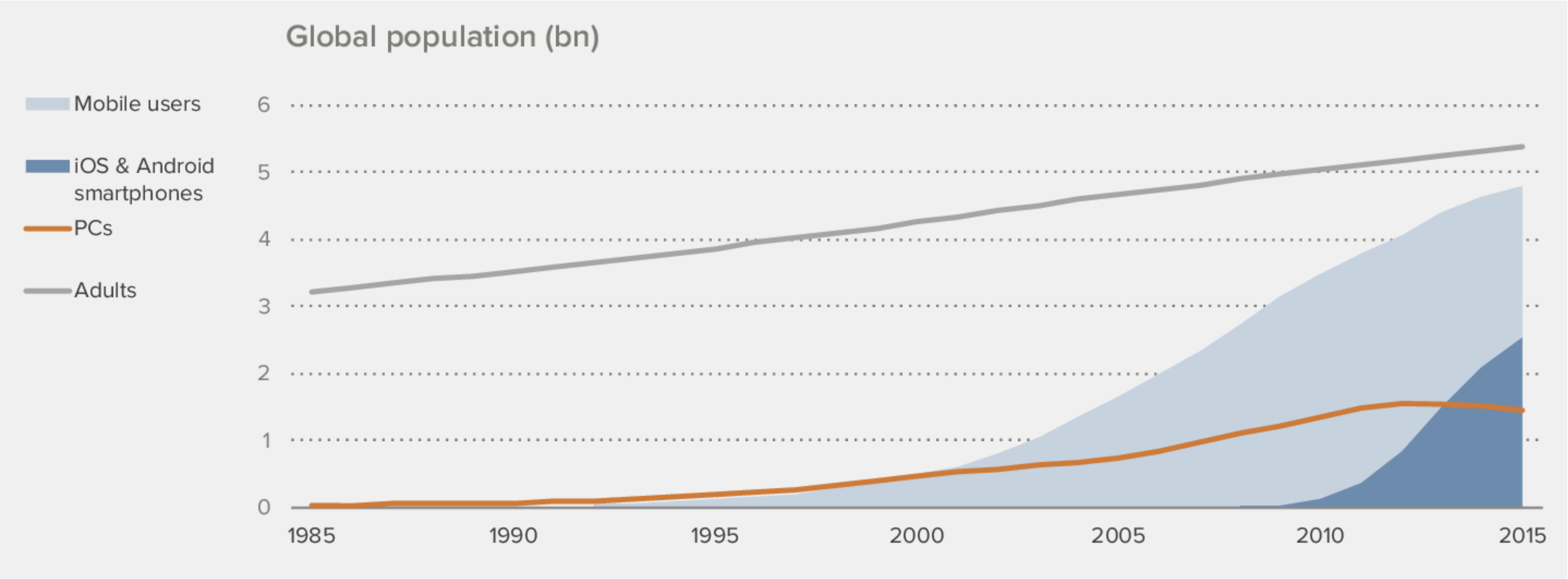

https://www.ben-evans.com/benedictevans/2016/12/8/mobile-is-eating-the-world

Machine learning can map features in data from smartphones & wearables to disease

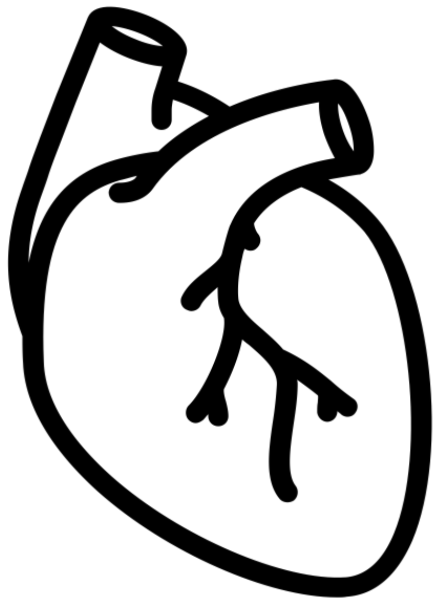

Richer attributes of time series beyond simple summary statistics may better reflect illness

Irregularity

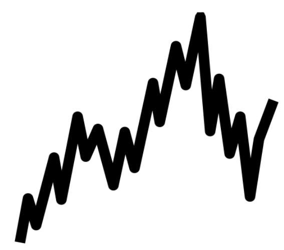

Nonstationarity

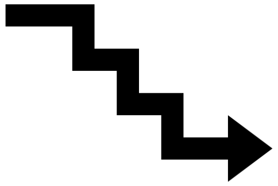

Time scale

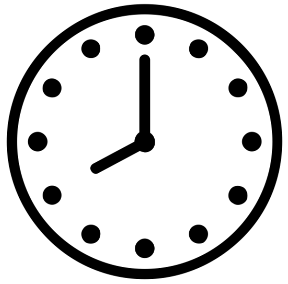

Interaction

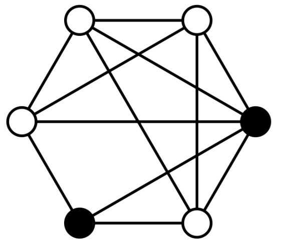

Indices reflecting these attributes and could be better features for classifying illness via ML

Irregularity	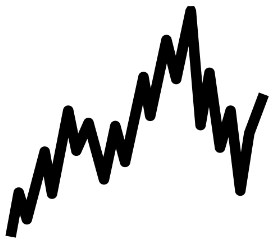	**Entropy**
Nonstationarity	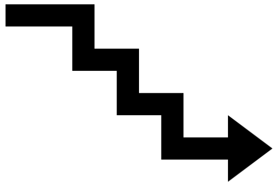	**Segmentation**
Time scale	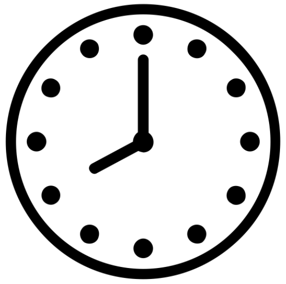	**Multiscale**
Interaction	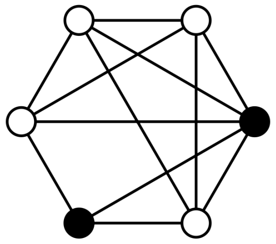	**Network features**

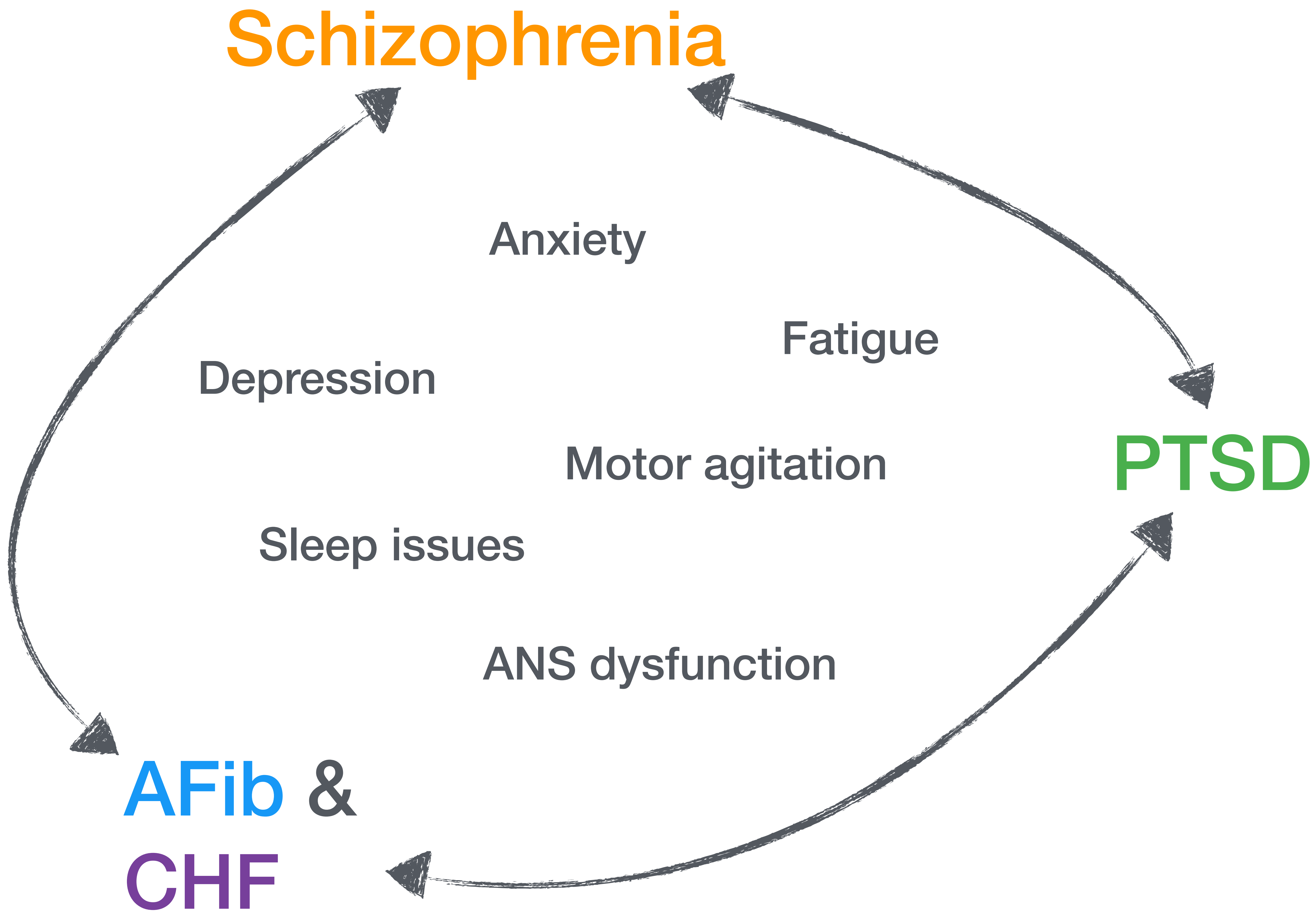
Schizophrenia
Anxiety
Fatigue
Depression
PTSD
Motor agitation
Sleep issues
ANS dysfunction
AFib &
CHF

	Cohort	Hypothesis
1	Schizophrenia	
2	PTSD	
3	Schizophrenia & atrial fibrillation	
4	Heart failure	

	Cohort	Hypothesis
1	Schizophrenia	Classification & type of feature varies with time scale of data.
2	PTSD	
3	Schizophrenia & atrial fibrillation	
4	Heart failure	

Schizophrenia

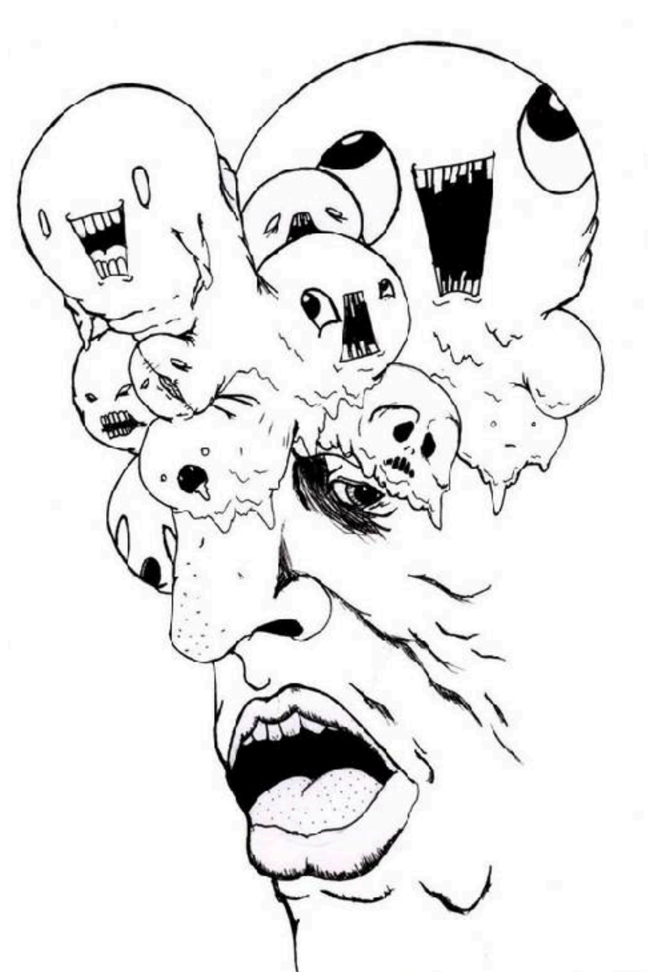

Co-morbidities[1,2]

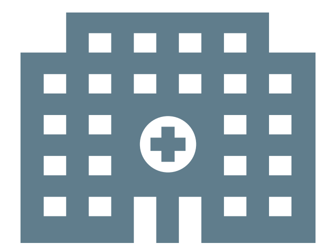

$134B[3]

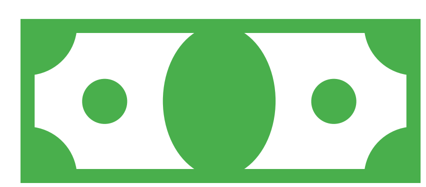

1. P. F. Buckley et al. Psychiatric comorbidities and schizophrenia., Schizophrenia Bulletin. 2009.
2. K. Hor and M. Taylor. Suicide and schizophrenia: a systematic review of rates and risk factors. Journal of psychopharmacology. 2010.
3. M Cloutier et al. The economic burden of schizophrenia in the United States in 2013. Journal of Clinical Psychiatry. 2013.

Schizophrenia associated with decreased entropy of HR[1] and lower & more structured activity[2]

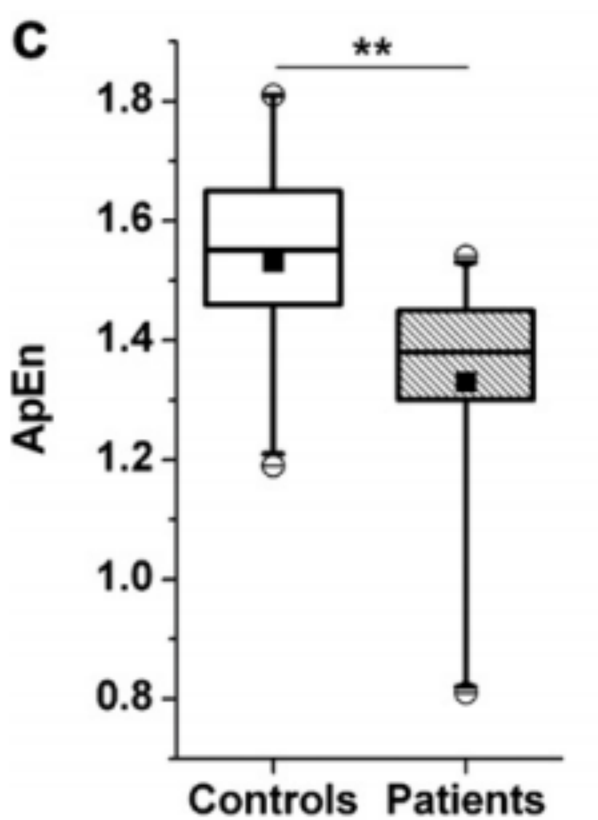

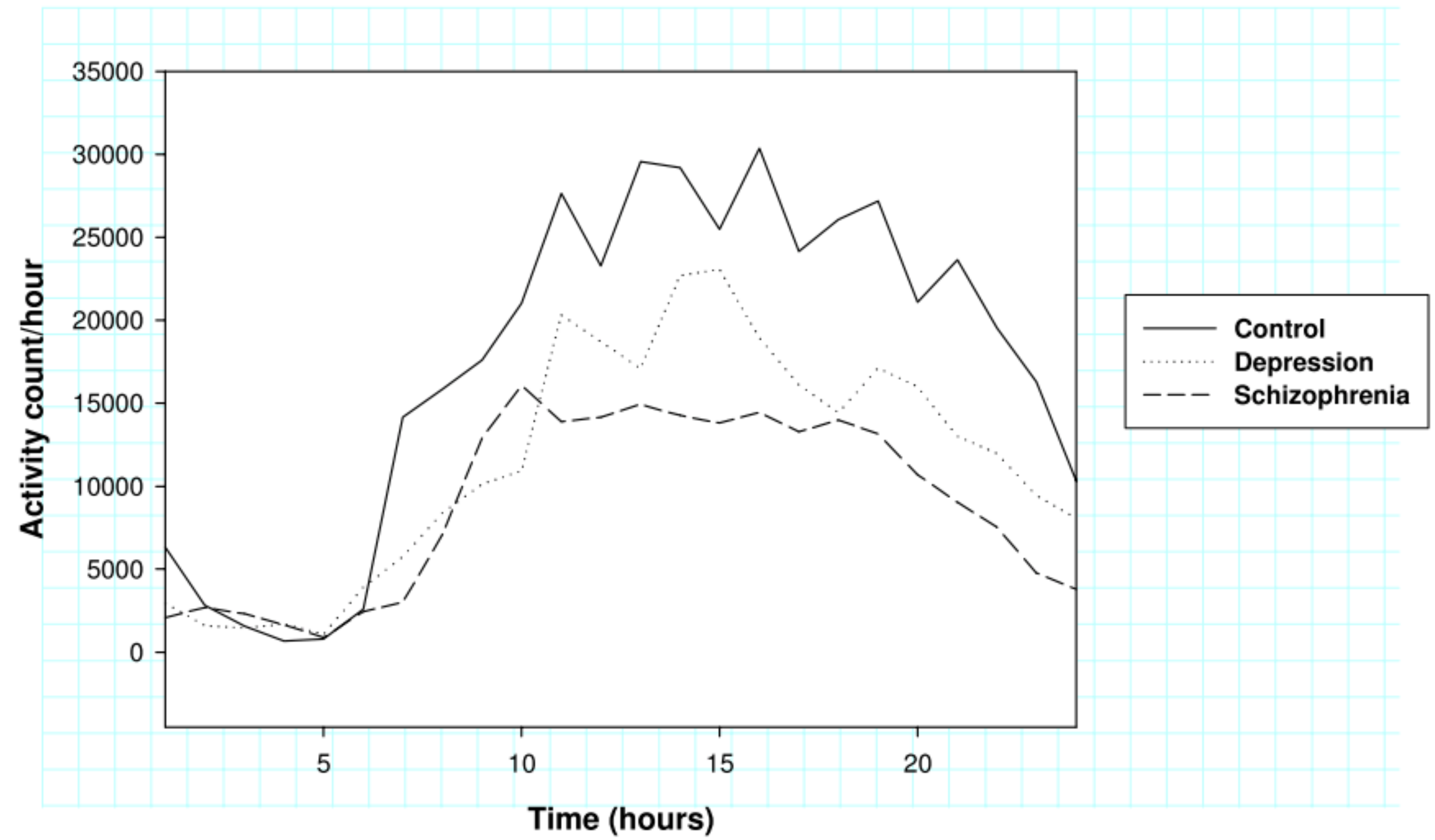

1. Bär, K.-J. et al. Non-linear complexity measures of heart rate variability in acute schizophrenia. Clin. Neurophysiol. 118, 2009–2015 (2007).
2. Berle, J. O., Hauge, E. R., Oedegaard, K. J., Holsten, F. & Fasmer, O. B. Actigraphic registration of motor activity reveals a more structured behavioural pattern in schizophrenia than in major depression. BMC Res. Notes 3, 149 (2010).

Cohort of 16 schizophrenia patients and 19 healthy controls

16 medicated outpatients diagnosed with schizophrenia but in symptomatic remission

19 healthy controls

All subjects unemployed

HR and activity monitored for 3-4 weeks using Zio XT patch

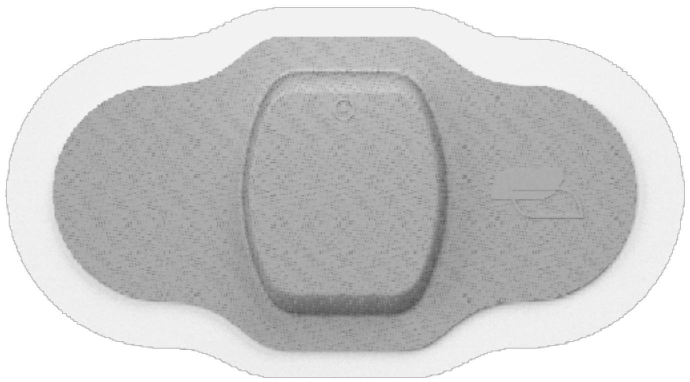

Osipov, M., Behzadi, Y., Kane, J. M., Petrides, G. & Clifford, G. D. Objective identification and analysis of physiological and behavioral signs of schizophrenia. J. Ment. Heal. 24, 276–282 (2015).

Does **window length** affect type of features and classifier performance in schizophrenia?

<u>Hours to days</u>
circadian rhythms, sleep

<u>Days to weeks</u>
social activity, behavior

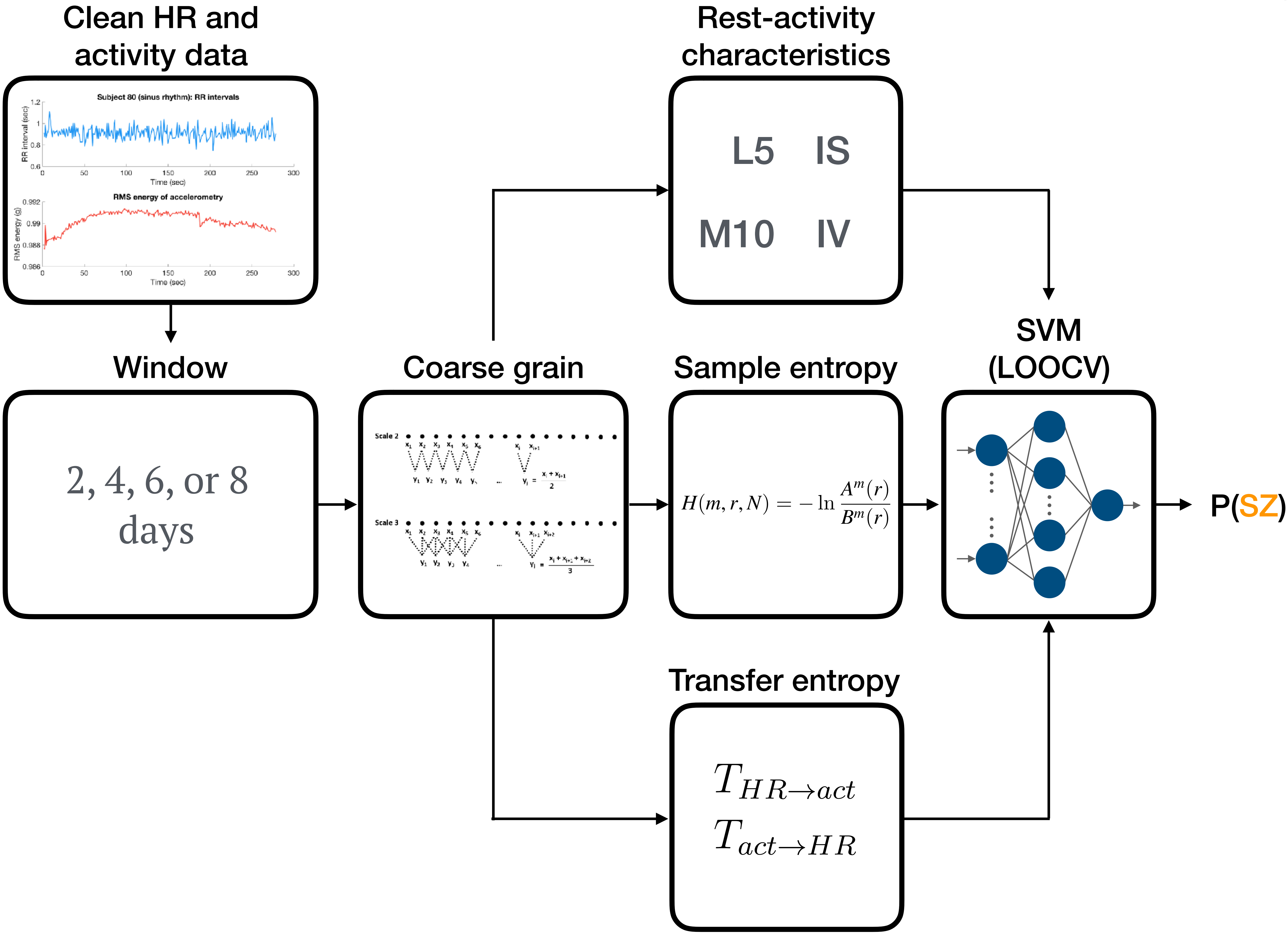
Clean HR and activity data
Subject 80 (sinus rhythm): RR intervals
RR interval (sec)
Time (sec)
RMS energy of accelerometry
RMS energy (g)
Time (sec)
Window
2, 4, 6, or 8 days
Coarse grain
Scale 2
Scale 3
Rest-activity characteristics
L5
IS
M10
IV
Sample entropy
$H(m,r,N) = -\ln \frac{A^m(r)}{B^m(r)}$
Transfer entropy
$T_{HR \rightarrow act}$
$T_{act \rightarrow HR}$
SVM (LOOCV)
P(SZ)

Extract features from **two-day** window sliding through HR and activity time series data

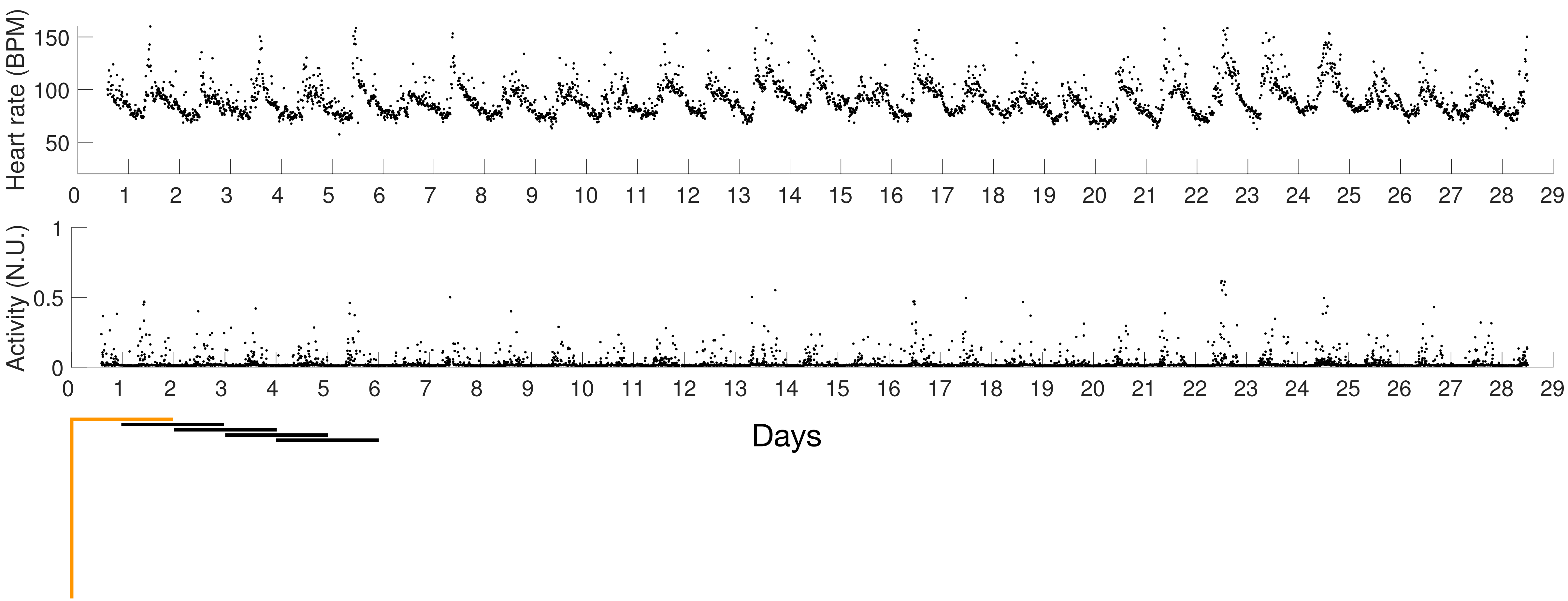

First window: days 0-2

Reinertsen, E. et al. Continuous assessment of schizophrenia using heart rate and accelerometer data. Physiol. Meas. 38, 1456–1471 (2017).

Extract features from **eight-day** window sliding through HR and activity time series data

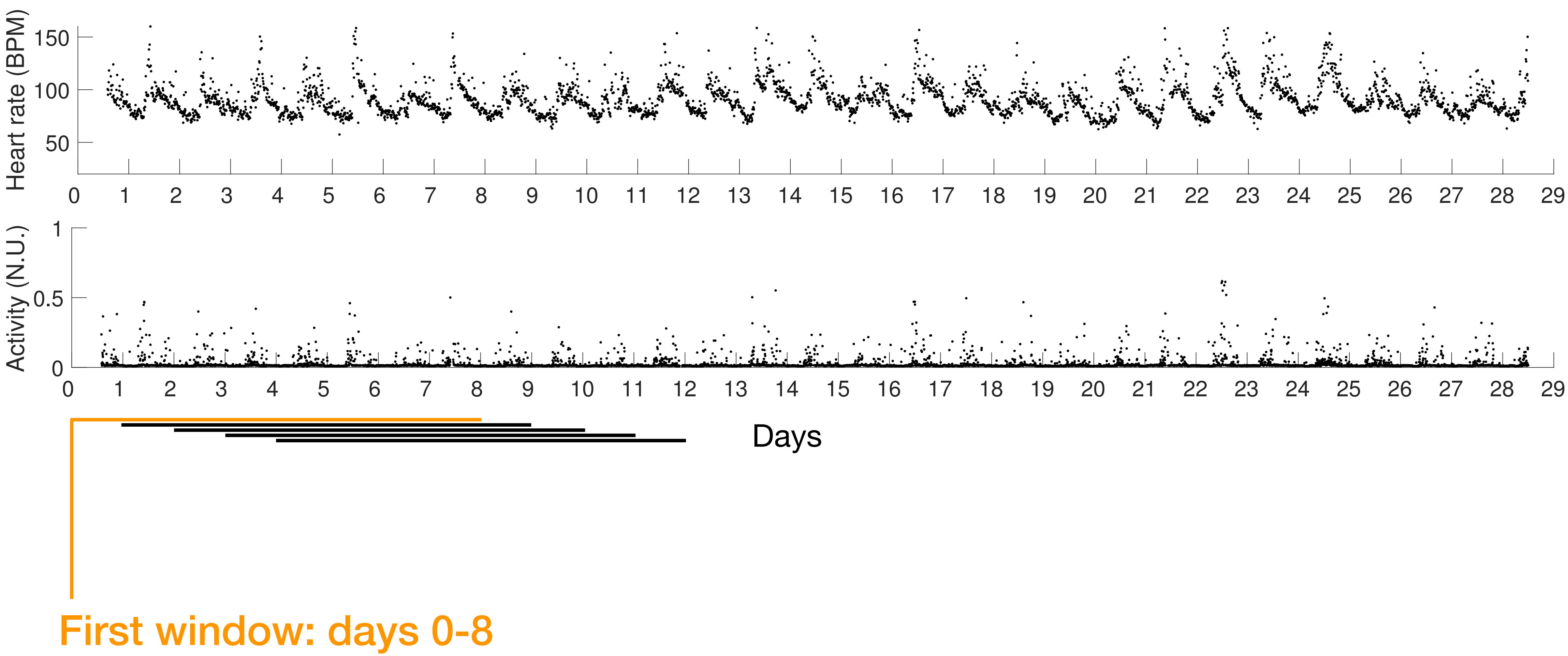

Reinertsen, E. et al. Continuous assessment of schizophrenia using heart rate and accelerometer data. Physiol. Meas. 38, 1456–1471 (2017).

Most predictive features using two-day windows reflect variance and irregularity of activity

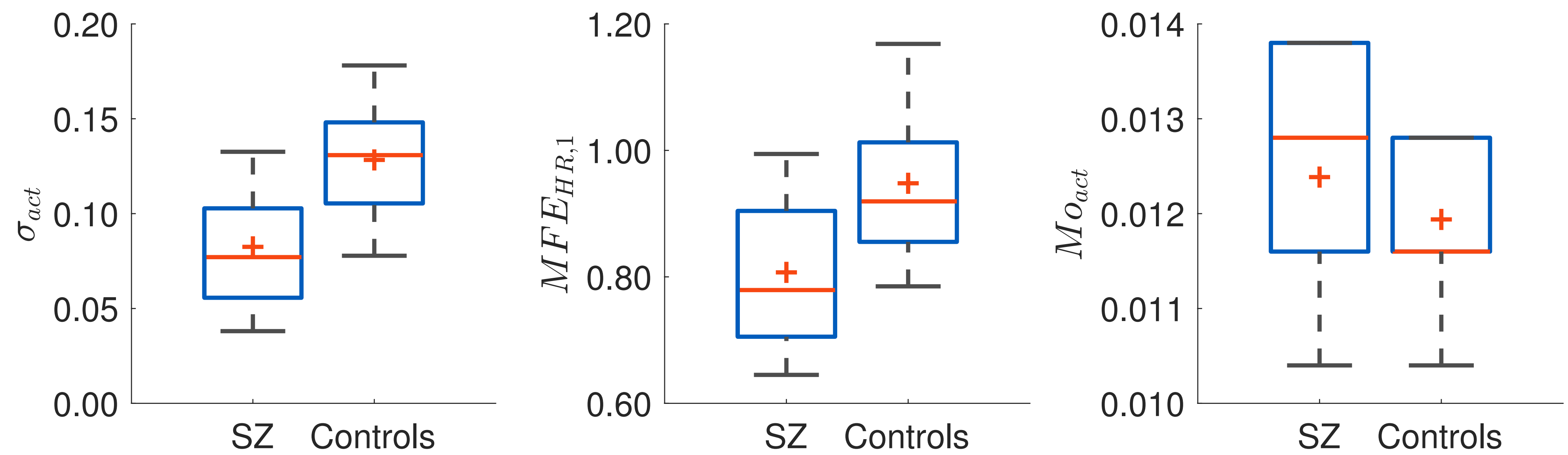

σ_{activity} Entropy $\text{Mode}_{\text{activity}}$

Reinertsen, E. et al. Continuous assessment of schizophrenia using heart rate and accelerometer data. Physiol. Meas. 38, 1456–1471 (2017).

Most predictive features using eight-day windows reflect transfer entropy and irregularity over broader time scales

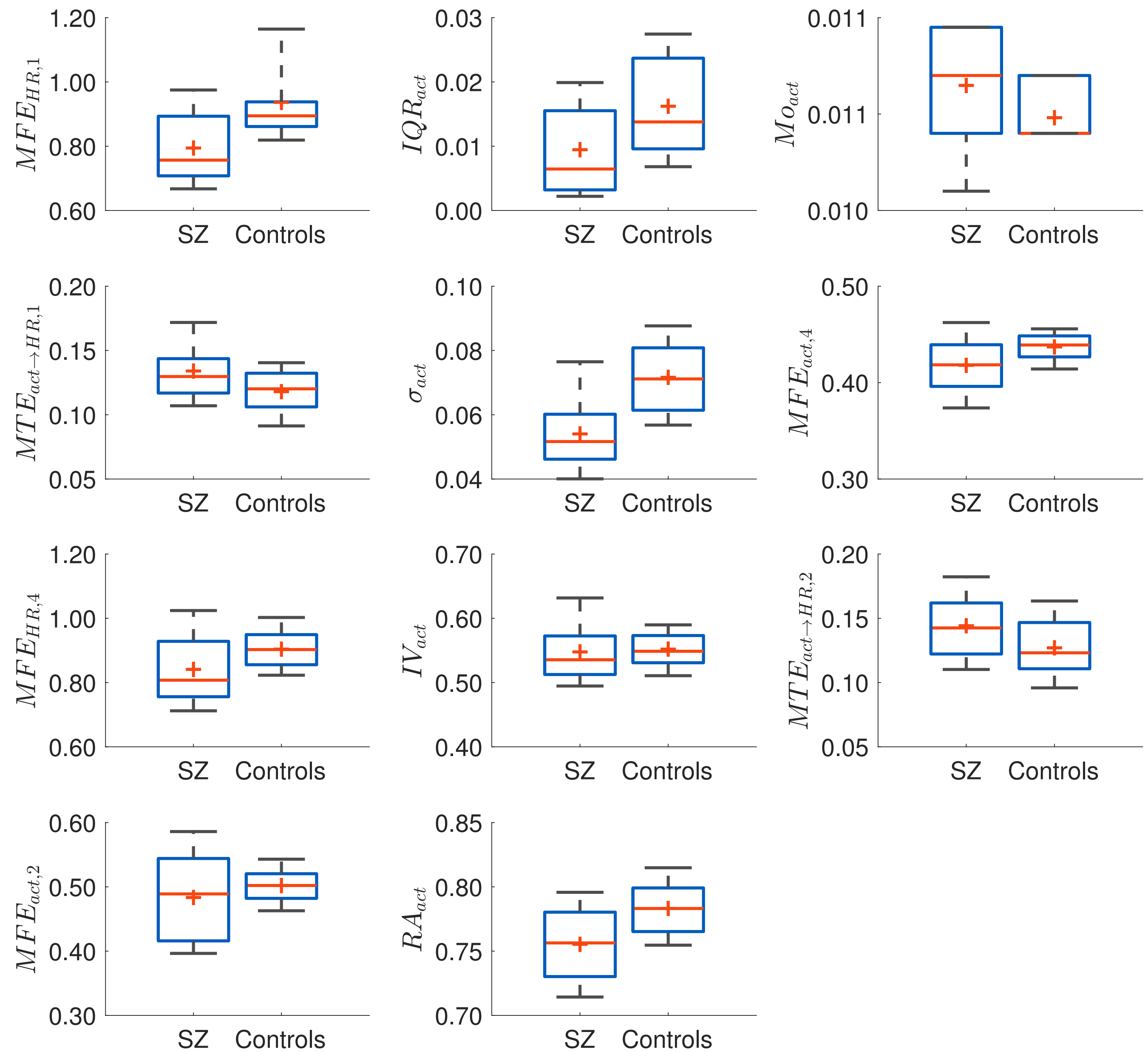

Reinertsen, E. et al. Continuous assessment of schizophrenia using heart rate and accelerometer data. Physiol. Meas. 38, 1456–1471 (2017).

ROC curves vary with window length

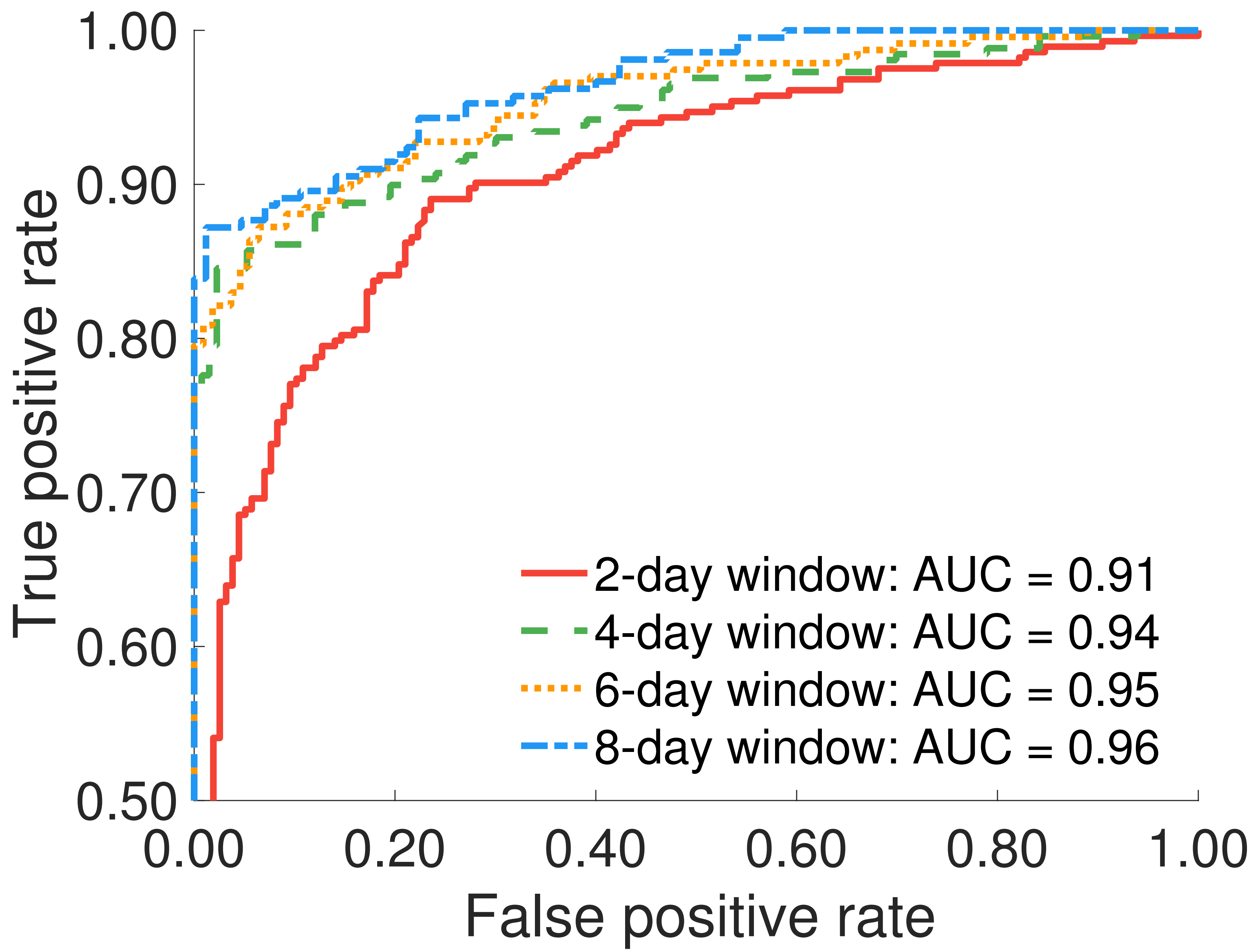

Reinertsen, E. et al. Continuous assessment of schizophrenia using heart rate and accelerometer data. Physiol. Meas. 38, 1456–1471 (2017).

Window length affects features and classifier performance in schizophrenia, but relating features to time scale is challenging

<ins>2 days</ins>
circadian rhythms, sleep

<ins>8 days</ins>
social activity, behavior

	Cohort	Hypothesis
1	Schizophrenia	Classification & type of feature varies with time scale of data.
2	PTSD	
3	Schizophrenia & atrial fibrillation	
4	Heart failure	

	Cohort	Hypothesis
1	Schizophrenia	Classification & type of feature varies with time scale of data.
2	PTSD	Segmenting data into quiescent periods improves signal:noise and classification.
3	Schizophrenia & atrial fibrillation	
4	Heart failure	

Post Traumatic Stress Disorder (PTSD)

1. Osipov, M. et al. Objective identification and analysis of physiological and behavioral signs of schizophrenia. J. Ment. Heal. 24, 276–282 (2015).
2. Mellman, T. A. et al. Heart rate variability during sleep and the early development of post traumatic stress disorder. Biol. Psychiatry 55, 953–956 (2004).

Decreased HRV is associated with current PTSD

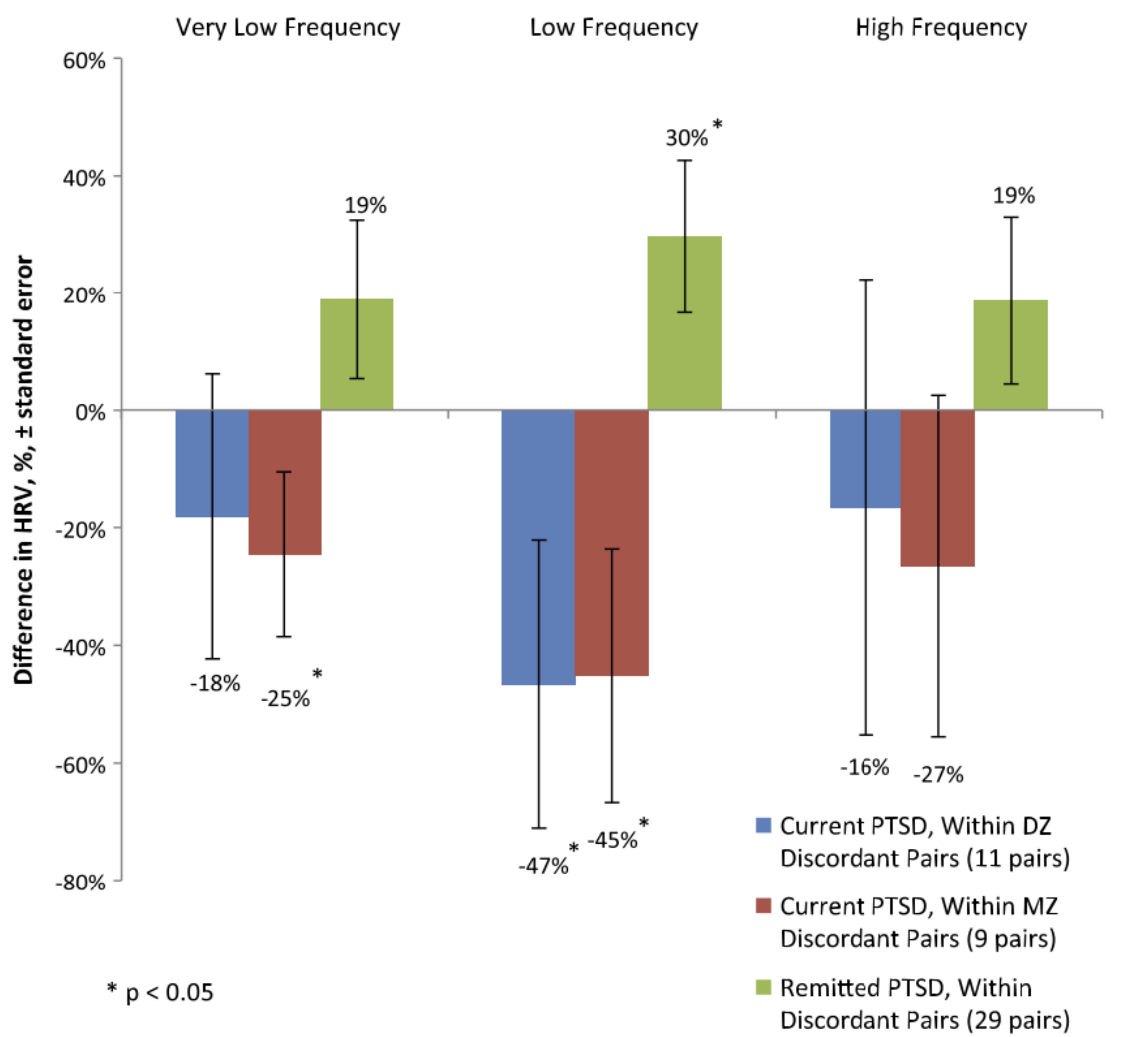

Shah, A. J. et al. PTSD and impaired autonomic modulation in male twins. Biol. Psychiatry 73, 1103–1110 (2013).

Classify PTSD in 48 male veterans using HR data

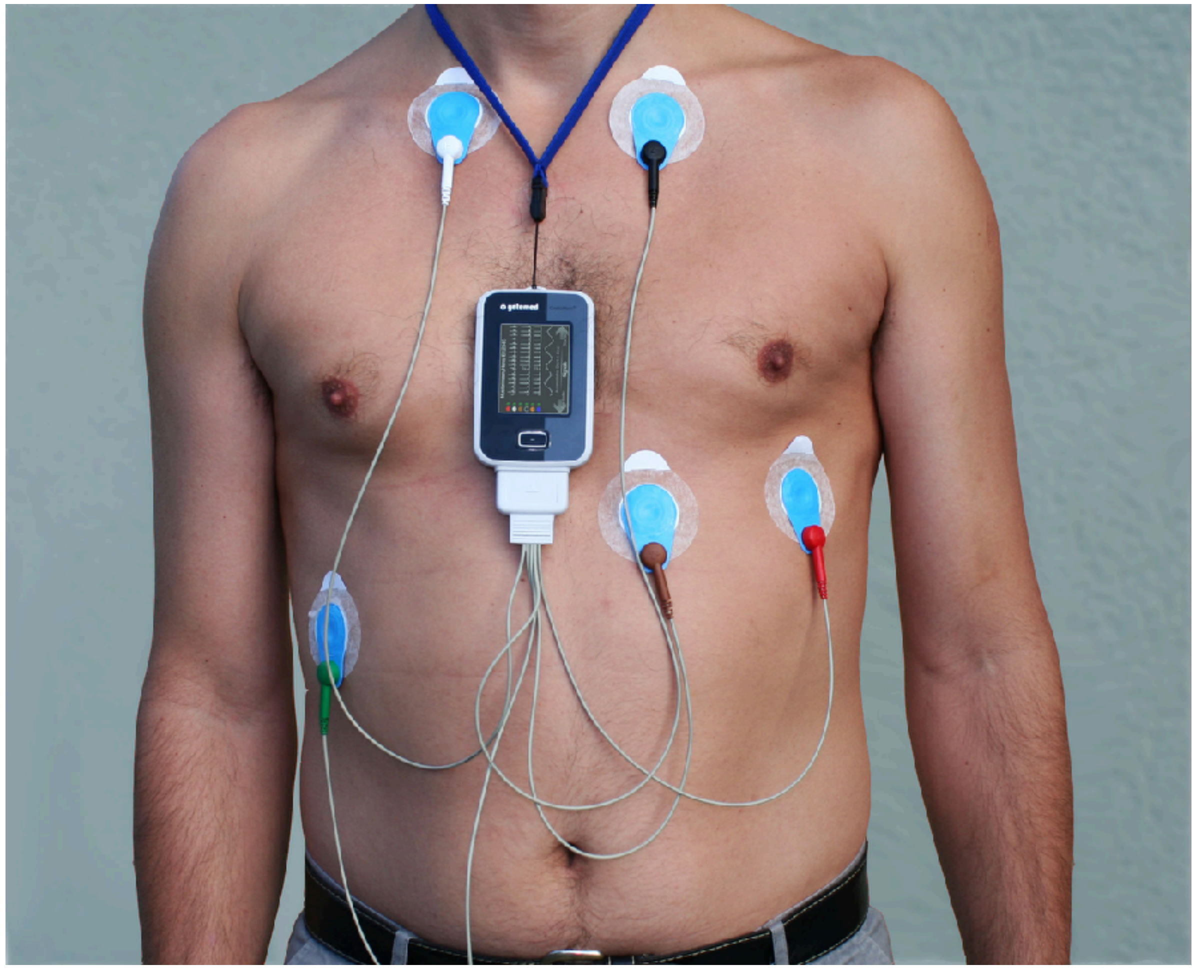

- Prior work used machine learning to predict PTSD from EMR data with AUC of 0.75[2]
- No prior work using passive physiological data to *classify* PTSD
- Emory Twins Studies[1]
- 23 diagnosed PTSD and 25 controls
- 24-hour ECG

1. Shah, A. J. et al. PTSD and impaired autonomic modulation in male twins. Biol. Psychiatry 73, 1103–1110 (2013).
2. Karstoft, K.-I., Galatzer-Levy, I. R., Statnikov, A., Li, Z. & Shalev, A. Y. Bridging a translational gap: using machine learning to improve the prediction of PTSD. BMC Psychiatry 15, 30 (2015).

Does segmenting HR data into quiescent periods improve classification of PTSD?

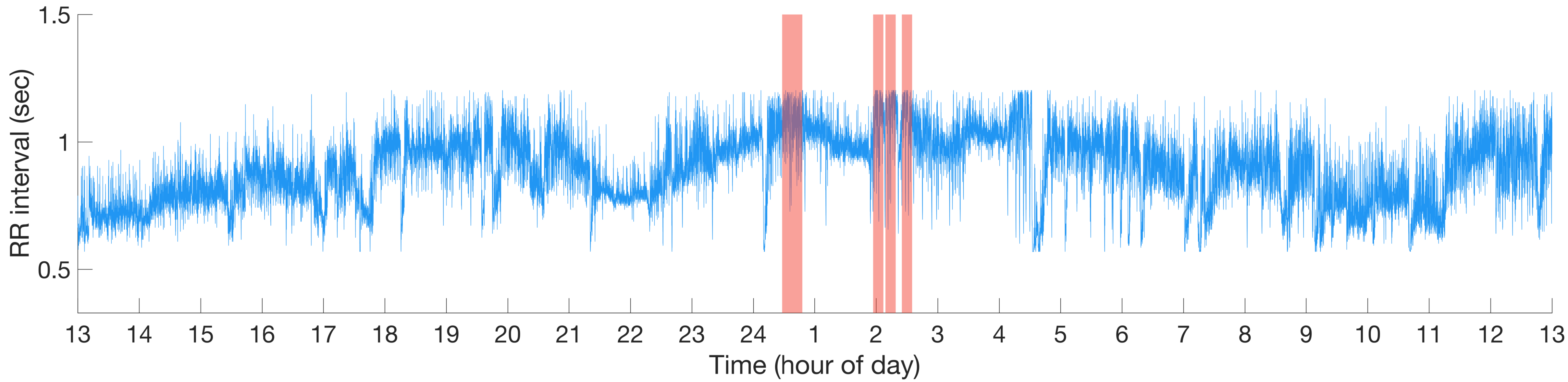

Reinertsen, E. et al. Heart rate-based window segmentation improves accuracy of classifying posttraumatic stress disorder using heart rate variability measures. Physiol. Meas. (2017).

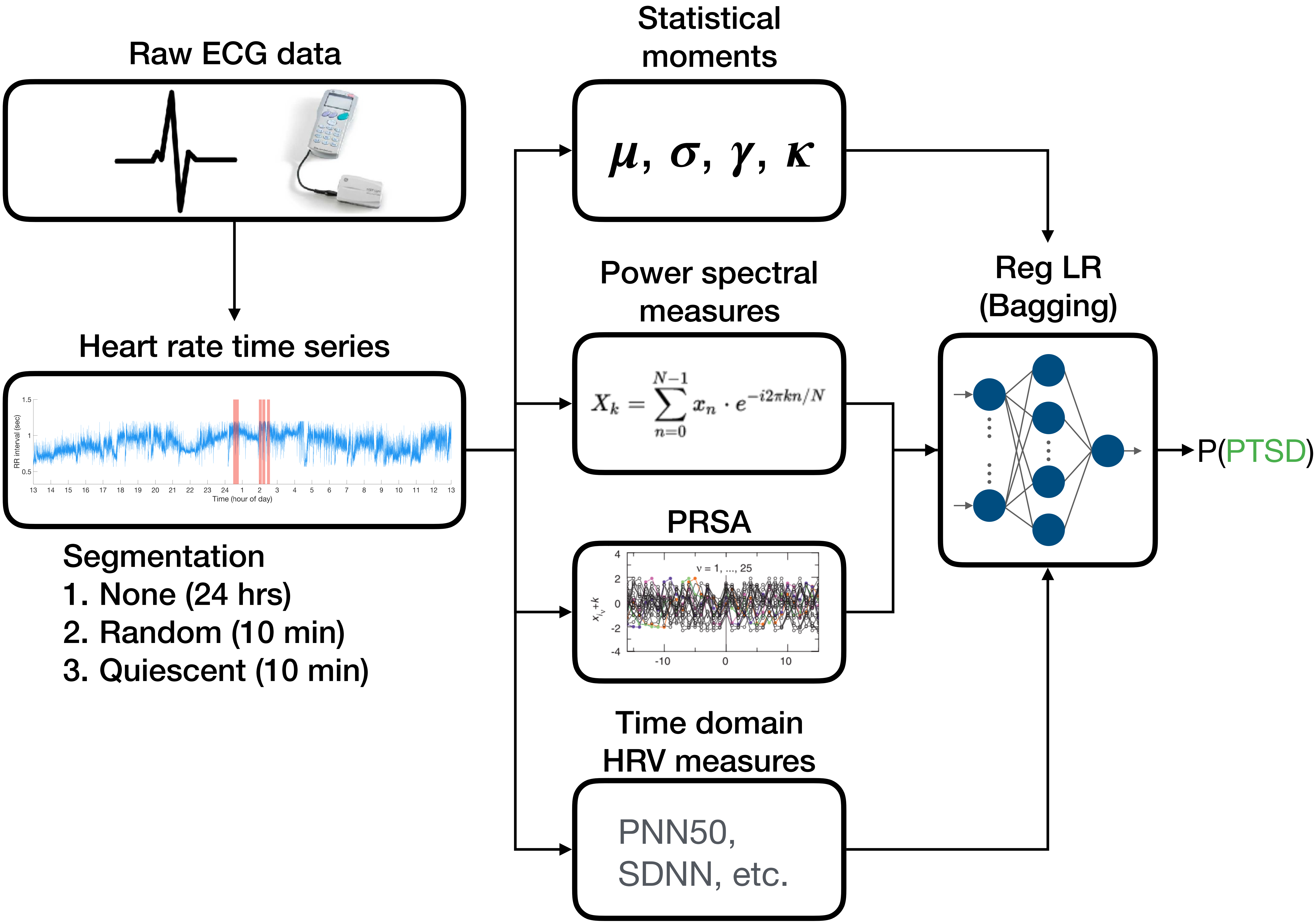
Raw ECG data
Heart rate time series
RR interval (sec)
Time (hour of day)
Segmentation
1. None (24 hrs)
2. Random (10 min)
3. Quiescent (10 min)
Statistical moments
$\mu, \sigma, \gamma, \kappa$
Power spectral measures
$X_k = \sum_{n=0}^{N-1} x_n \cdot e^{-i2\pi kn/N}$
PRSA
v = 1, ..., 25
Time domain HRV measures
PNN50, SDNN, etc.
Reg LR (Bagging)
P(PTSD)

Segmentation into quiescent segments improves classifier performance

	Segmentation approach		
Metric	24 hours	Random segments	Quiescent segments
AUC	0.67 [0.62 0.71]	0.70 [0.62 0.79]	0.86 [0.75 0.88]
Accuracy	0.73 [0.67 0.73]	0.73 [0.67 0.80]	0.80 [0.73 0.80]
Sensitivity	0.57 [0.43 0.71]	0.43 [0.43 0.57]	0.71 [0.57 1.00]
Specificity	0.94 [0.75 1.00]	1.00 [0.88 1.00]	0.94 [0.88 1.00]
PPV	0.92 [0.71 1.00]	1.00 [0.78 1.00]	0.94 [0.83 1.00]
NPV	0.69 [0.67 0.75]	0.67 [0.64 0.73]	0.79 [0.73 0.88]

First report of classification of PTSD using non-invasive physiological features.

Reinertsen, E. et al. Heart rate-based window segmentation improves accuracy of classifying posttraumatic stress disorder using heart rate variability measures. Physiol. Meas. (2017).

medibio

INNOVATION IN MIND

	Cohort	Hypothesis
1	Schizophrenia	Classification & type of feature varies with time scale of data.
2	PTSD	Segmenting data into quiescent periods improves signal:noise and classification.
3	Schizophrenia & atrial fibrillation	
4	Heart failure	

	Cohort	Hypothesis
1	Schizophrenia	Classification & type of feature varies with time scale of data.
2	PTSD	Segmenting data into quiescent periods improves signal:noise and classification.
3	Schizophrenia & atrial fibrillation	Interactions between HR and activity improve classification of mental illness, not arrhythmia.
4	Heart failure	

Interactions between HR and activity could improve classification of schizophrenia but not AFib

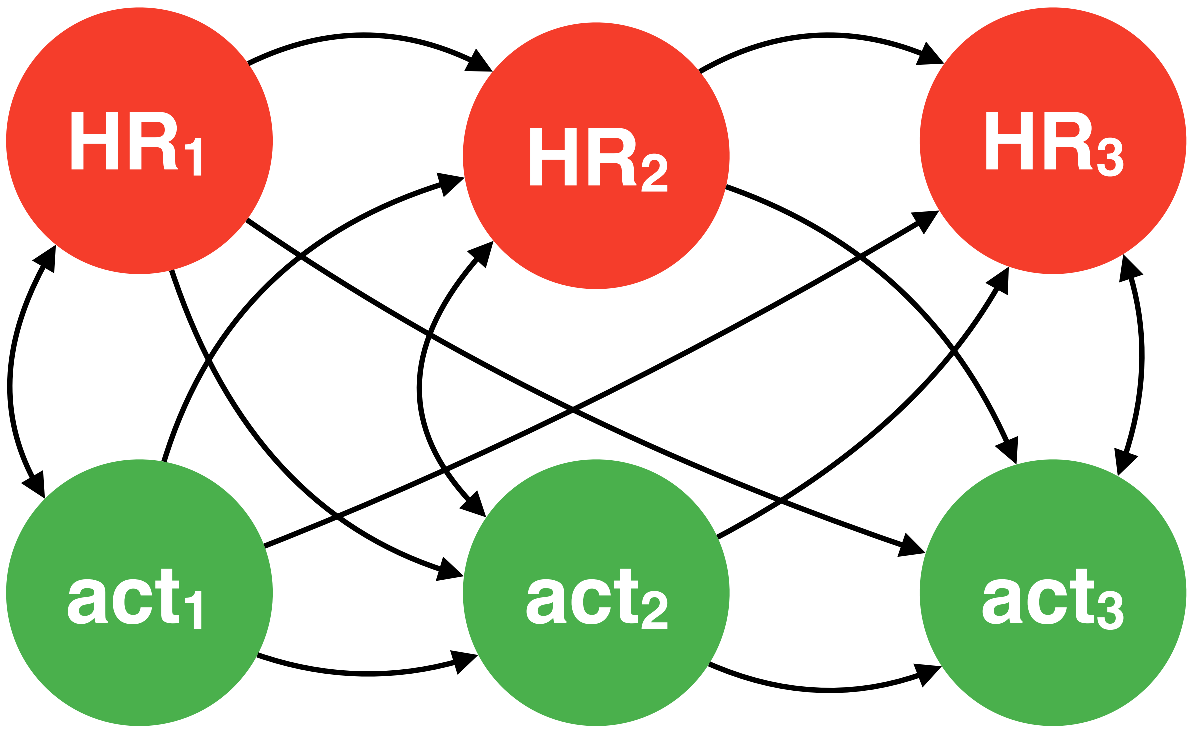

AFib is the most common cardiac rhythm disorder

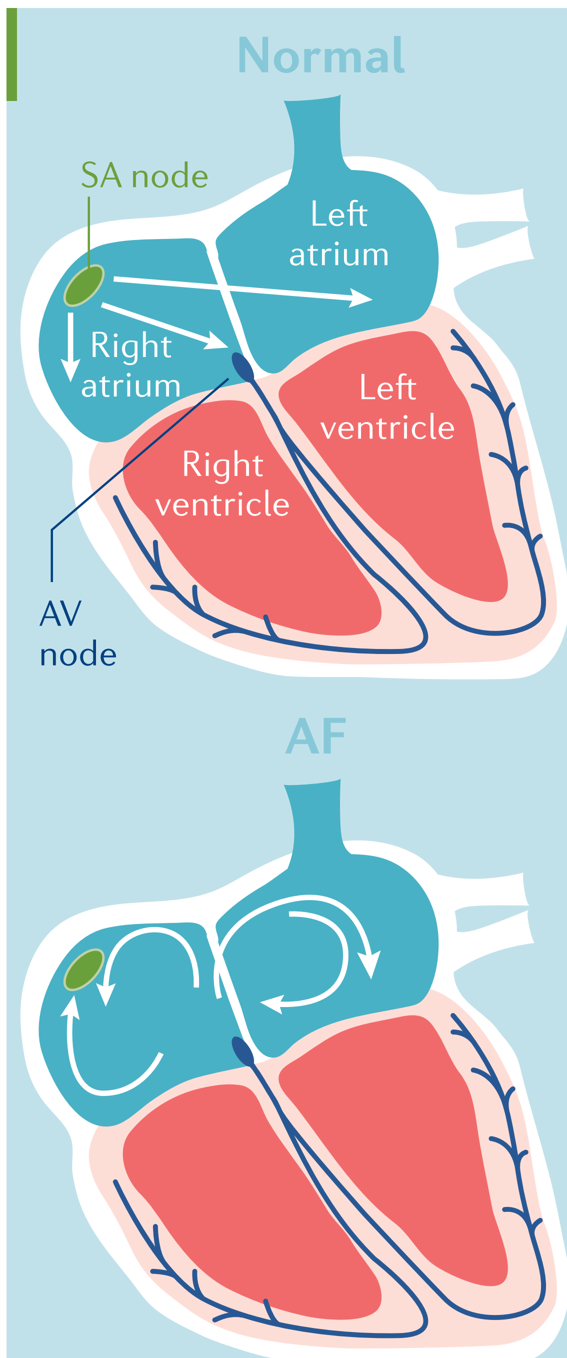

Disorganized electrical impulses that can result in rapid rate and irregular rhythm.[1]

↑risk of stroke and heart failure.

Cost >1% of health expenditures.[2]

1. Lip, G. Y. H. et al. Atrial fibrillation. Nat. Rev. Dis. Prim. 2, 16016 (2016).
2. Ball, J., Carrington, M. J., McMurray, J. J. V & Stewart, S. Atrial fibrillation: Profile and burden of an evolving epidemic in the 21st century. Int. J. Cardiol. 167, 1807–1824 (2013).

AFib is associated with low LF power[1] and altered multiscale entropy[2]

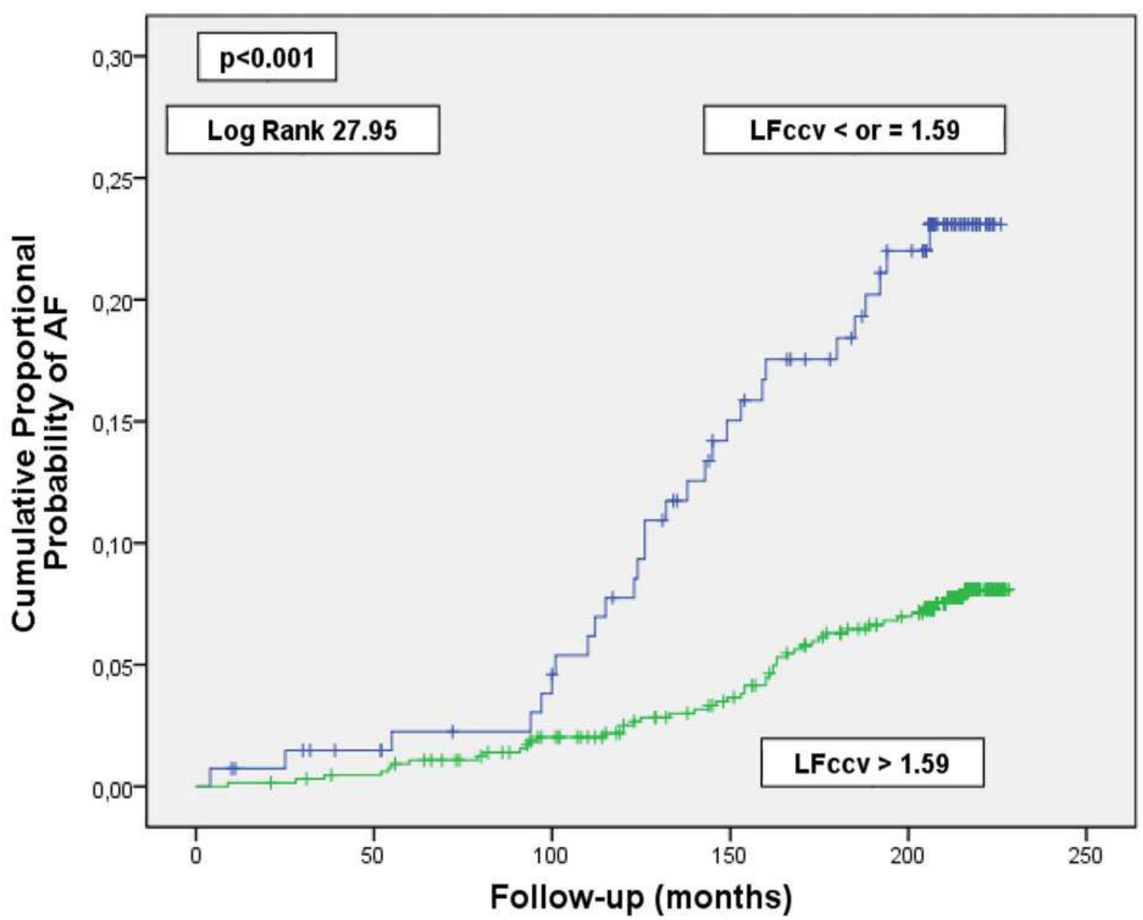

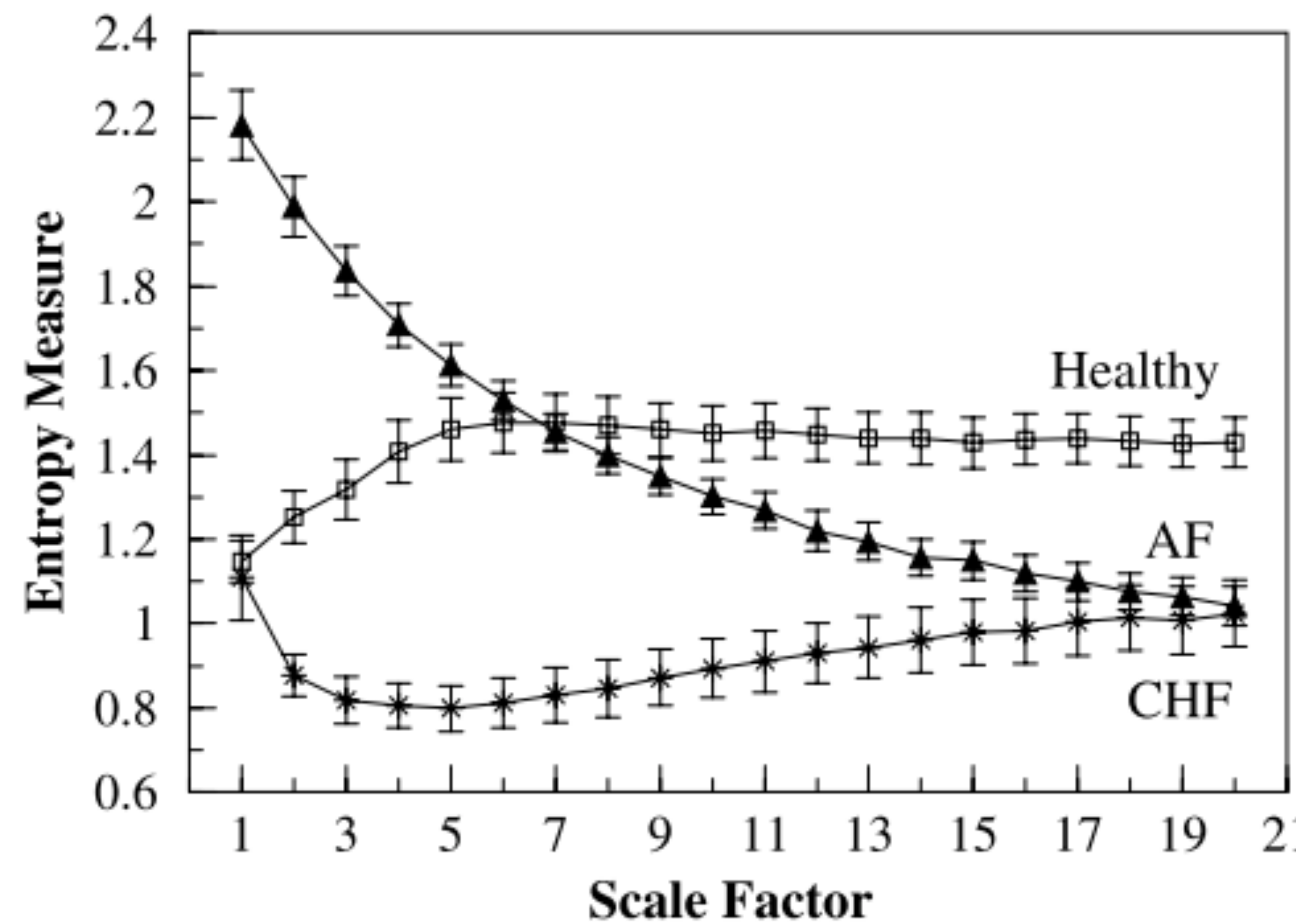

1. Perkiömäki, J. et al. Heart rate variability findings as a predictor of atrial fibrillation in middle-aged population. J. Cardiovasc. Electrophysiol. 25, 719–724 (2014).
2. Costa, M., Goldberger, A. & Peng, C.-K. Multiscale entropy analysis of complex physiologic time series. Phys. Rev. Lett. (2002).

Detecting AFib using ML and wearables

1. Shashikumar, S. P., Shah, A. J., Li, Q., Clifford, G. D. & Nemati, S. A deep learning approach to monitoring and detecting atrial fibrillation using wearable technology. 2017 IEEE EMBS Int. Conf. Biomed. Heal. Informatics 141–144 (2017).
2. Bumgarner, J. M. et al. Automated atrial fibrillation detection algorithm using smartwatch technology. J. Am. Coll. Cardiol. 71, 2381–2388 (2018).
3. Gladstone, R. A. et al. Passive Detection of Atrial Fibrillation Using a Commercially Available Smartwatch. JAMA Cardiol. 0124, 409–416 (2018).

Compare transfer entropy and network features for classifying 1. schizophrenia and 2. AFib

44 AFib

53 controls

Shashikumar, S. P., Shah, A. J., Li, Q., Clifford, G. D. & Nemati, S. A Deep Learning Approach to Monitoring and Detecting Atrial Fibrillation using Wearable Technology. IEEE EMBS International Conference on Biomedical & Health Informatics 141–144 (2017).

Samsung Simbands used to record ECG, photoplethysmography (PPG), and accelerometry

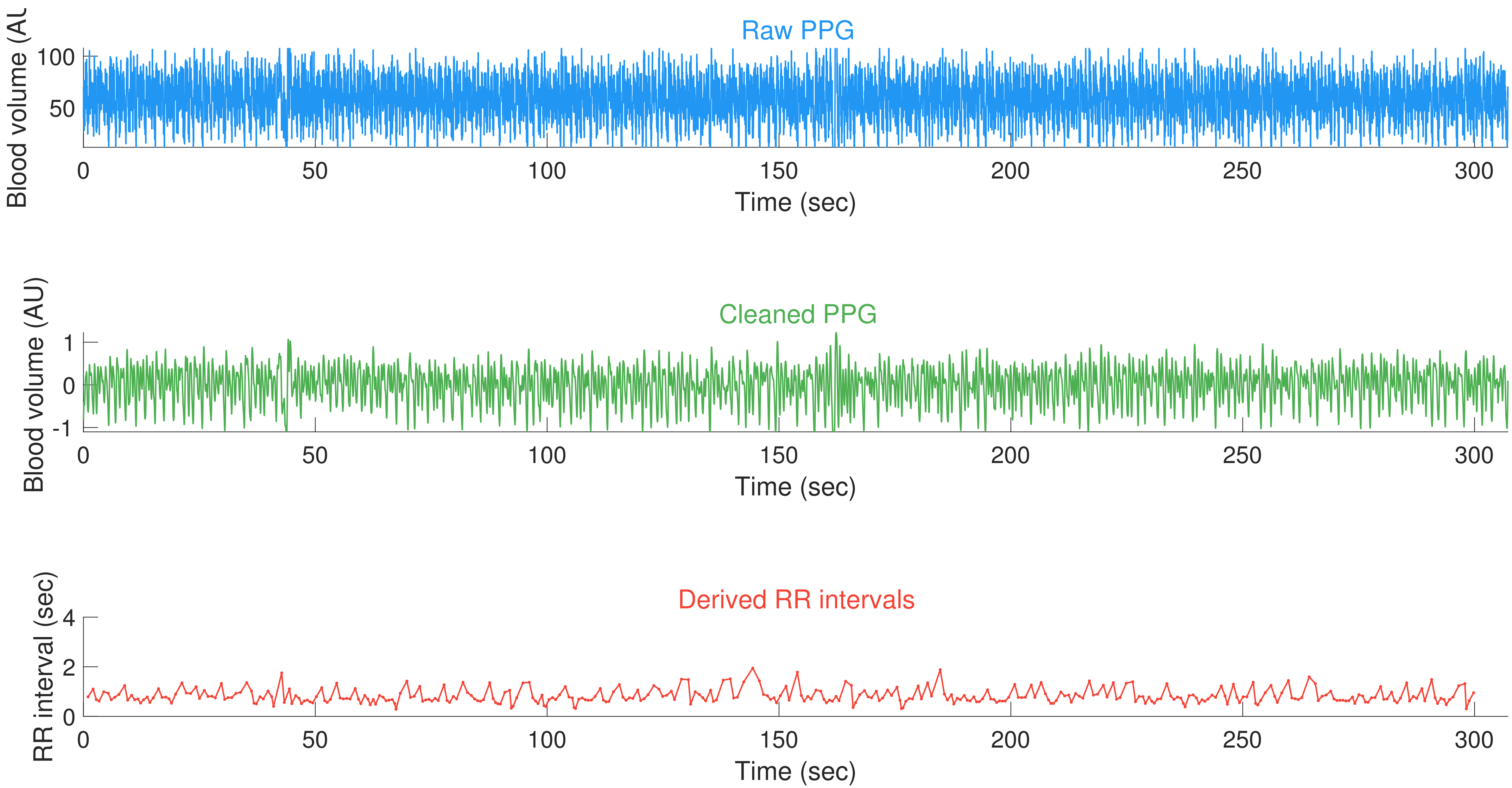

Shashikumar, S. P., Shah, A. J., Li, Q., Clifford, G. D. & Nemati, S. A Deep Learning Approach to Monitoring and Detecting Atrial Fibrillation using Wearable Technology. IEEE EMBS International Conference on Biomedical & Health Informatics 141–144 (2017).

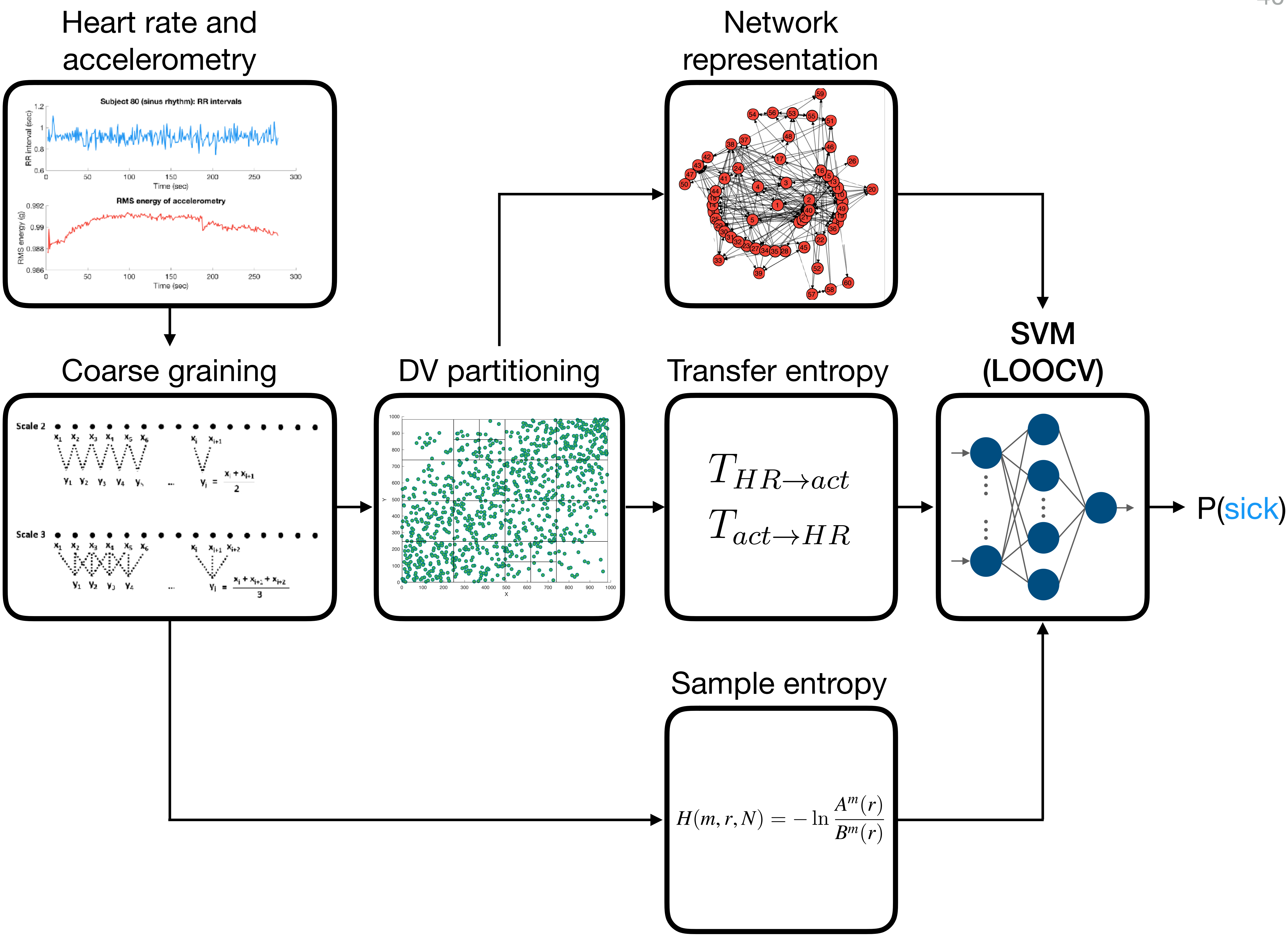
Heart rate and accelerometry
Subject 80 (sinus rhythm): RR intervals
RR interval (sec)
Time (sec)
RMS energy of accelerometry
RMS energy (g)
Time (sec)
Network representation
Coarse graining
Scale 2
Scale 3
DV partitioning
Transfer entropy
$T_{HR \to act}$
$T_{act \to HR}$
SVM (LOOCV)
P(sick)
Sample entropy
$H(m, r, N) = -\ln \frac{A^m(r)}{B^m(r)}$

Network representations of data from controls differ from schizophrenia patients

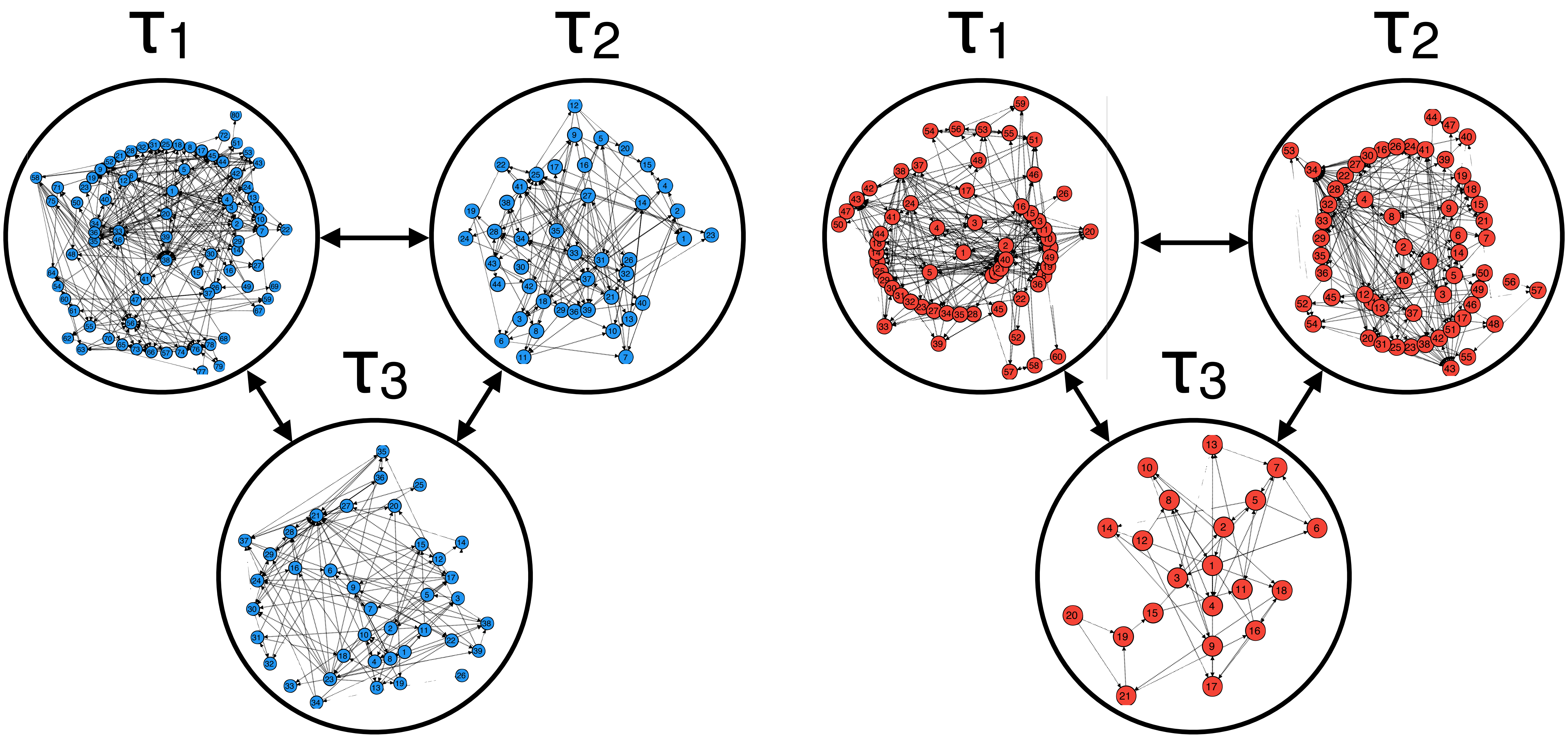

Reinertsen, E. et al. Multiscale network dynamics between heart rate and locomotor activity are altered in schizophrenia. Physiol. Meas. 0, 7–10 (2018).

For classifying schizophrenia, multiscale network representation (MSNR) outperformed multiscale transfer entropy (MTE)

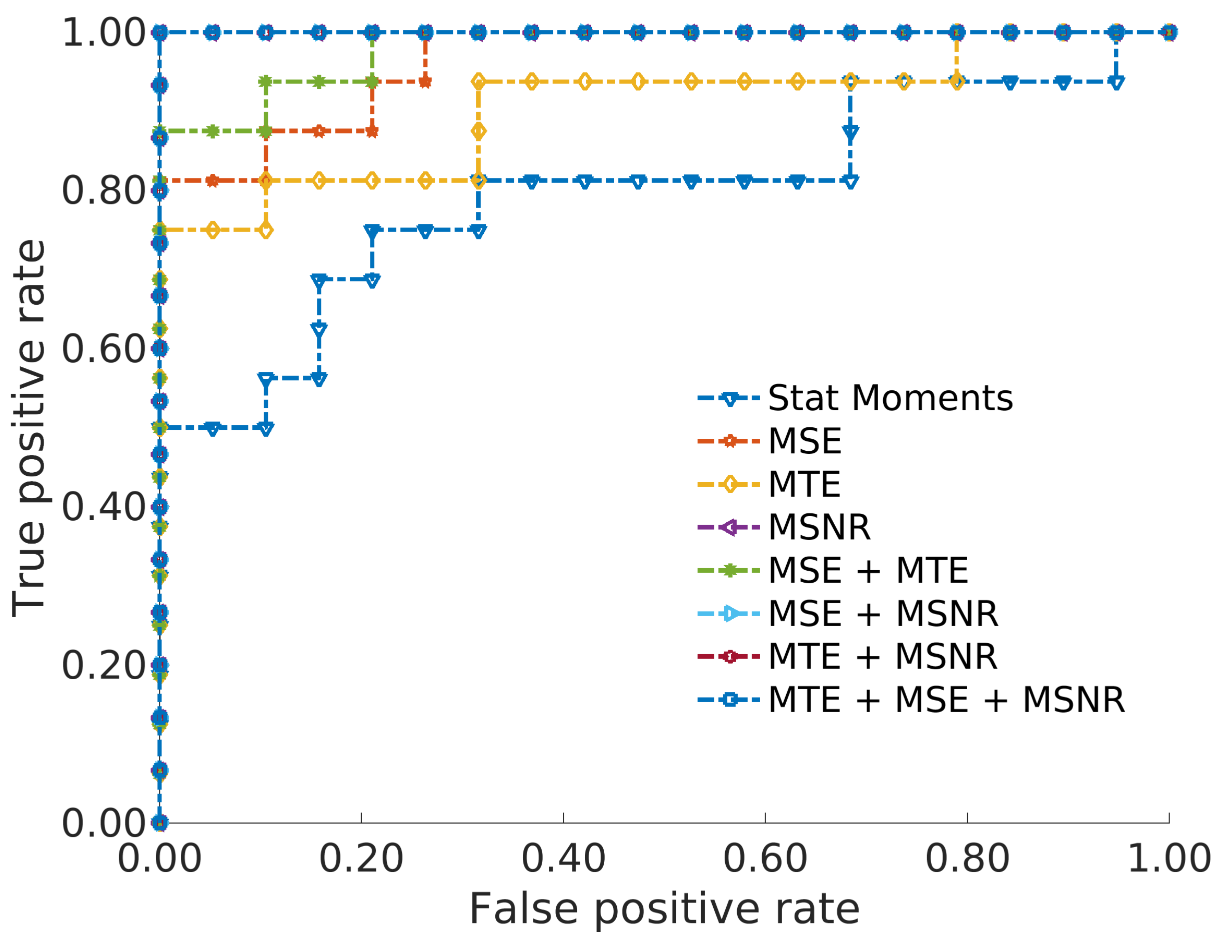

Model	Training AUC	Testing AUC
Statistical moments	0.95	0.80
MSE	0.98	0.96
MTE (all)	1.00	0.94
MSNR	1.00	1.00
MSE + MTE	1.00	1.00
MSE + MSNR	1.00	1.00
MTE + MSNR	1.00	1.00
MTE + MSE + MSNR	1.00	1.00

Reinertsen, E. et al. Multiscale network dynamics between heart rate and locomotor activity are altered in schizophrenia. Physiol. Meas. 0, 7–10 (2018).

Network representations of data from controls differ from AF patients

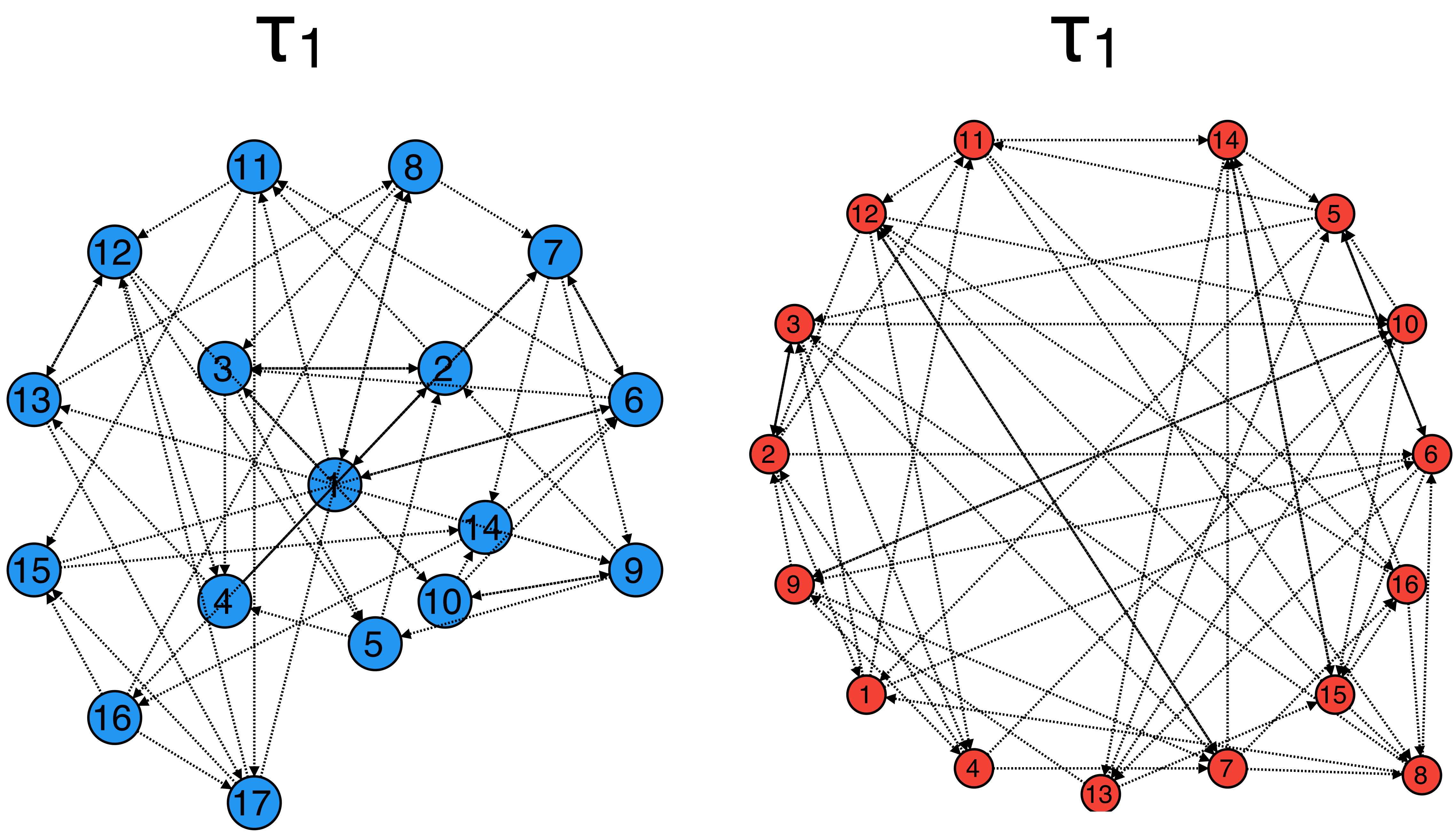

Reinertsen, E. et al. Multiscale network dynamics between heart rate and locomotor activity are altered in schizophrenia. Physiol. Meas. 0, 7–10 (2018).

For classifying AFib, MSE generalized well, and MTE slightly overfit but surpassed MSNR

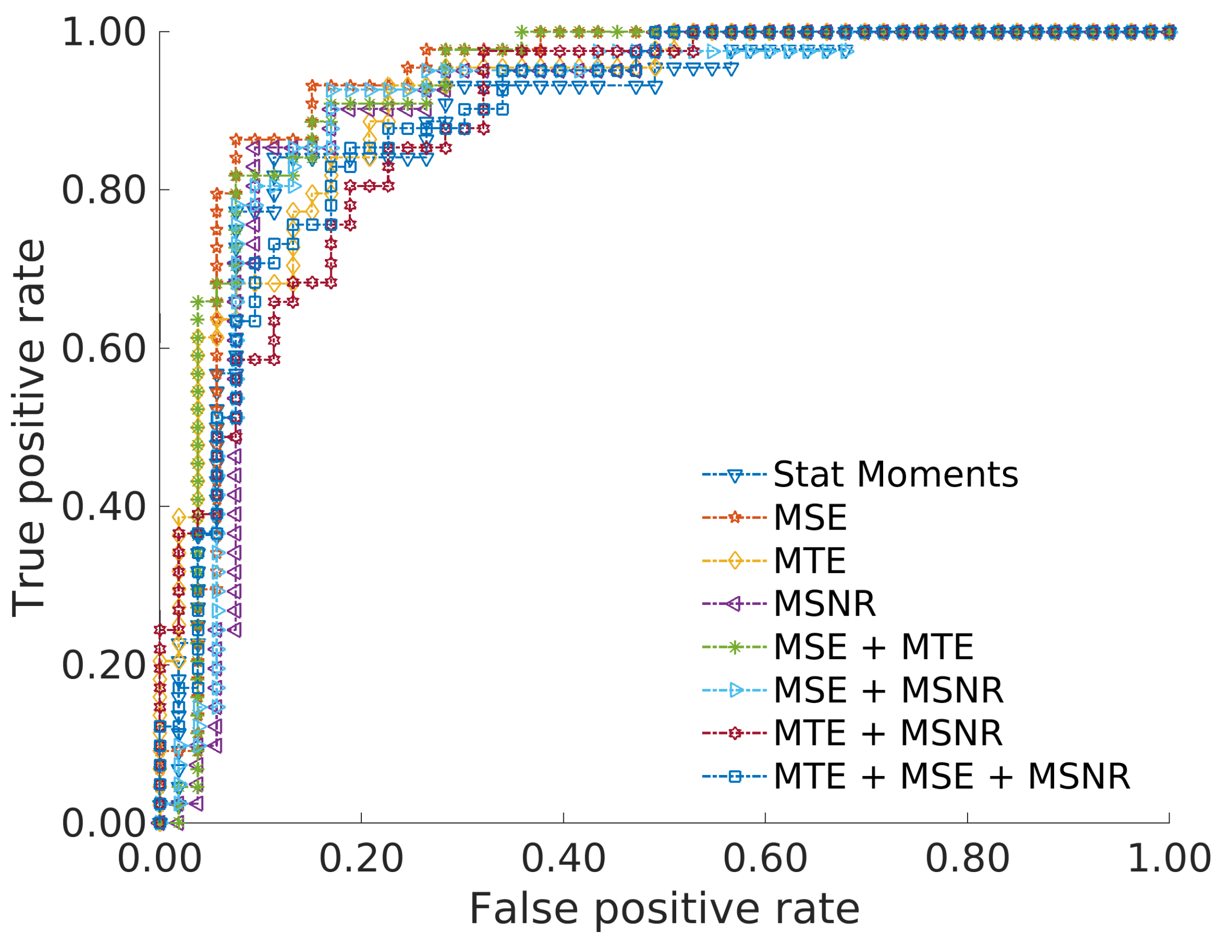

Model	Training AUC	Testing AUC
Statistical moments	0.92	0.89
MSE	0.94	0.93
MTE (all)	0.96	0.91
MSNR	0.92	0.90
MSE + MTE	0.98	0.93
MSE + MSNR	0.96	0.90
MTE + MSNR	0.99	0.89
MTE + MSE + MSNR	0.99	0.89

Reinertsen, E. et al. Multiscale network dynamics between heart rate and locomotor activity are altered in schizophrenia. Physiol. Meas. 0, 7–10 (2018).

Networks may capture transitions, trends, and latent variables better than transfer entropy

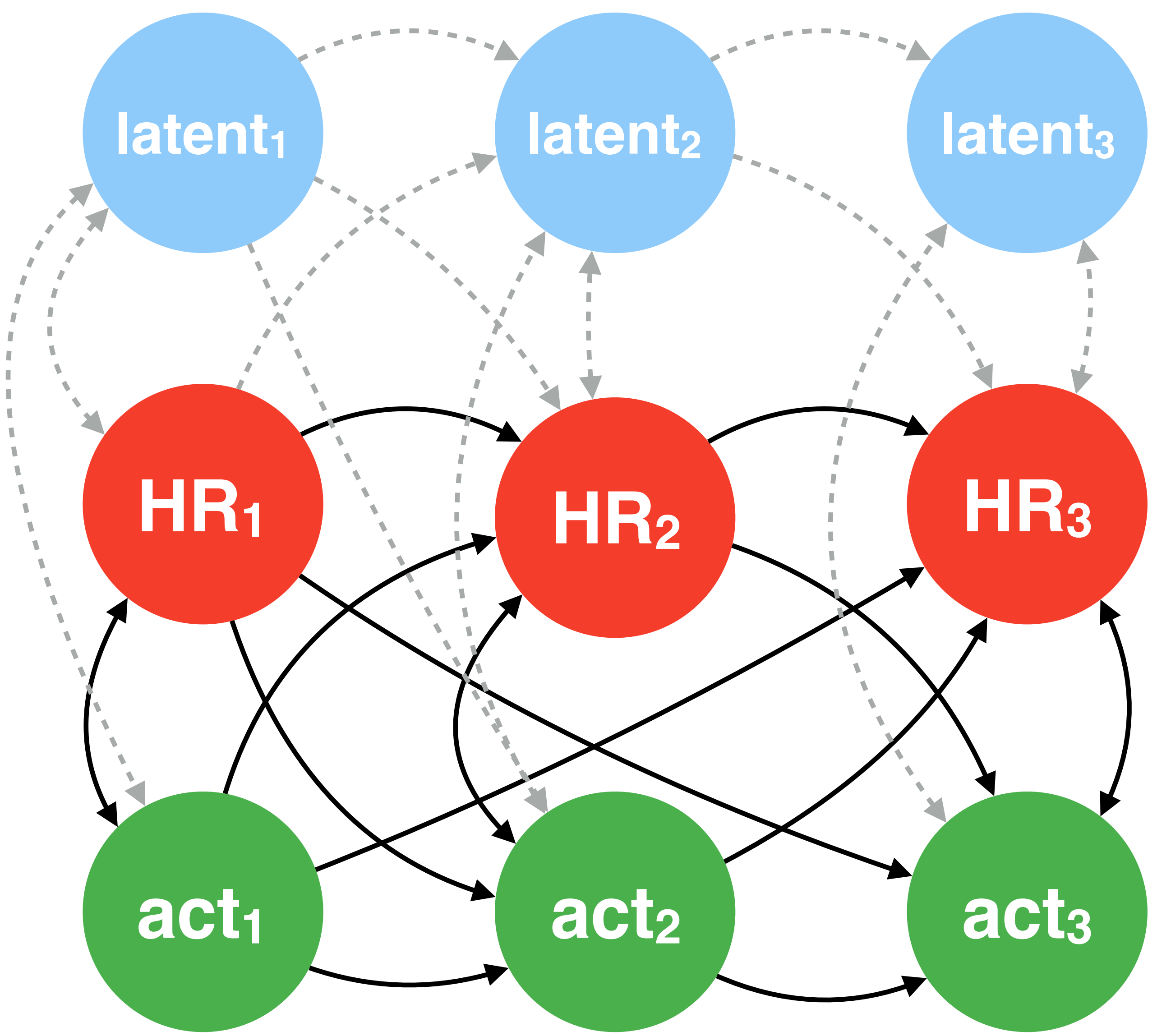

Summary

Schizophrenia: measures of **interaction** between physiology and activity were better features than univariate measures.

AFib: univariate measure of **irregularity** was a better feature than measures of interaction between physiology and activity.

	Cohort	Hypothesis
1	Schizophrenia	Classification & type of feature varies with time scale of data.
2	PTSD	Segmenting data into quiescent periods improves signal:noise and classification.
3	Schizophrenia & atrial fibrillation	Interactions between HR and activity improve classification of mental illness, not arrhythmia.
4	Heart failure	Passive smartphone data can be used to estimate quality of life.

Personalized CHF severity estimates from 680M movement, 9K location, and 11K contact activity data points (ten patients)

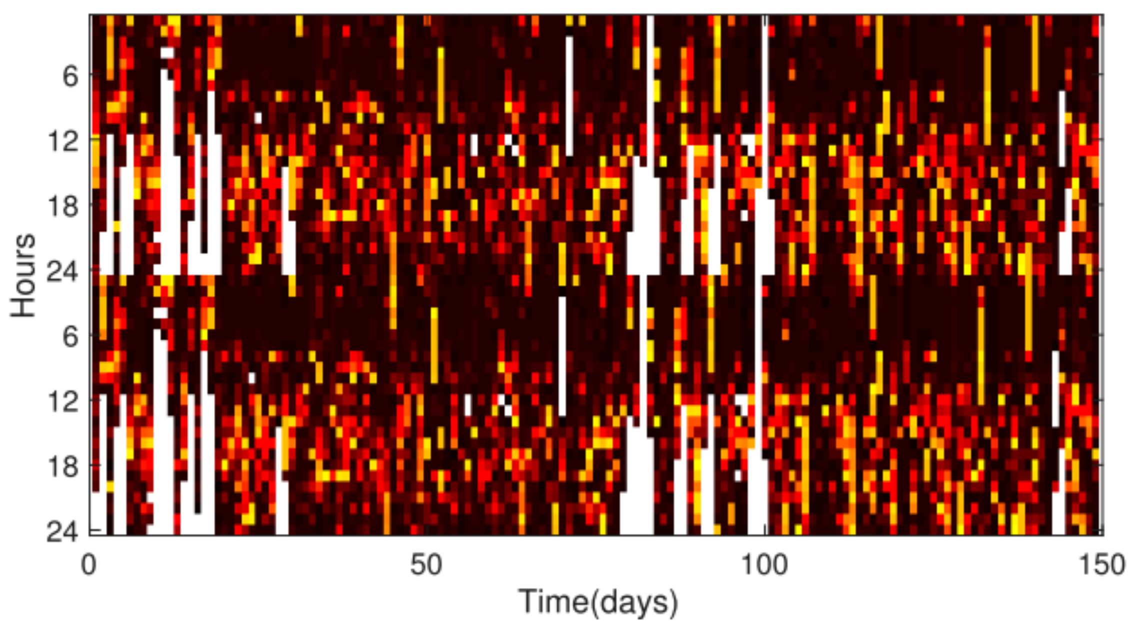

(a) Actigraphy levels.

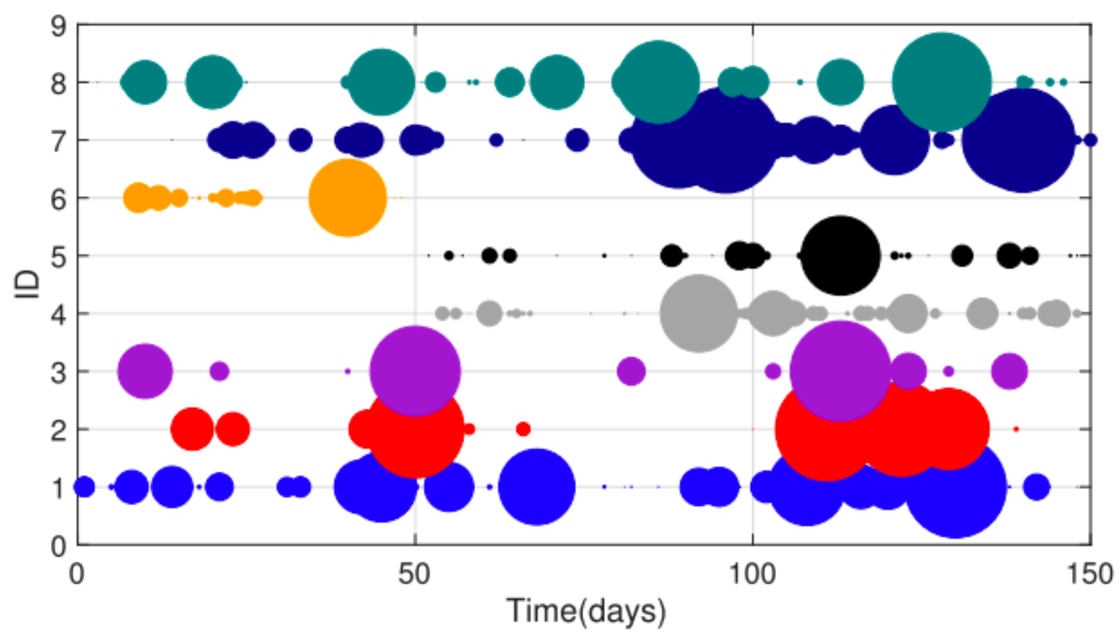

(b) Contact activity levels.

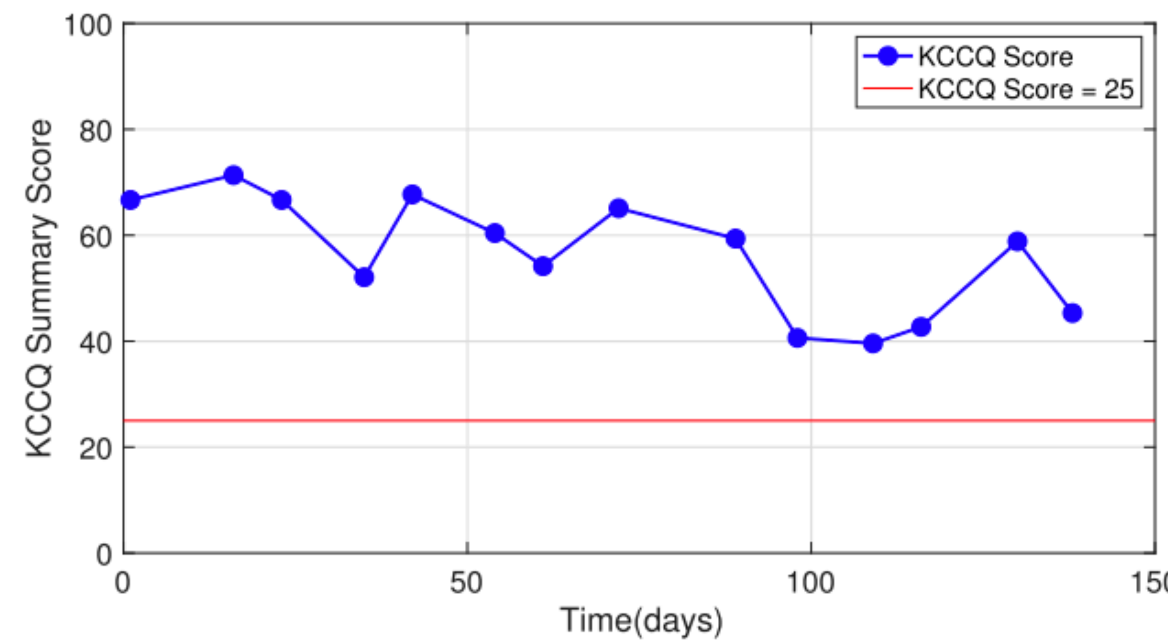

(c) KCCQ scores over time.

Figure 1: Daily actigraphy levels over a period of 150 days for one individual are shown in figure (a). Darker colors indicate lower activity and white indicates missing data. Subject's contact activity levels are shown in figure (c). The y-axis shows de-identified contacts while the x-axis shows time. Circle radius is proportional to call duration, and unique individuals are encoded by color. Figure (c) shows the KCCQ score over days for the same subject.

Cakmak, A., Reinertsen, E., Taylor, H. A., Shah, A. J. & Clifford, G. D. Personalized heart failure severity estimates using passive smartphone data. IEEE Int. Conf. Big Data (2018).

Addressing limitations of this preliminary work requires larger & more focused studies

1. Small sample size
2. Single institution
3. Simple learning algorithms
4. Broad classification — clinically useful?

Reflections on informatics in the trenches

1. Wearables not yet relevant for most patient care.
2. Low hanging fruit in sales, operations, logistics.
3. Clinical context surprisingly helpful.
4. Bilingual speakers rare.
5. More hype than expertise.
6. Technology alone insufficient; also requires policy, economics, culture, workflow.

Outline

1. HR and accelerometer data contain disease-relevant information.
2. Simple statistical measures do not address complexity, time scales, or interactions.
3. My work explores these limitations using data from different patient cohorts.
4. Entrepreneurship & VC are important to translation.
5. Future direction.

“Entrepreneurship is the rawest form of the translational impulse” -David Shaywitz

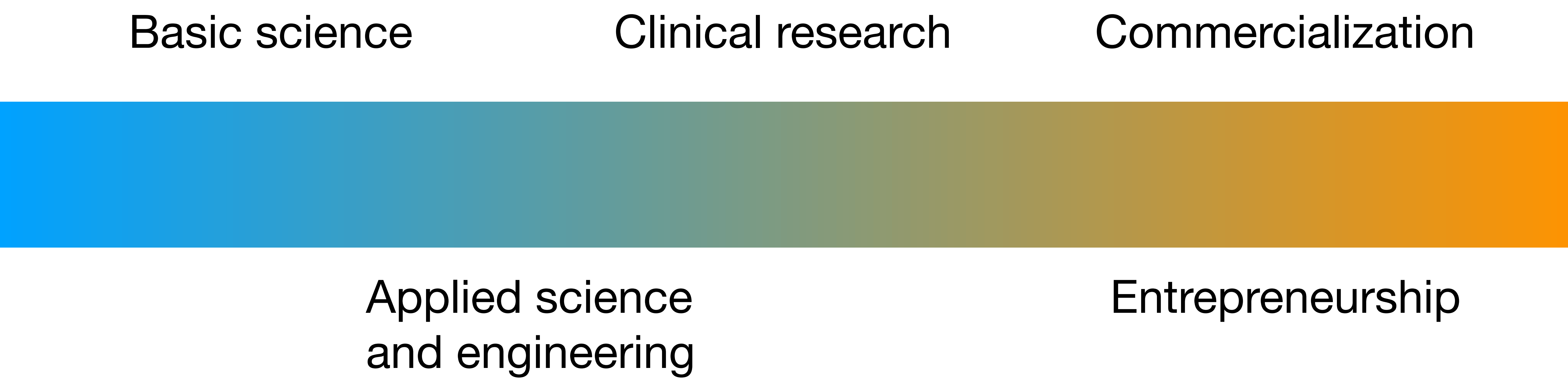

FORGE

Takeda

TAKEDA VENTURES, INC.

Takeda

TAKEDA VENTURES, INC.

David Shaywitz, MD, PhD

Senior Partner, TVI

Life science VC firm

$1-25M per investment

Palo Alto, San Diego, Boston, London

Team members have PhD +/- MD

Data Science & Tech = DST

I helped David diligence DST startups

Takeda

TAKEDA VENTURES, INC.

GI	Onc
Neuro	Rare Dz

TAKEDA VENTURES, INC.

GI	Onc	
Neuro	Rare Dz	DST?

Takeda
TAKEDA VENTURES, INC.

TAKEDA VENTURES, INC.

1. Disconnect between c-suite and trenches.
2. Pharma values assets, not platforms.
3. Hard to share best practices in large firms.
4. DST is a tool for domain experts, not a replacement of.
5. Many startups have glaring issues with fundamental statistics & ML.
6. Pharma wants to work with academic experts in DST space (DBMI?).

Outline

1. HR and accelerometer data contain disease-relevant information.
2. Simple statistical measures do not address complexity, time scales, or interactions.
3. My work explores these limitations using data from different patient cohorts.
4. Entrepreneurship & VC are important to translation.
5. Future direction.

Interests: 1. critical care / sepsis, 2. mapping physiology to drug dev / discovery, 3. EHR data fusion, and 4. informatics consults

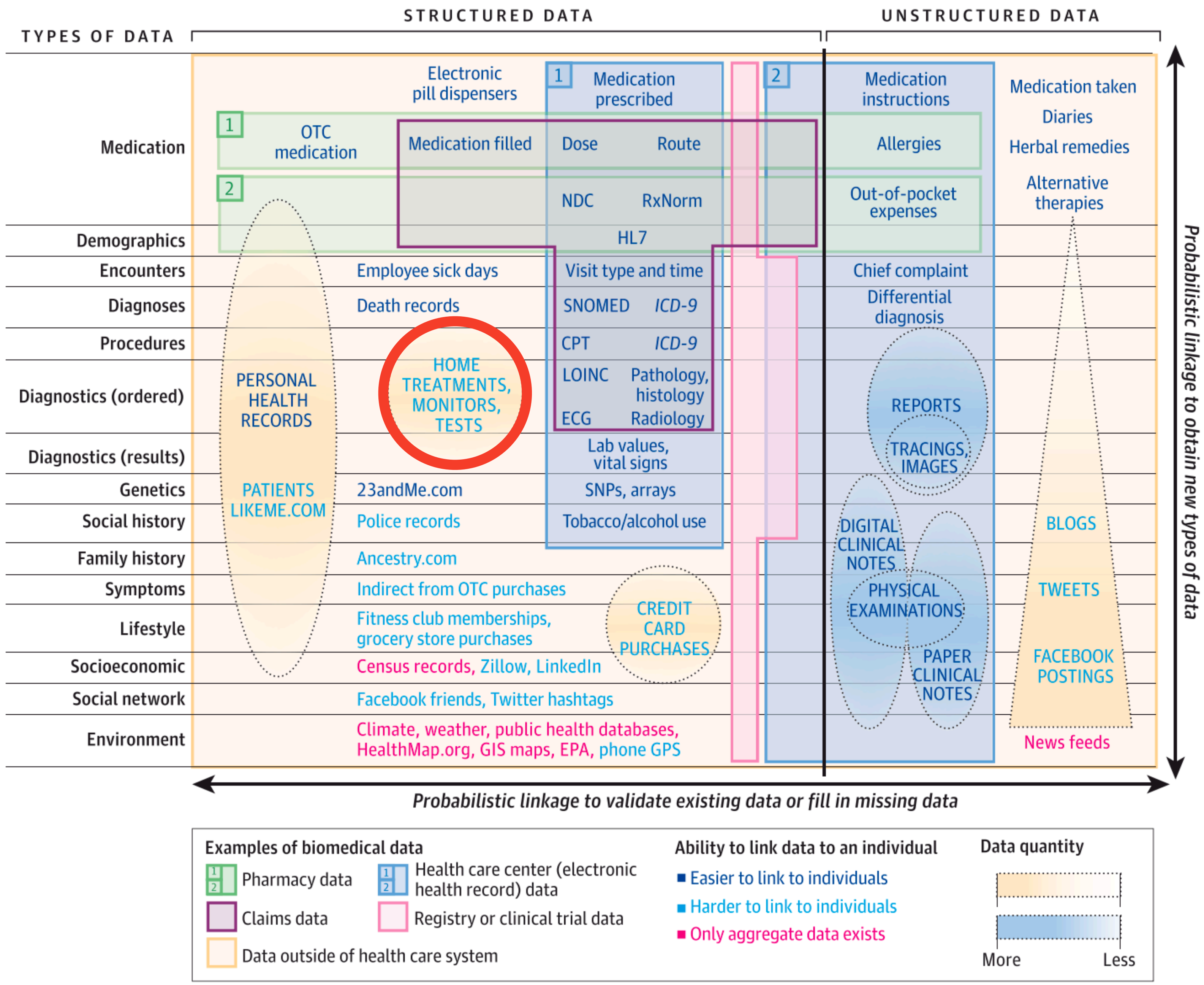

1. Nemati, S. et al. An Interpretable Machine Learning Model for Accurate Prediction of Sepsis in the ICU. Crit. Care Med. 1 (2017).
2. Weber, G. M., Mandl, K. D. & Kohane, I. S. Finding the Missing Link for Big Biomedical Data. JAMA 311, (2014).
3. Longhurst, C, Harrington, R & Shah, N 'green button' for using aggregate patient data at the point of care. Health Aff. (2014).

Thanks to Gari Clifford, Shamim Nemati, colleagues, collaborators, patients, and funders















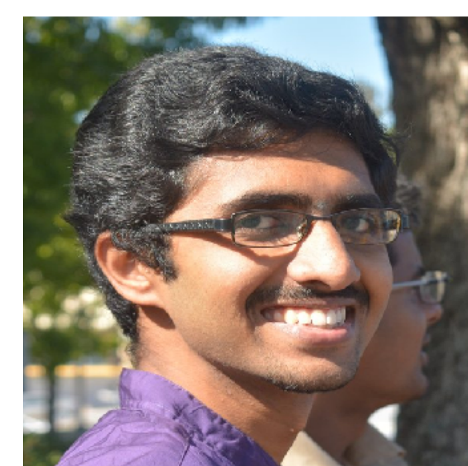

Appendix

Heart rate variability (HRV) measures are derived from RR intervals

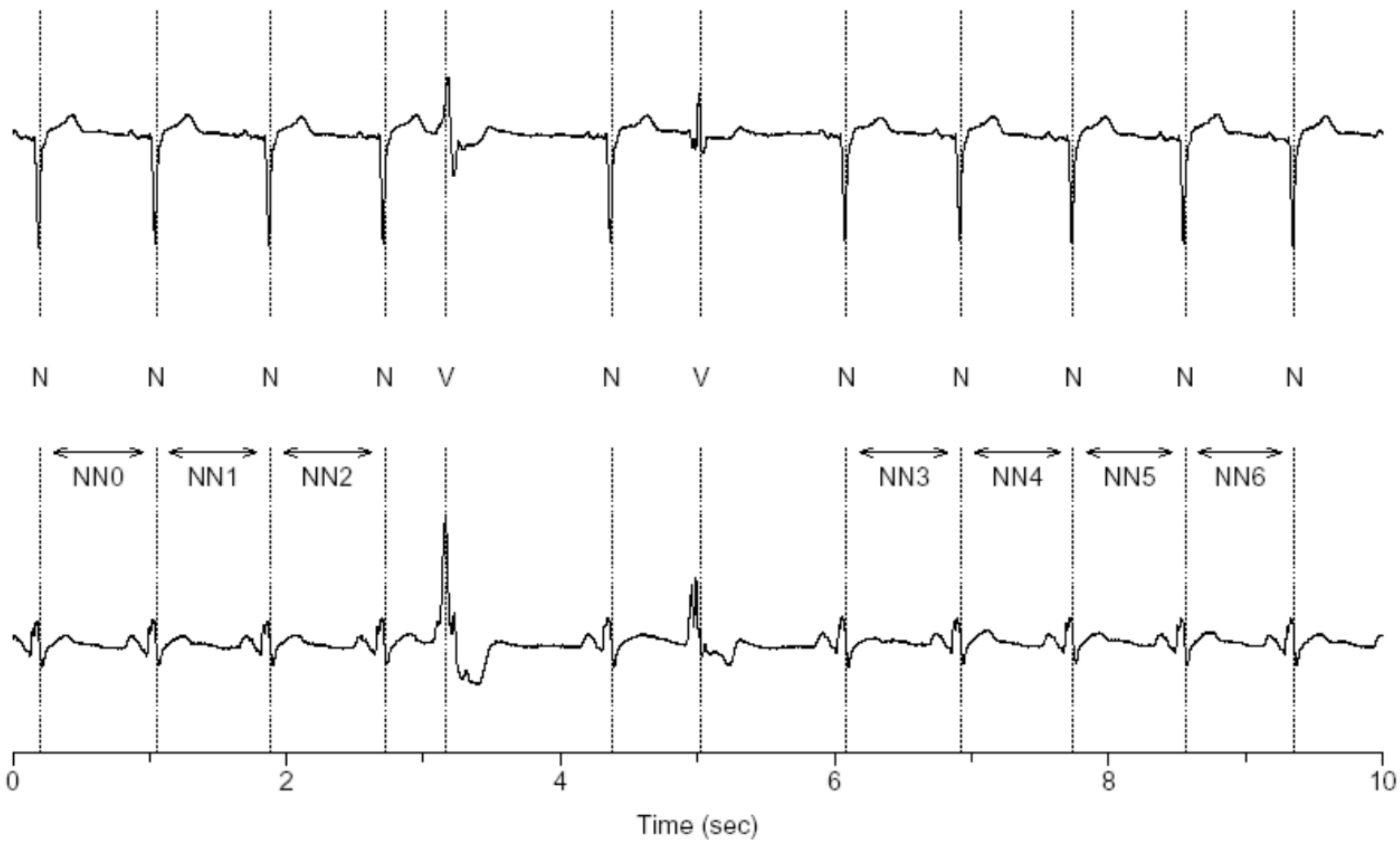

Mietus J. Time Domain Measures: From Variance to pNNx. 2006.

Time-domain HRV measures

AVNN: Average of all NN intervals

SDNN: Standard deviation of all NN intervals

SDANN: Standard deviation of the average of NN intervals in all 5- minute segments of a **24-h recording**

SDNNIDX (ASDNN): Mean of the standard deviation in all 5-minute segments of a **24-h recording**

rMSSD: Square root of the mean of the squares of the differences between adjacent NN intervals

pNN50: Percentage of differences between adjacent NN intervals that are >50 msec; this is one member of the larger pNNx family

M. Malik, "Heart Rate Variability: Standards of Measurement, Physiological Interpretation, and Clinical Use," Circulation, vol. 17, pp. 354–381, 1996.

Frequency HRV measures reflect sympathetic & parasympathetic activity

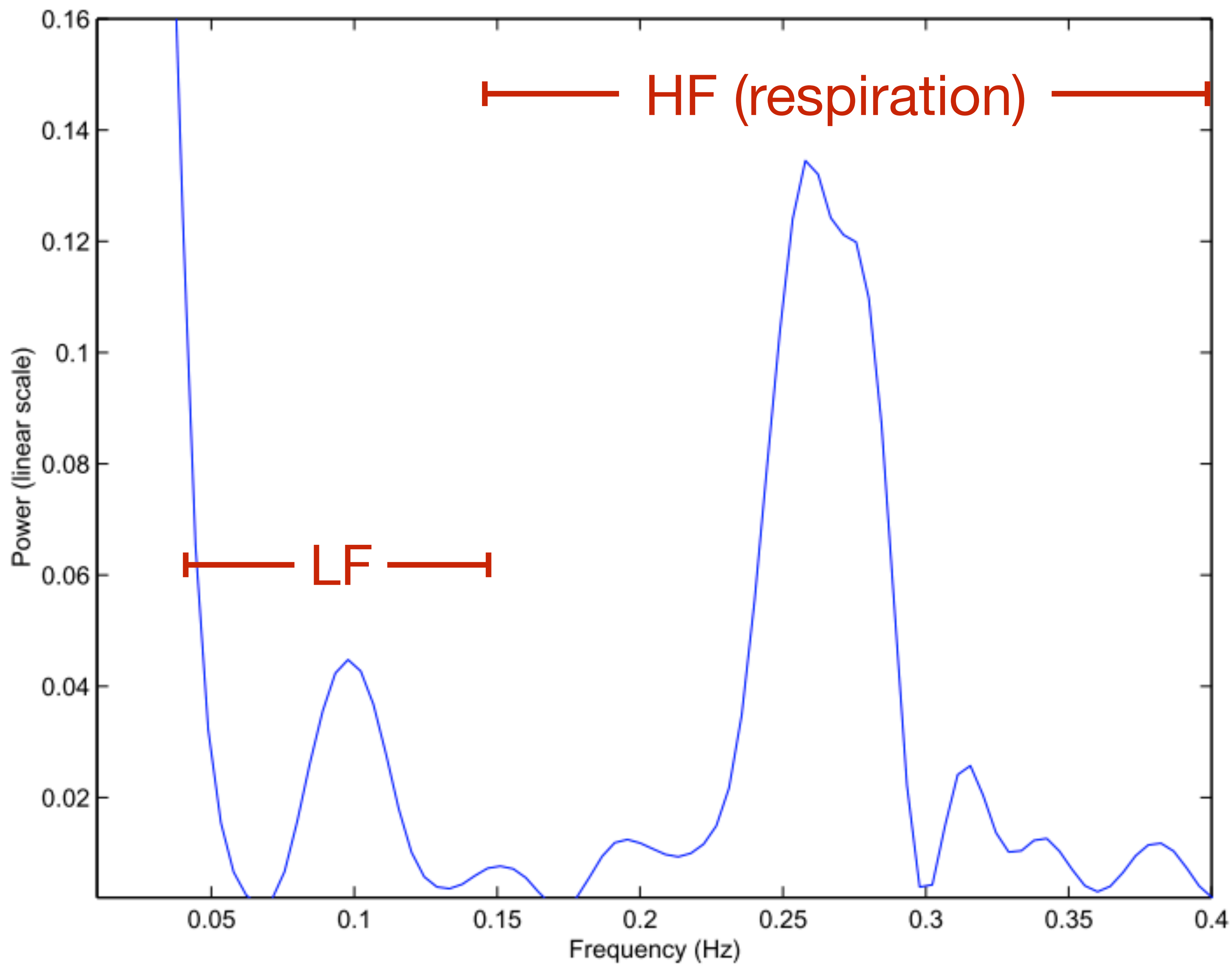

Clifford GD. Signal processing methods for heart rate variability. PhD thesis. 2002.

The LF/HF ratio does not measure the complex cardiac sympathovagal balance

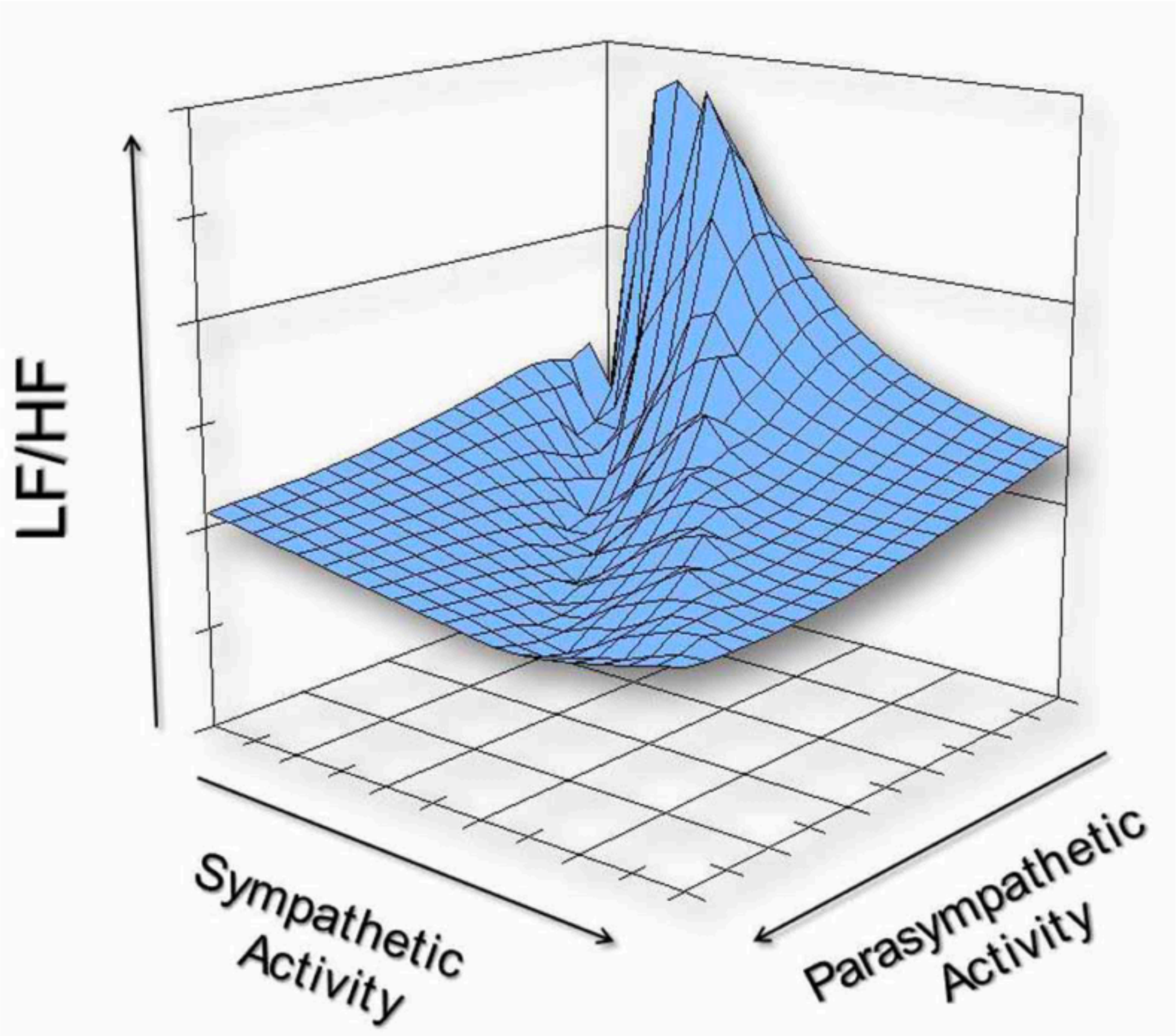

Billman, G. E. The LF/HF ratio does not accurately measure cardiac sympatho-vagal balance. Front. Physiol. 4 FEB, 1–5 (2013).

The Fourier transform of the auto-correlation function is called the PSD:

$$S_x(f) = \int_{-\infty}^{\infty} R_x(\tau) e^{-2\pi i f \tau} d\tau$$

$$R_x(\tau) = E[x(t)x(t+\tau)]$$

The PSD is also the expectation of the Fourier transformation magnitude squared, over a large time interval:

$$S_x(f) = \lim_{T \to \infty} E\left\{ \frac{1}{2T} \left| \int_{-T}^{T} x(t) e^{-j2\pi i f t} dt \right|^2 \right\}$$

The discrete Fourier transform (DFT) requires *O(n^2)* operations:

Given N discrete samples of $f(x)$, sampled in uniform steps,

$$F(u) = \frac{1}{N} \sum_{x=0}^{N-1} f(x) e^{-i2\pi ux/N}$$

for $u = 0, 1, 2, \ldots, N-1$, and

$$f(x) = \sum_{u=0}^{N-1} F(u) e^{i2\pi ux/N}$$

for $x = 0, 1, 2, \ldots, N-1$.

each *F(u)* involves N-1 multiplications, and there are N *F(u)*s.

The radix-2 DIT FFT expresses the DFT of length N recursively in terms of two interleaved DFTs (even- and odd-indexed) each of size N/2. Convergence occurs in *O(n log n).*

Algorithm speed is achieved by re-using the results of intermediate computations to compute multiple DFT outputs.

Yoo, Y. Tutorial on Fourier theory. March 2001. www.cs.otago.ac.nz/cosc453/student_tutorials/fourier_analysis.pdf

Phase-rectified signal averaging (PRSA) quantifies acceleration and deceleration capacity

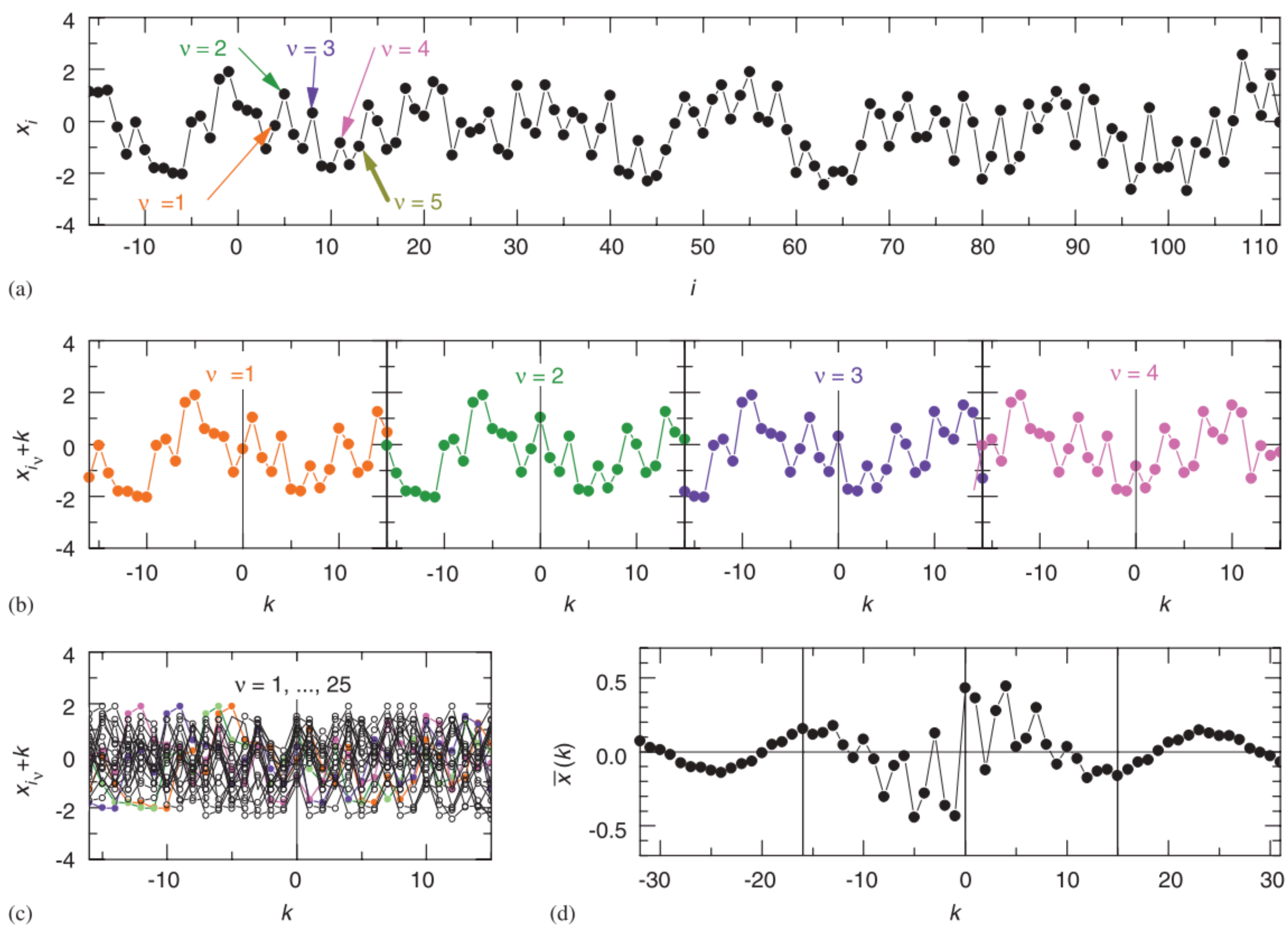

Bauer A. et al. Phase-rectified signal averaging detects quasi-periodicities in non-stationary data. Phys. A, vol. 364, pp. 423–434 (2006).

Two time series can have similar μ, σ, and PSD, but different complexity

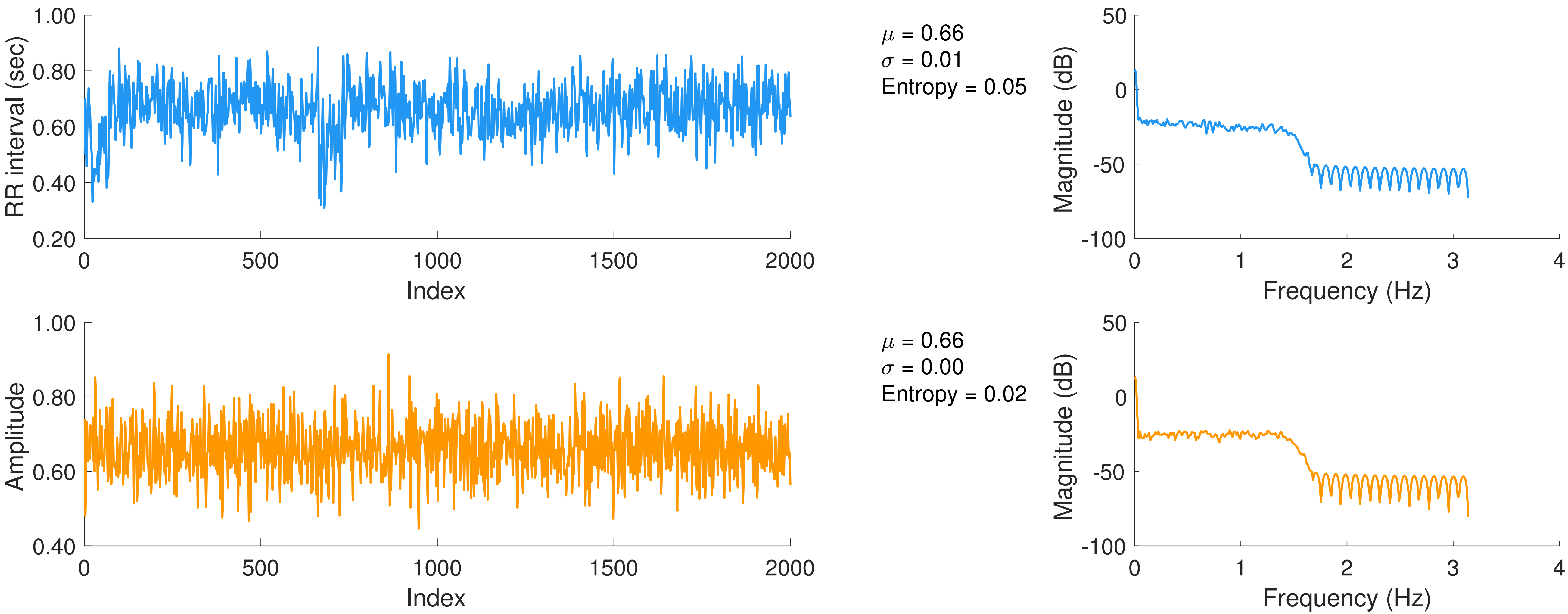

McSharry, P. E. & Clifford, G. D. A statistical model of the sleep-wake dynamics of the cardiac Rhythm. in Computers in Cardiology 32, 591–594 (2005).

Sample entropy (SampEn) measures complexity, or "expected surprise"

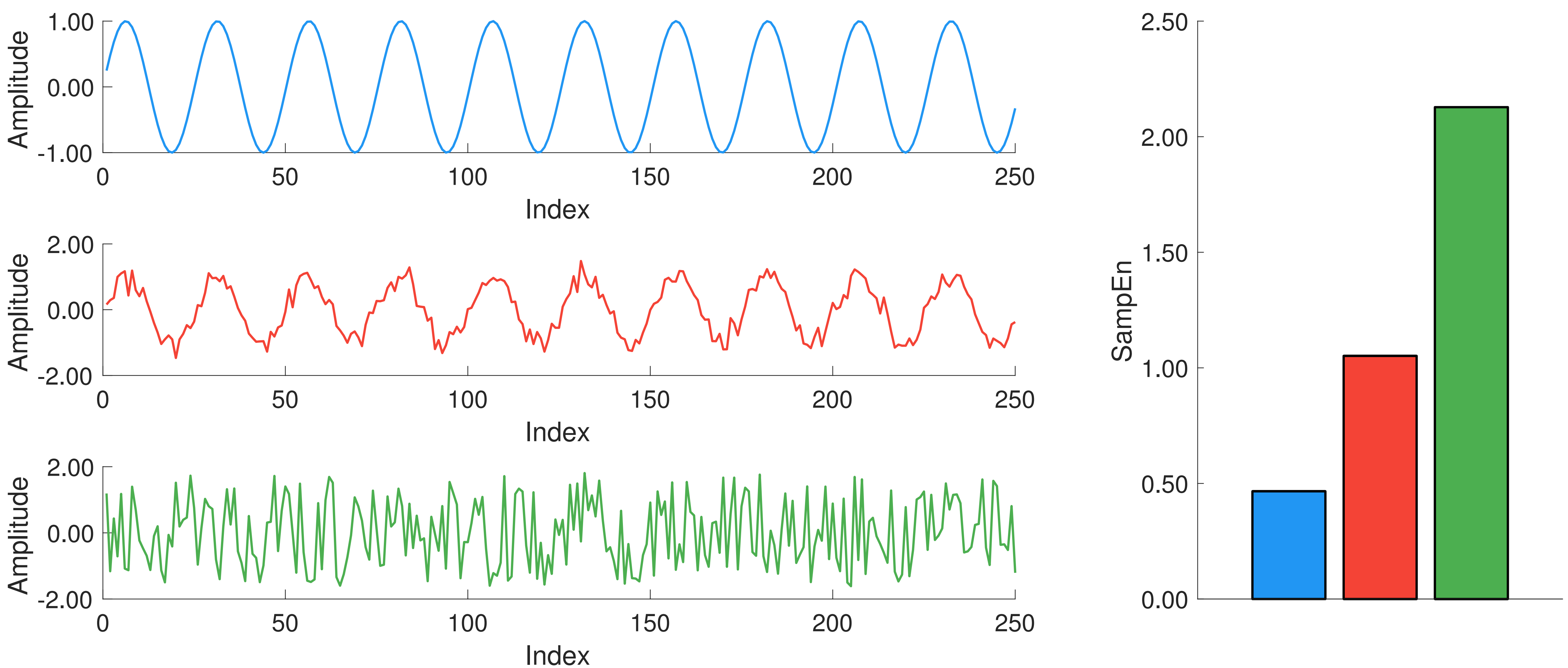

SampEn estimates regularity by counting pattern matches of template length *m*

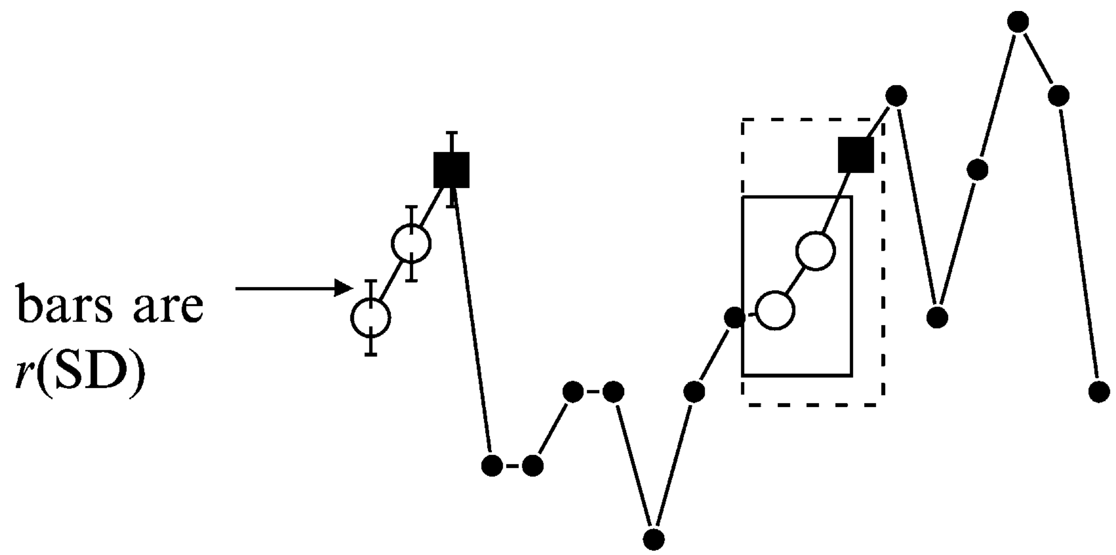

■ A_i = number of matches of length $m+1$ with ith template

○ B_i = number of matches of length m with ith template

$$SampEn = -\log \frac{A}{B}$$

Where

A = number of template vector pairs having $d[X_{m+1}(i), X_{m+1}(j)] < r$ of length $m+1$

B = number of template vector pairs having $d[X_m(i), X_m(j)] < r$ of length m

Richman, J. S., Lake, D. E. & Moorman, J. R. Sample Entropy. Methods Enzymol. 384, 172–184 (2004).

Sample entropy

1. underestimates conditional entropy in the presence of sinusoidal trends.
2. is less sensitive to spikes compared to linear estimators.
3. is sensitive to local alterations in signal variance in terms of bias, although the relationship between conditional entropy and AR amplitude is not impaired.
4. significantly overestimates conditional entropy in the presence of power-law long-range correlations (both negative and positive), i.e. "slow trends"
5. is sensitive to sample size (which we knew).
6. significantly overestimates conditional entropy in the presence of both short-term AR dependencies and power-law long range correlations.
7. calculated from RR intervals of CHF patients is sensitive to normalization, high-pass filtering to remove slow trends, and sleep status

Xiong, W., Faes, L. & Ivanov, P. C. Entropy measures, entropy estimators, and their performance in quantifying complex dynamics: Effects of artifacts, nonstationarity, and long-range correlations. Phys. Rev. E 95, 1–37 (2017).

SampEn is derived from conditional entropy

$$C(X) = H(X_n | X_n^-) = H(X_n^-, X_n) - H(X_n^-)$$
$$= -\mathbb{E}[\log p(x_n | x_1, \ldots, x_{n-1})],$$

C(X) quantifies information in the present of the process X that cannot be explained by its past history X^-

Xiong, W., Faes, L. & Ivanov, P. C. Entropy measures, entropy estimators, and their performance in quantifying complex dynamics: Effects of artifacts, nonstationarity, and long-range correlations. Phys. Rev. E 95, 1–37 (2017).

Entropy measures non-Gaussianity and is proportional to skewness and kurtosis

Negentropy ***J(y)*** is based on differential entropy ***H(y)***, where $\boldsymbol{y_{gauss}}$ is a Gaussian variable with the same covariance matrix as ***y.***

$$H(y) = -\int P(y)\ log_2 P(y) dy$$

J(y) can be estimated from skewness **γ** and kurtosis **κ**

$$\mathcal{J}(y) = H(y_{gauss}) - H(y)$$

κ is not robust and is sensitive to outliers

$$\mathcal{J}(y) \approx \frac{1}{12}\gamma(y)^2 + \frac{1}{48}\kappa(y)^2$$

Gaussians are maximally random

24-hr RR tachograms exhibit different dynamics over various time scales

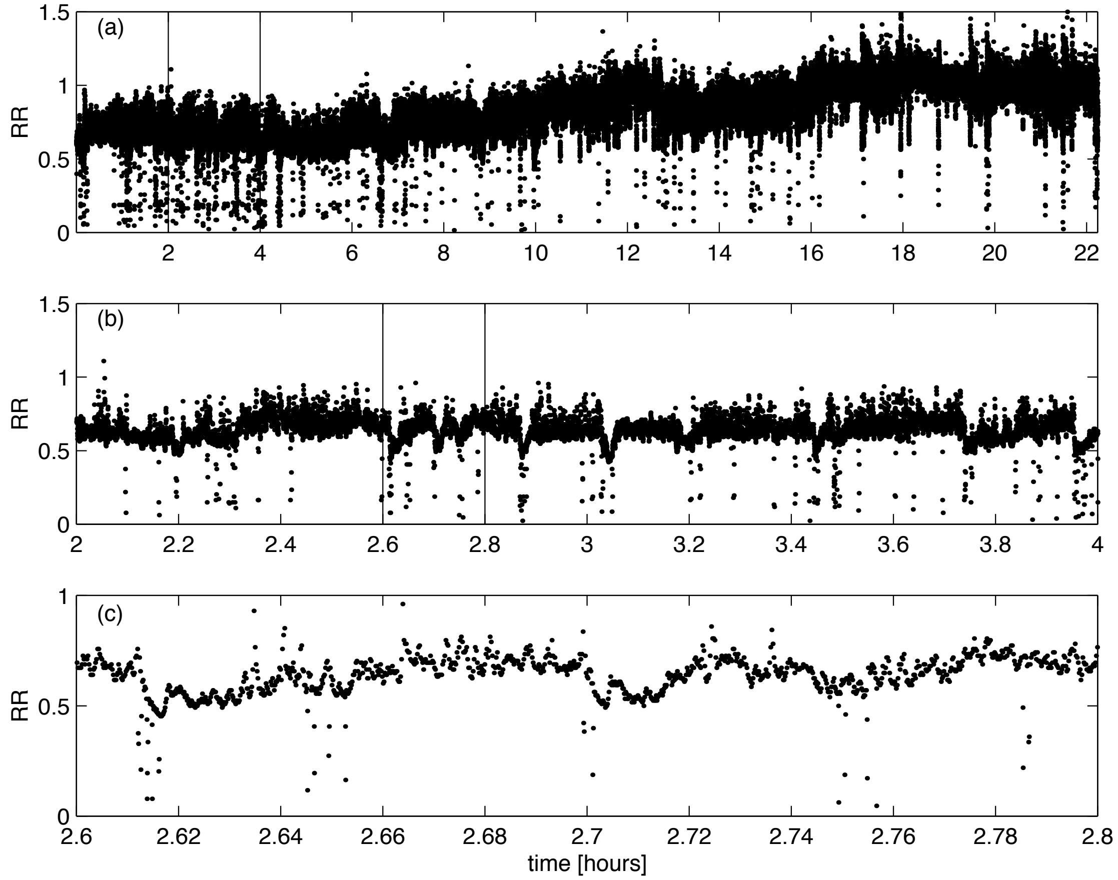

Respiratory sinus arrhythmia

Mayer waves

Circadian rhythm

Sleep stage

Physical activity

Social routine

1. McSharry, P. E., Clifford, G. D., Tarassenko, L. & Smith, L. A. Method for generating an artificial RR tachogram of a typical healthy human over 24-hours. in Computers in Cardiology 225–228 (2002).
2. Clifford, G. D., McSharry, P. E. & Tarassenko, L. Characterizing artefact in the normal human 24-hour RR time series to aid identification and artificial replication of circadian variations in human beat to beat heart rate using a simple threshold. in Computers in Cardiology 129–132 (2002).

Time series can be evaluated at different time scales via coarse-graining

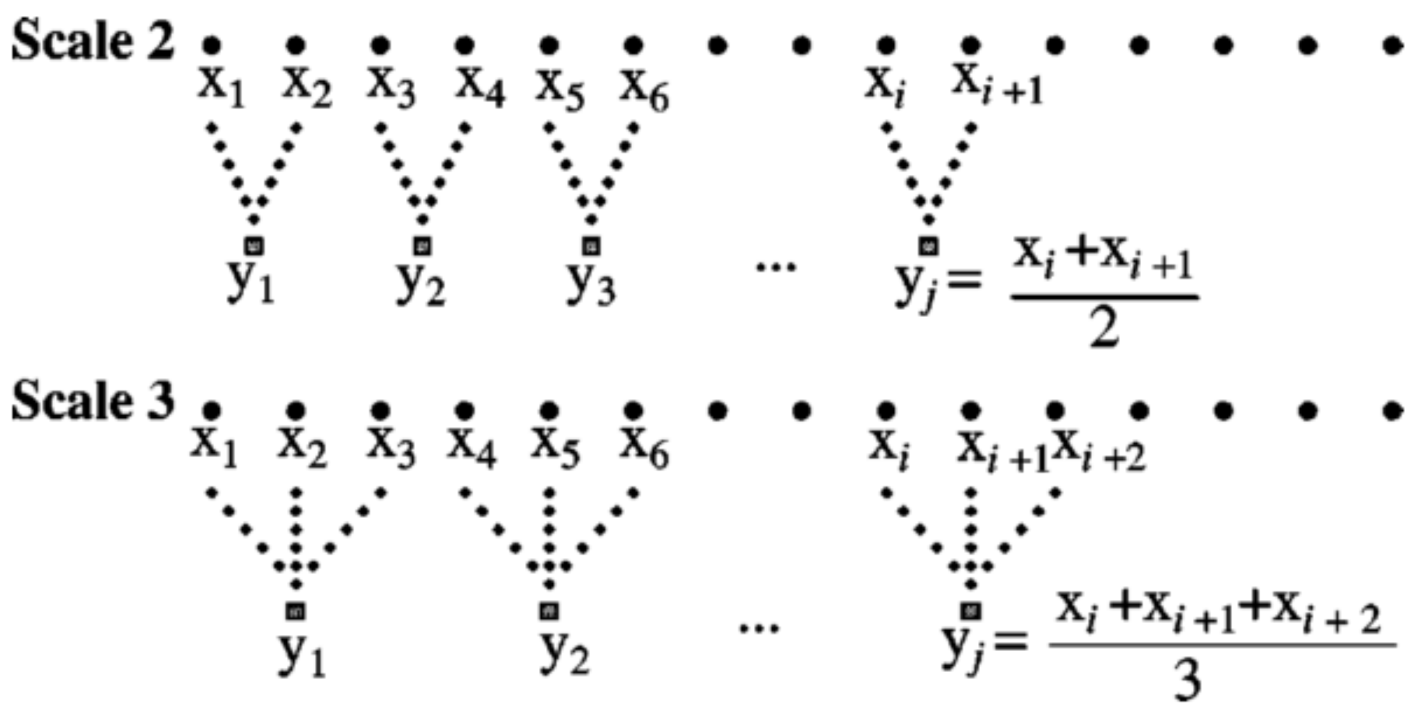

$$y_j^{(\tau)} = \frac{1}{\tau} \sum_{i=(j-1)\tau+1}^{j\tau} x_i$$

https://www.physionet.org/physiotools/mse/tutorial/node1.html

M. Costa, A. Goldberger, and C.-K. Peng, “Multiscale entropy analysis of biological signals,” Phys. Rev. E, 2005.

SampEn over various time scales is MultiScale Entropy (MSE), which differs in illness

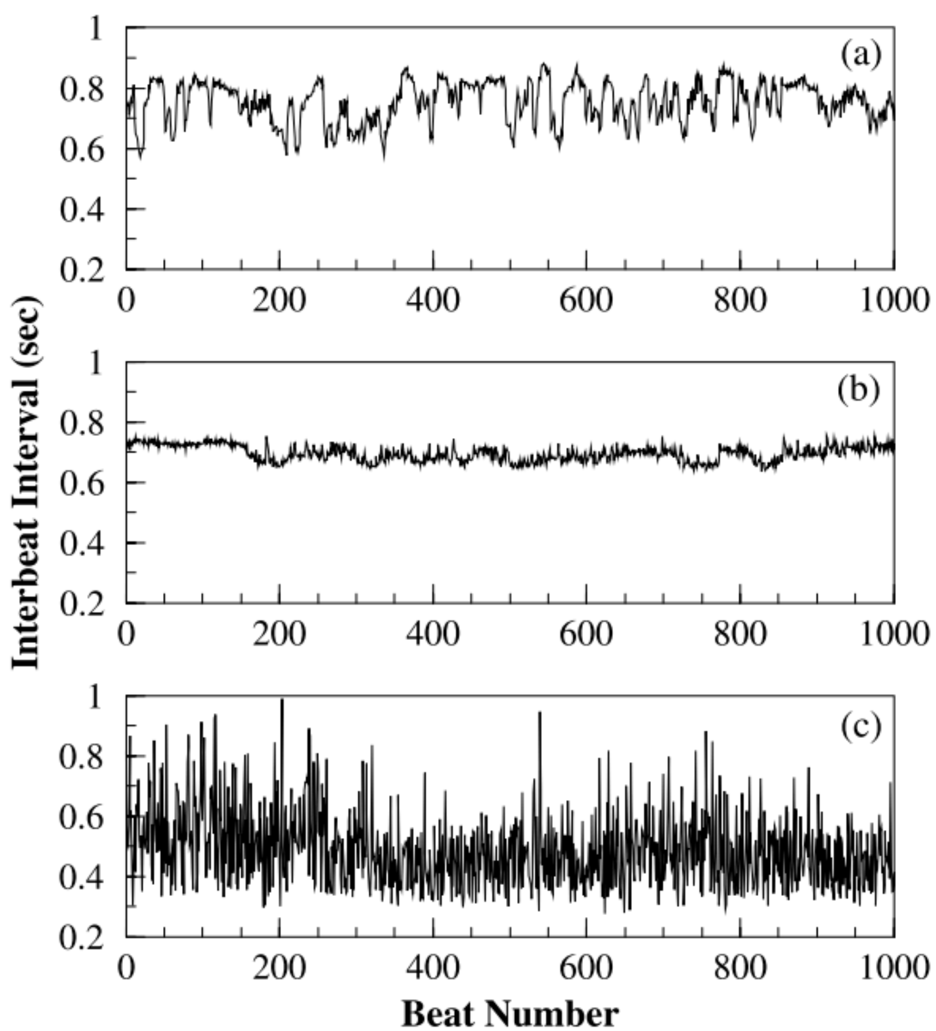

FIG. 2. Representative heartbeat intervals time series from (a) healthy individual (sinus rhythm), (b) subject with congestive heart failure (sinus rhythm), and (c) subject with the cardiac arrhythmia, atrial fibrillation.

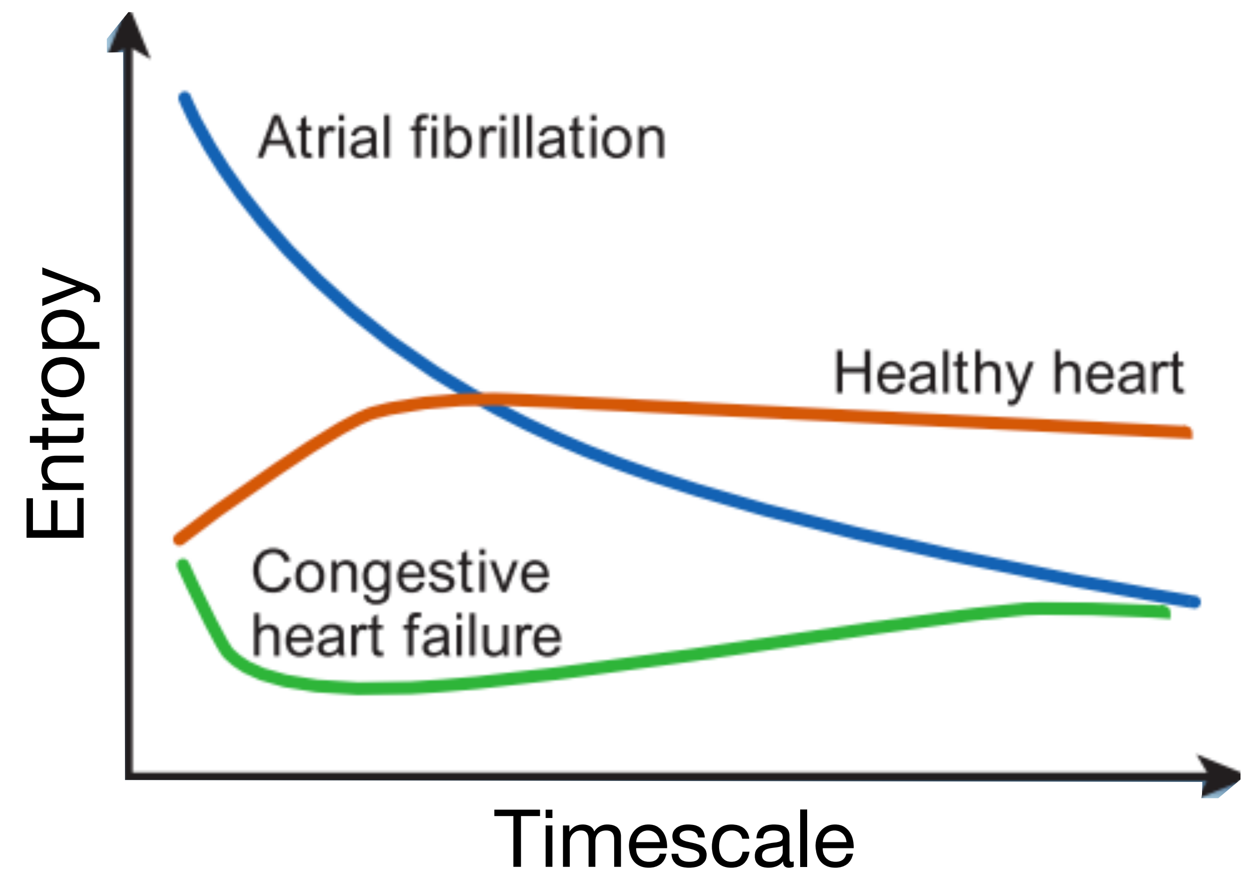

Costa M, Goldberger A, Peng C-K. Multiscale entropy analysis of complex physiologic time series. Phys Rev Lett. 2002.

D. R. Chialvo, “Unhealthy surprises.,” Nature, vol. 419, no. 6904, p. 263, 2002.

Univariate measures do not assess interaction

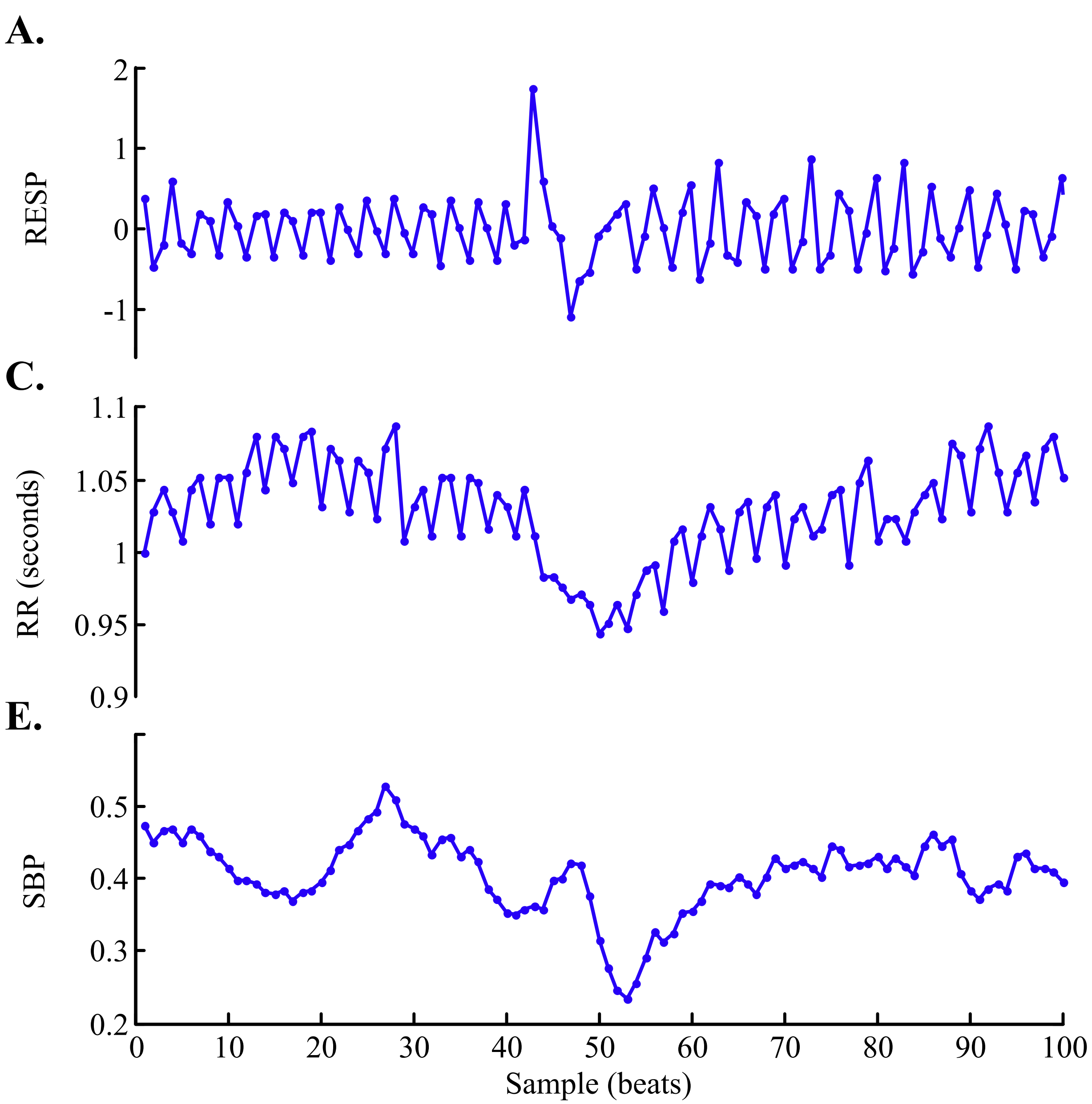

- Feedback
- Differential response to perturbation
- System dynamics differ with illness

Nemati, S. et al. Respiration and heart rate complexity: Effects of age and gender assessed by band-limited transfer entropy. Respir. Physiol. Neurobiol. 189, 159–163 (2013).

Is sunrise caused by the rooster crowing?

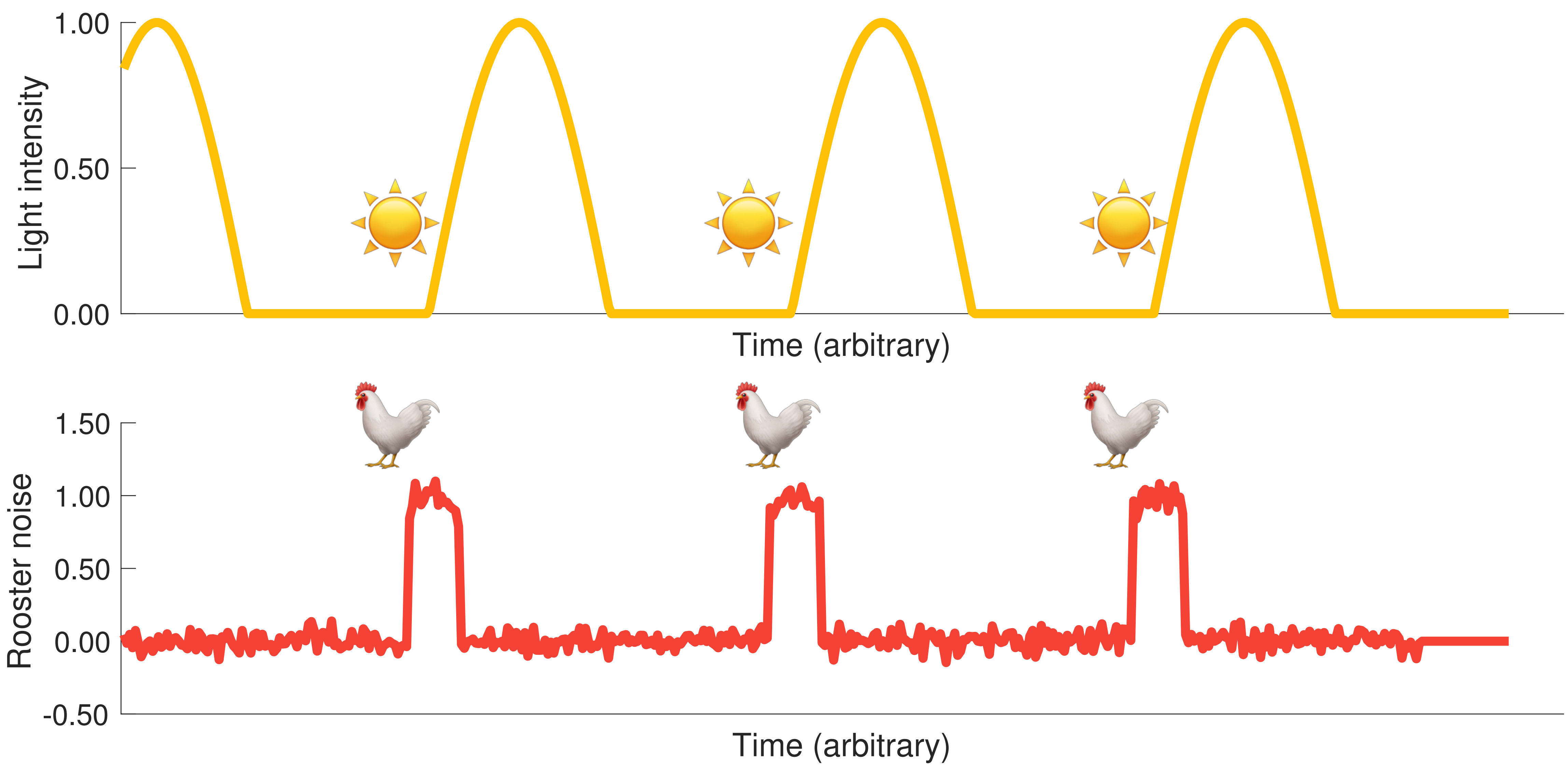

Does knowing about the rooster improve prediction of next sunrise, using past sunrises?

H(☀️ | ☀️$_{\text{past}}$)

vs.

H(☀️ | ☀️$_{\text{past}}$, 🐓$_{\text{past}}$)

Transfer entropy measures reduction in uncertainty given information about a 2nd variable

l = block length in X

k = block length in Y

τ = time lag in X

t = time lag in Y

TE from X to Y

$$T_{X\to Y} = H(y_i | y_{i-t}^{(l)}) - H(y_i | y_{i-t}^{(l)},\ x_{i-\tau}^{(k)})$$

Entropy of Y given past values of Y

Entropy of Y given past values of Y *and X*

Lee, J., Nemati, S. et al. Transfer Entropy Estimation and Directional Coupling Change Detection in Biomedical Time Series. Biomed. Eng. Online 11, 19 (2012).

Darbellay-Vajda (DV) partitioning

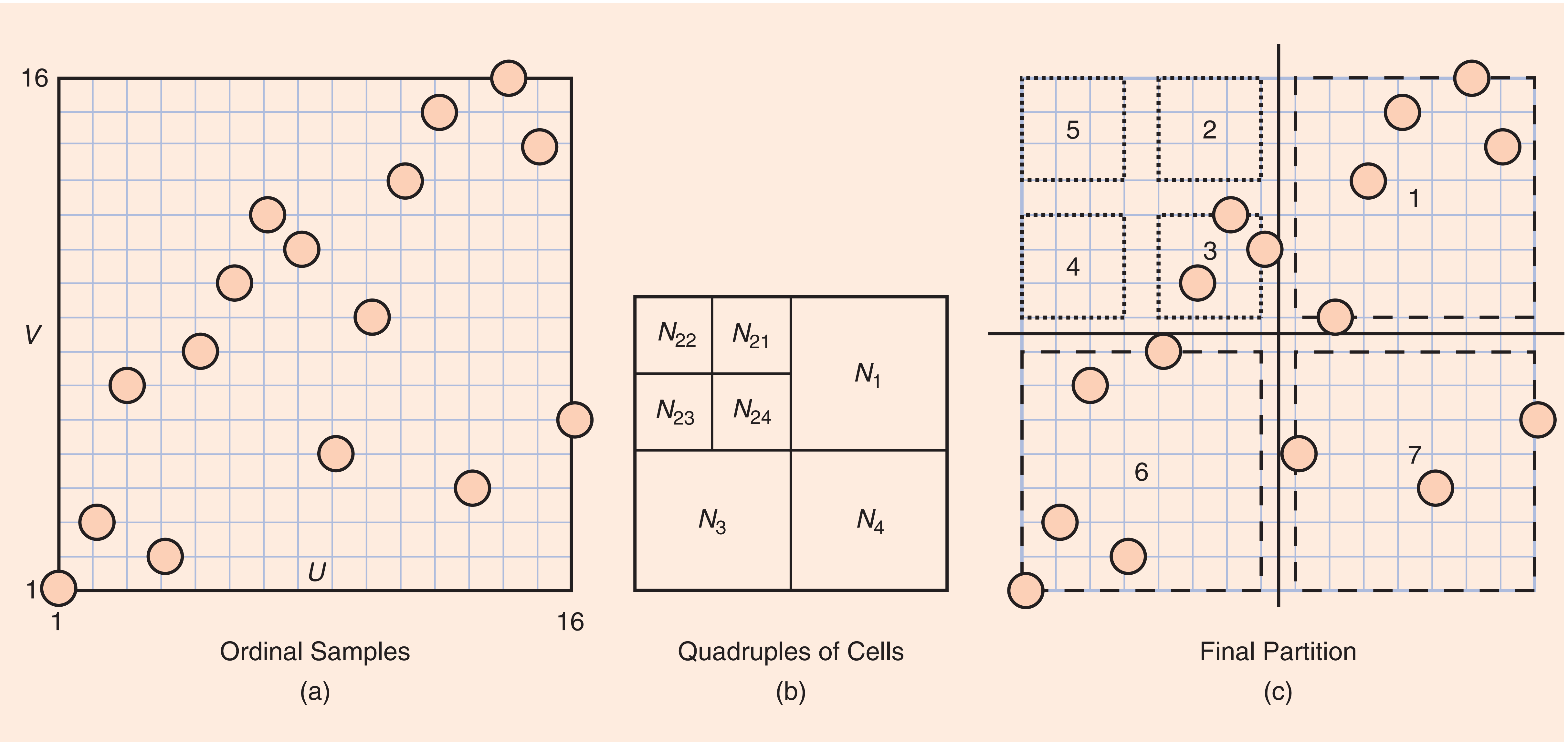

1. Hudson, J. E. Signal Processing Using Mutual Information. IEEE Signal Process. Mag. 23, 50–54 (2006).
2. Lee, J. et al. Transfer Entropy Estimation and Directional Coupling Change Detection in Biomedical Time Series. Biomed. Eng. Online 11, 19 (2012).

Partition represents a state in 6 dimensions

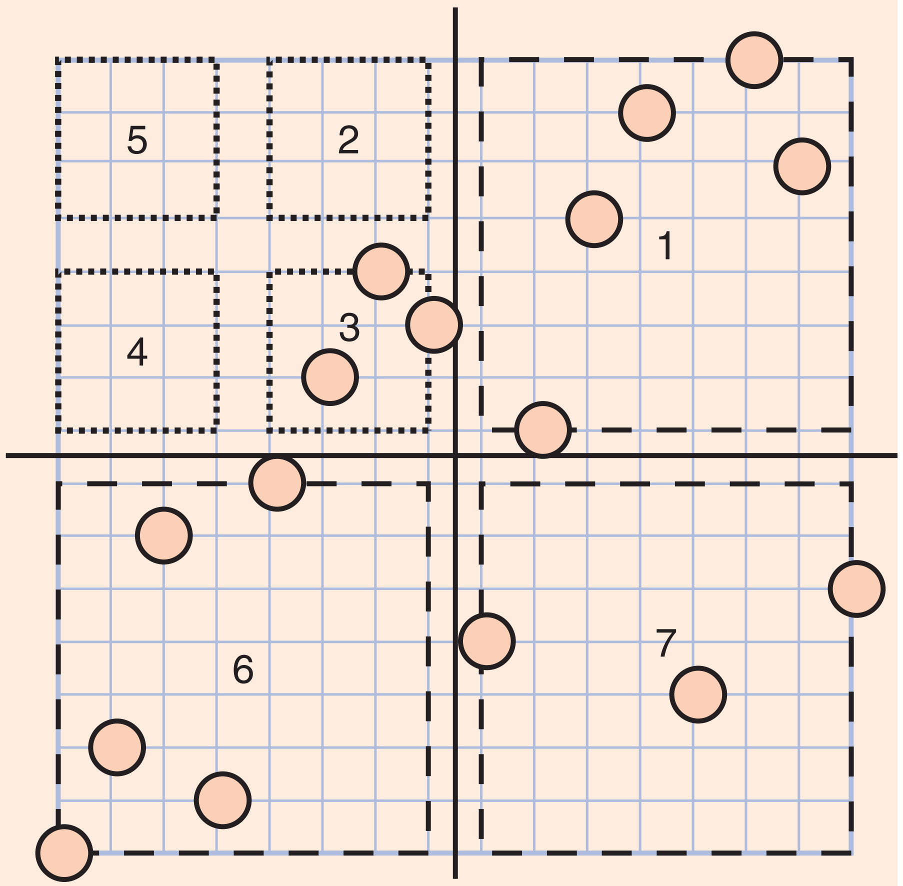

Final Partition

(c)

1. Six dimensions =
   two types of data, two lags

   HR_t, HR_{t-1}, HR_{t-2}
   act_t, act_{t-1}, act_{t-2}

2. Each partition is a node

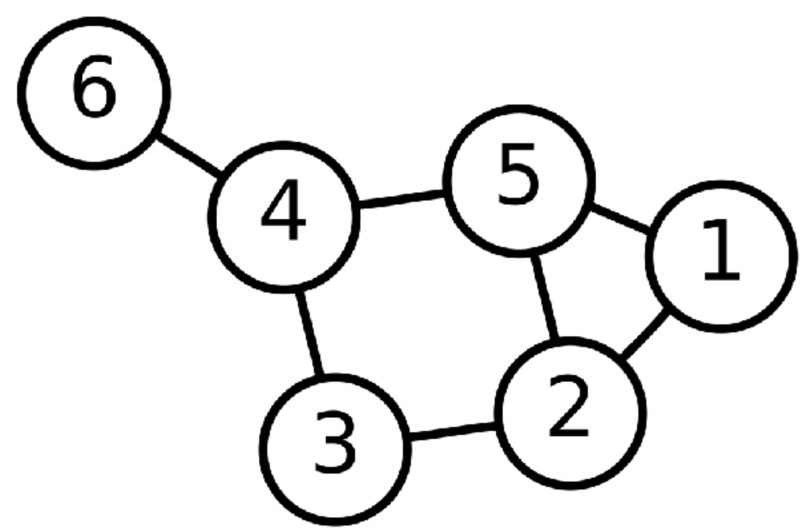

1. Shashikumar, S. P., Li, Q., Clifford, G. D. & Nemati, S. Multiscale network representation of physiological time series for early prediction of sepsis. Submitted (2017).

RR interval time series are non-stationary

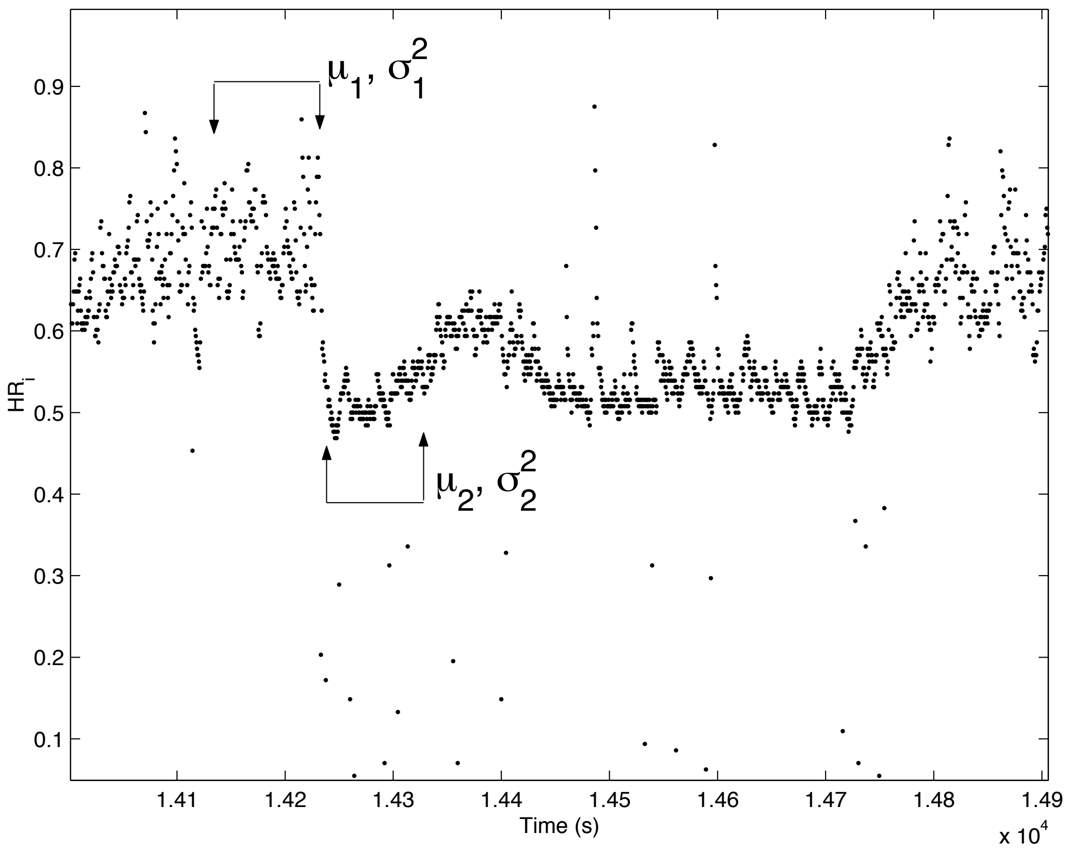

Figure 1. Fifteen minutes of RR interval data for a normal subject (16265) in the Physionet NSRDB. A state change is considered to have occured when adjacent 100 second segments have significantly different means (μ_1,μ_2) or variances (σ_1^2, σ_2^2).

- Sinusoidal trends
- Spikes
- $\Delta\sigma^2$
- Power-law correlations
- Autoregressive dependencies

1. Clifford, G. D., McSharry, P. E. & Tarassenko, L. Characterizing artefact in the normal human 24-hour RR time series to aid identification and artificial replication of circadian variations in human beat to beat heart rate using a simple threshold. in Computers in Cardiology 129–132 (2002).
2. Xiong, W., Faes, L. & Ivanov, P. C. Entropy measures, entropy estimators, and their performance in quantifying complex dynamics: Effects of artifacts, nonstationarity, and long-range correlations. Phys. Rev. E 95, 1–37 (2017).

Sample entropy of HR and locomotor activity differs in schizophrenia patients vs. controls

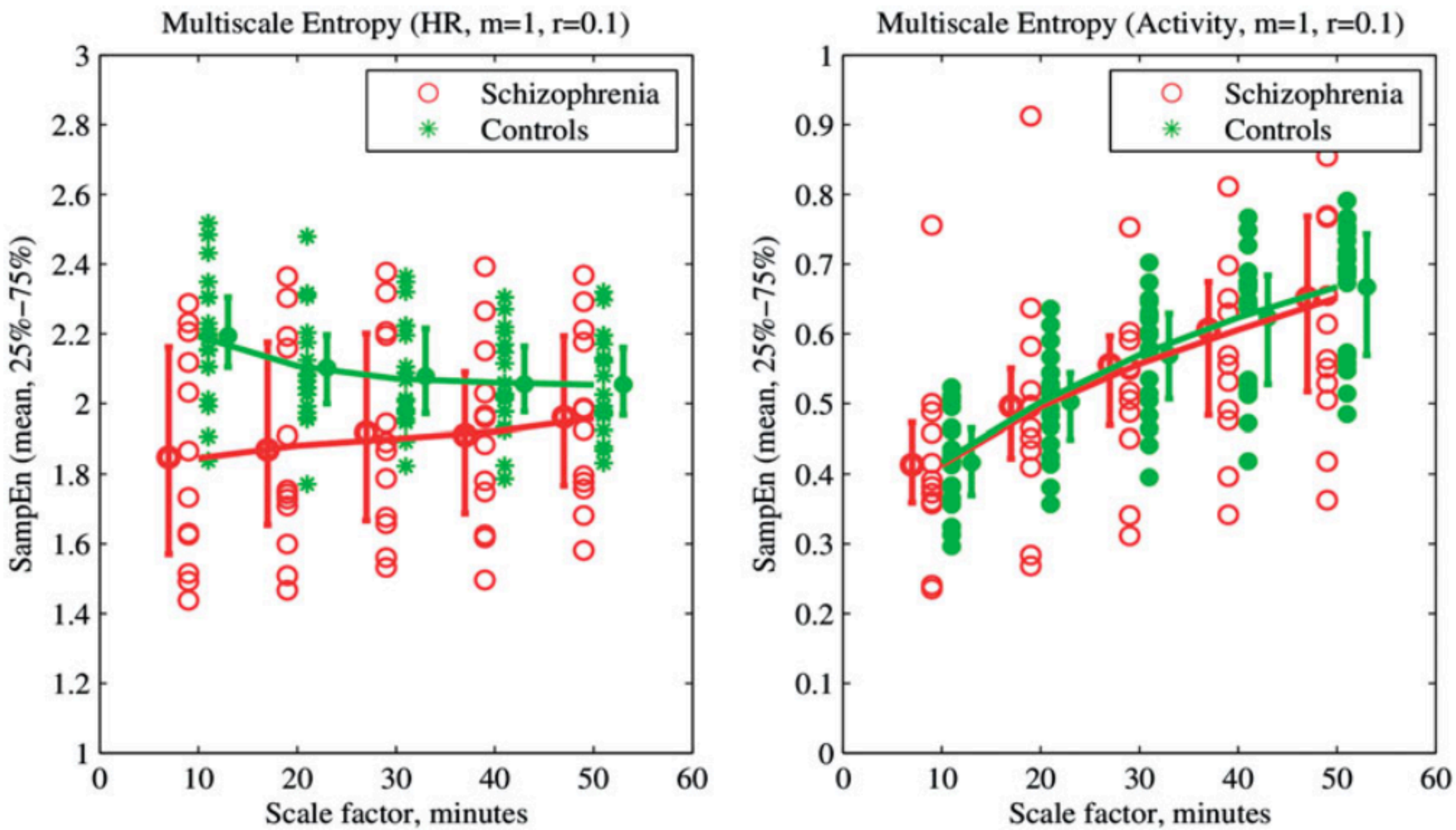

Osipov M, et al. Objective identification and analysis of physiological and behavioral signs of schizophrenia. J Ment Health (2015)

Feature selection via MRMR: Minimum Redundancy Maximum Relevance

minimizes mutual information between features

$$\boxed{\min\ R(S), R = \frac{1}{|S|^2} \sum_{x_i, x_j \in S} I(x_i; x_j)}$$

maximizes mutual information between features and classes

$$\boxed{\max\ D(S, c), D = \frac{1}{|S|} \sum_{x_i \in S} I(x_i; c)}$$

Support vector machines (SVMs): hyperplane that maximizes margin between classes

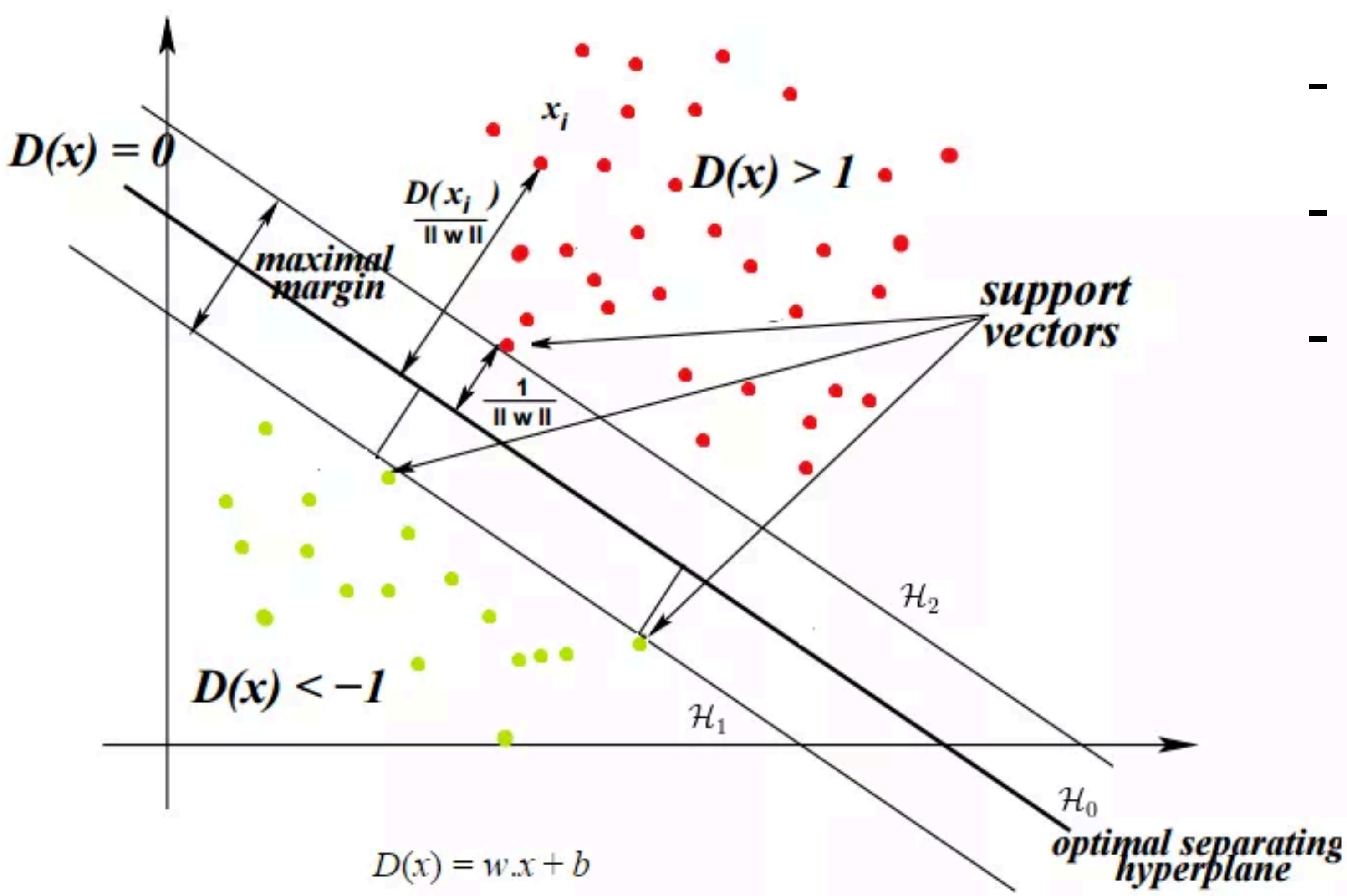

- Faster than elastic net
- Simple to implement in Matlab
- Few hyperparameters

Kernels implicitly map inputs x to high-dimensional feature space ϕ(x), enabling nonlinear classification

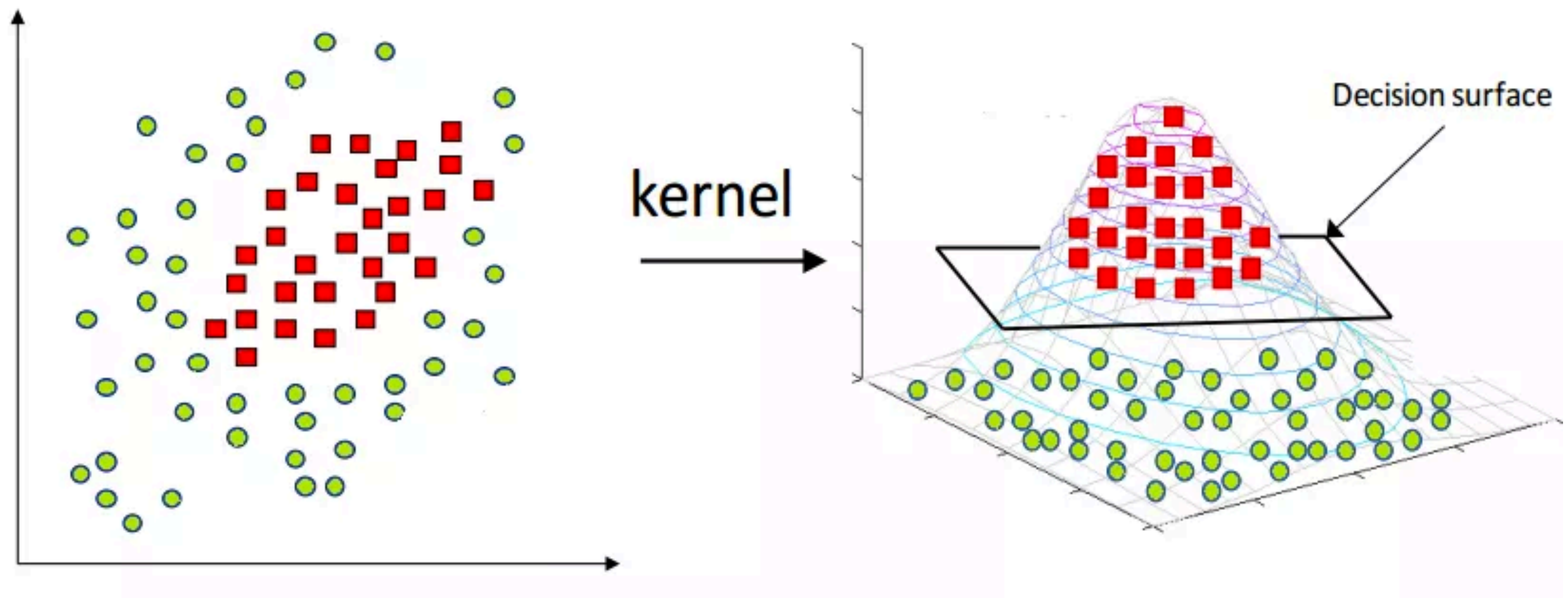

Gaussian kernel

$$K(x,z) = \exp\left(-\frac{||x-z||^2}{2\sigma^2}\right)$$

http://blog.hackerearth.com/simple-tutorial-svm-parameter-tuning-python-r
Andrew Ng's lecture notes from CS229: Machine Learning. Stanford University, CA.

Bayesian optimization searches for the maximum of an unknown but sampleable objective function

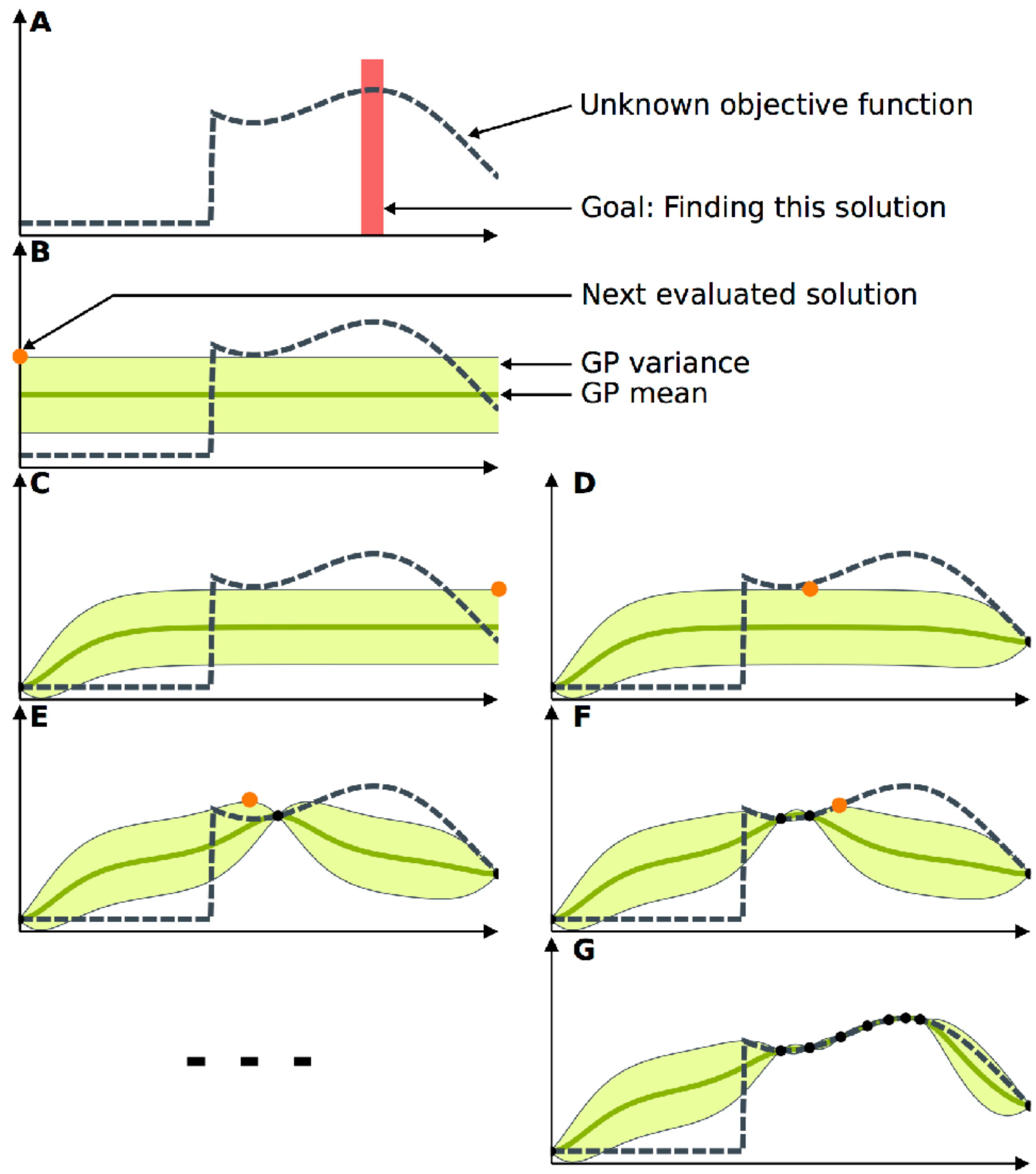

http://www.resibots.eu/limbo/guides/bo.html

Shahriari, B., Swersky, K., Wang, Z., Adams, R. P. & Freitas, N. de. Taking the human out of the loop: a review of Bayesian optimization. *Proc. IEEE* (2016).

Elastic net regularization

$$\min_{\beta_0,\beta}\left(\frac{1}{2N}\sum_{i=1}^{N}\left(y_i-\beta_0-x_i^T\beta\right)^2+\lambda P_\alpha(\beta)\right),$$

$$P_\alpha(\beta)=\frac{(1-\alpha)}{2}\|\beta\|_2^2+\alpha\|\beta\|_1$$

α = 1: Lasso

α = 0: Ridge regression

Optimal λ selected via internal crossvalidation

HR and activity data, classifier output, and data quantity for a control subject

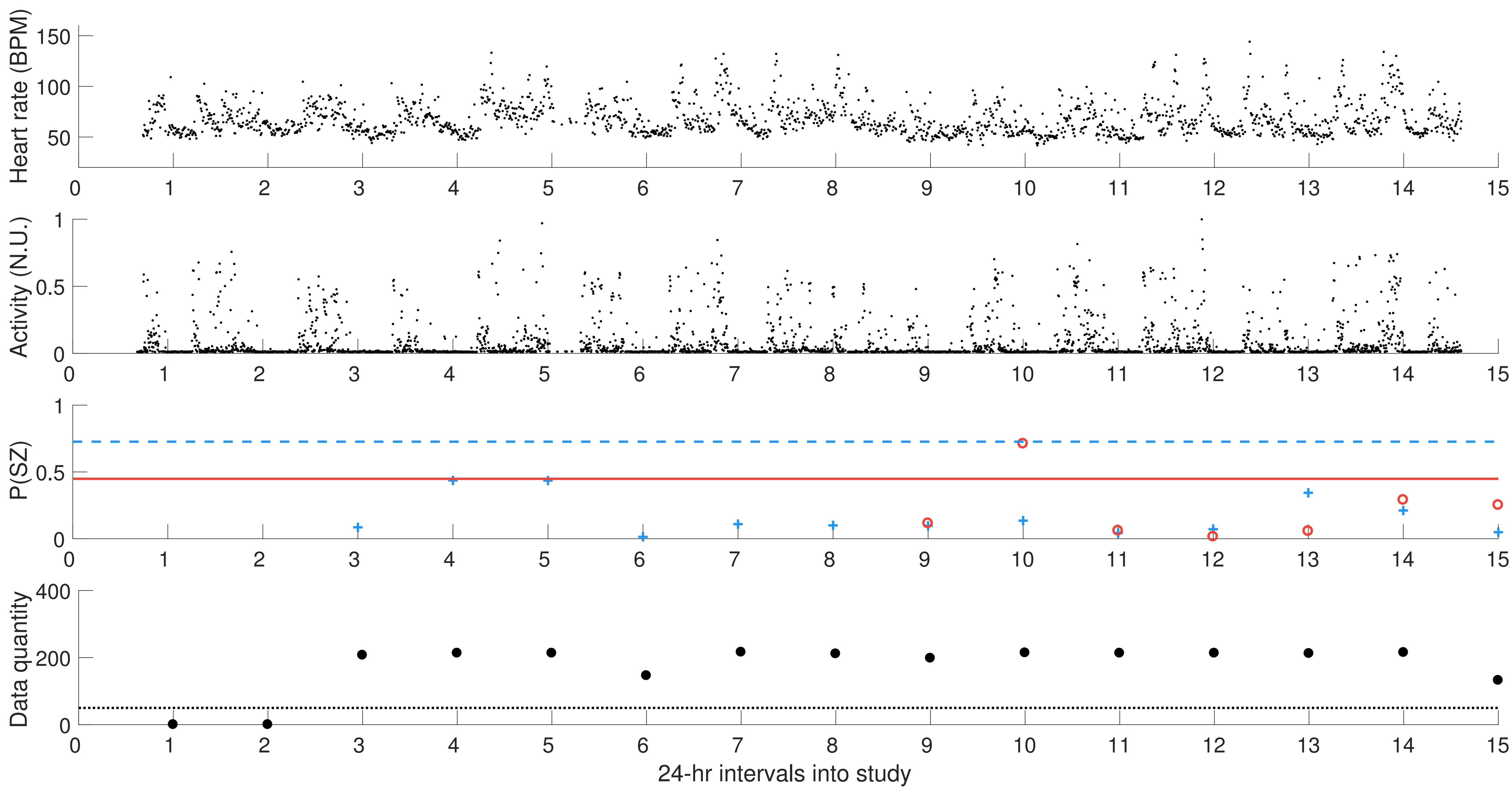

Reinertsen, E. et al. Continuous assessment of schizophrenia using heart rate and accelerometer data. Physiol. Meas. (2017).

HR and activity data, classifier output, and data quantity for a control subject

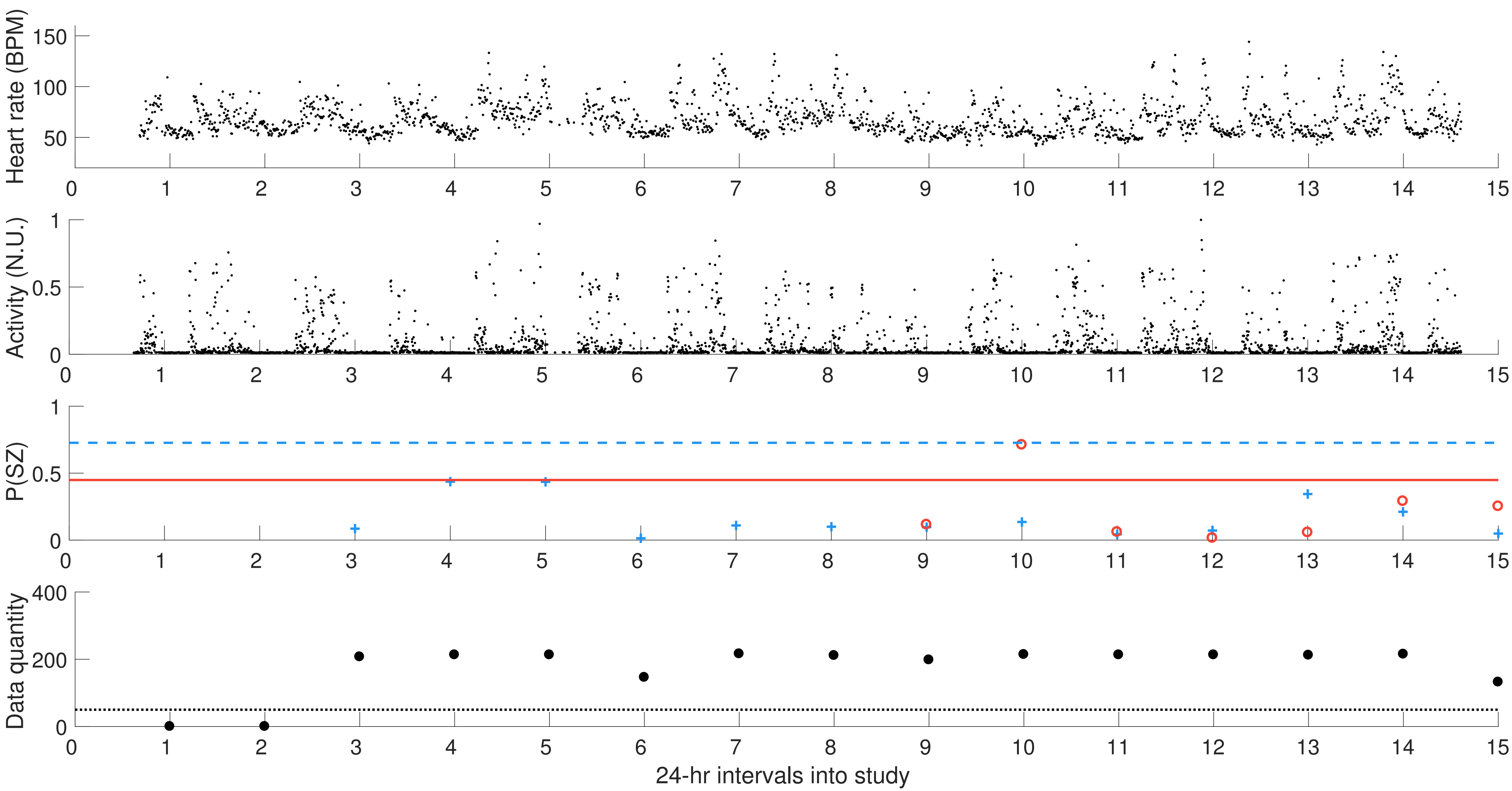

Reinertsen, E. et al. Continuous assessment of schizophrenia using heart rate and accelerometer data. Physiol. Meas. (2017).

Test AUC varies by number of most predictive features used and window length

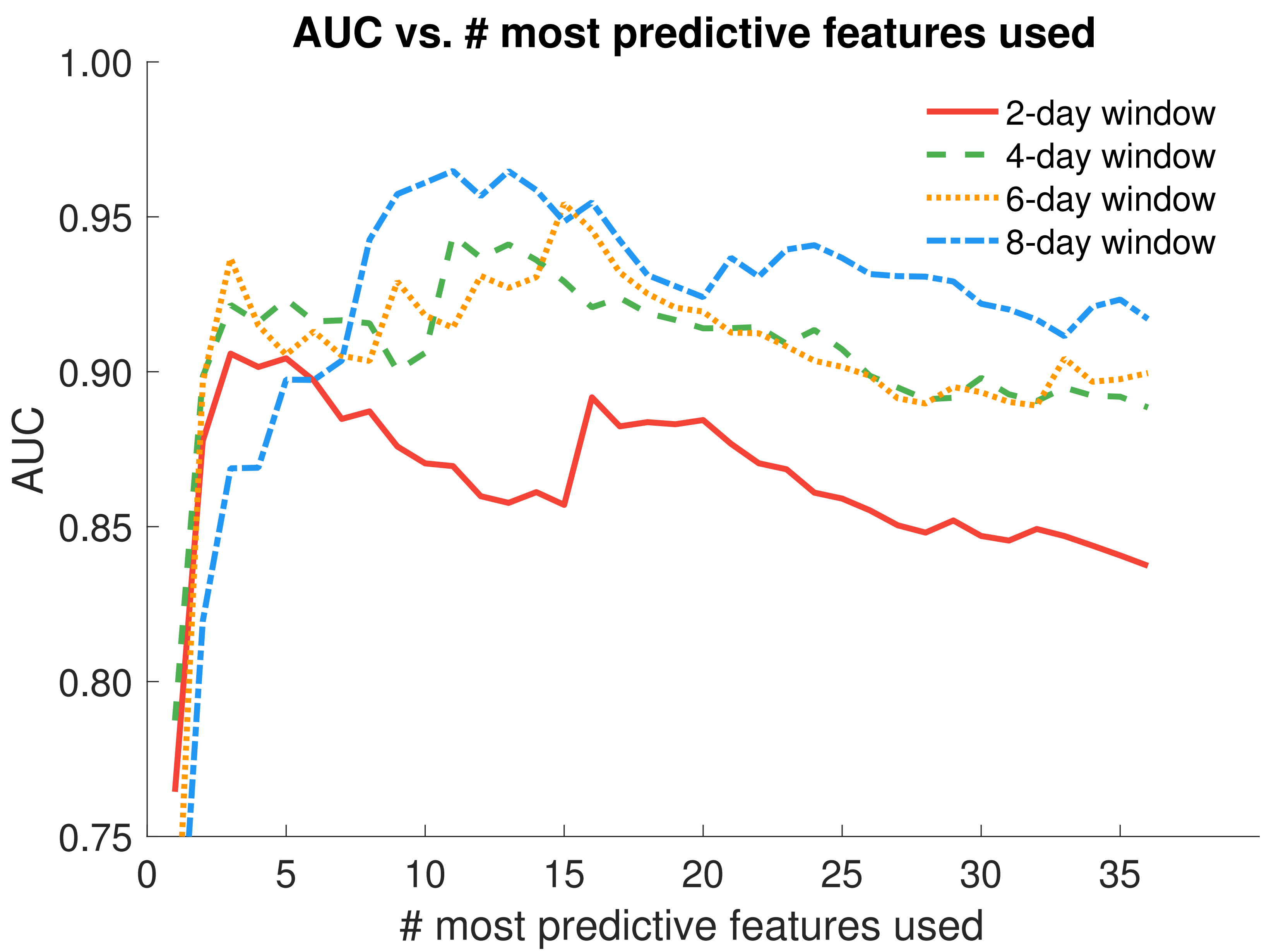

Reinertsen, E. et al. Continuous assessment of schizophrenia using heart rate and accelerometer data. Physiol. Meas. (2017).

Table 1: Classifier performance metrics vs. window length, using both HR and activity features. PPV indicates Positive Predictive Value and NPV indicates Negative Predictive Value.

	Window length (days)			
Metric	2	4	6	8
AUC	0.91	0.94	0.95	0.96
Accuracy	0.85	0.89	0.89	0.91
Sensitivity	0.89	0.85	0.87	0.87
Specificity	0.76	0.98	0.94	0.99
PPV	0.87	0.98	0.97	0.99
NPV	0.79	0.76	0.77	0.76

Table 2: Area under the ROC curve (AUC) vs. window length and feature type used to train support vector machine. AUCs calculated via leave-one-out-cross-validation (LOOCV).

	Window length (days)	
Feature type(s)	2	8
Heart rate (HR)	0.84	0.90
Activity	0.86	0.89
HR and activity	0.91	0.96

Reinertsen, E. et al. Continuous assessment of schizophrenia using heart rate and accelerometer data. Under review.

Temporal distribution of quiescent segments does not differ by PTSD status (P=0.23)

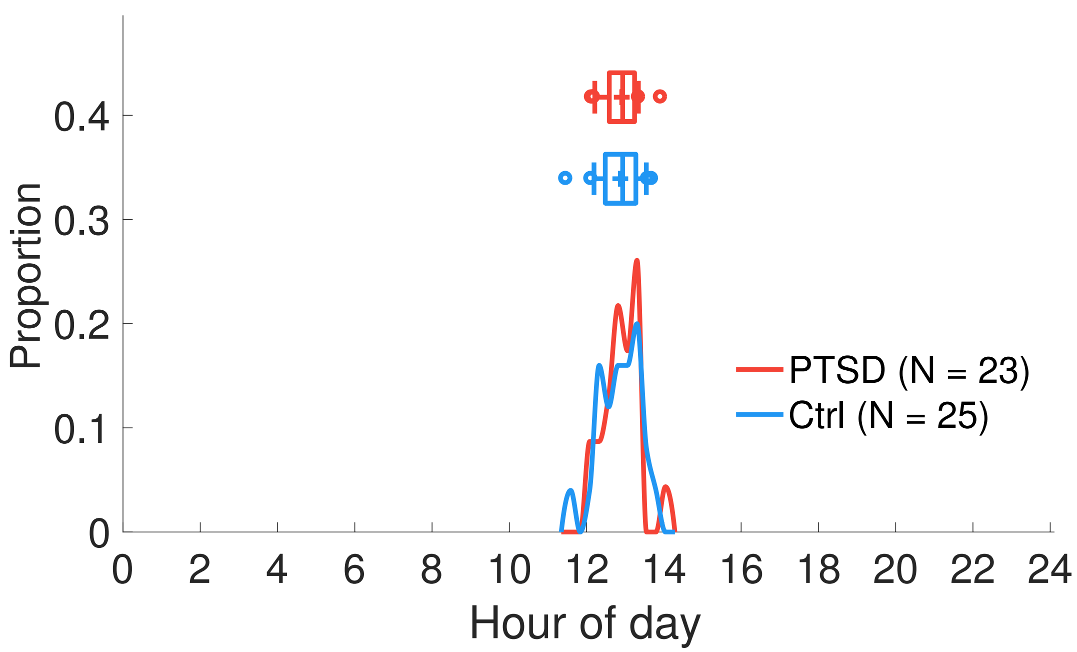

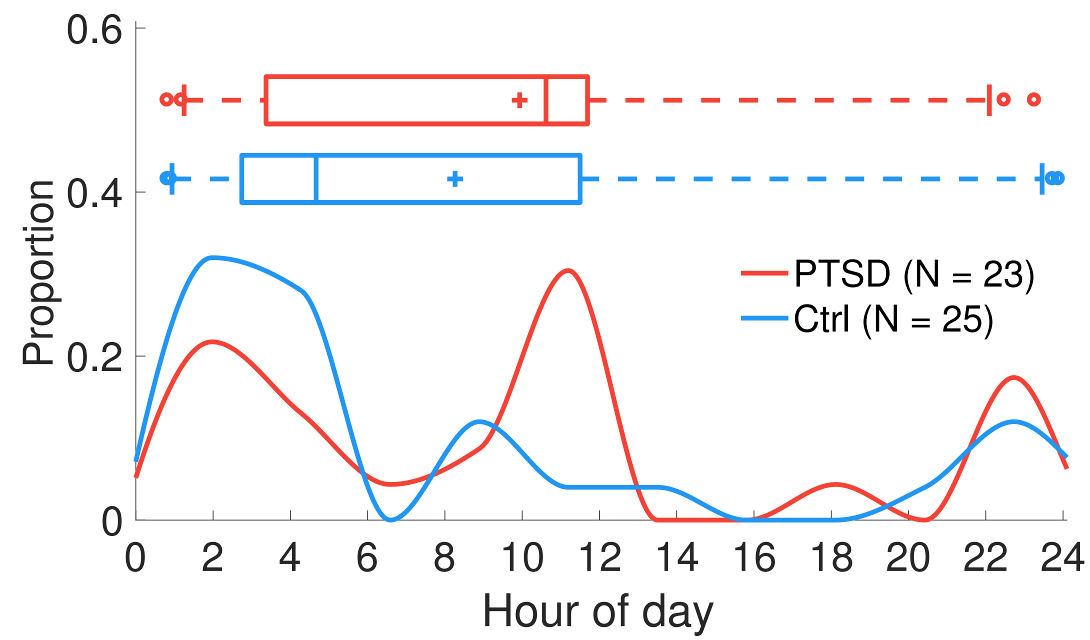

Reinertsen, E. et al. Heart rate-based window segmentation improves accuracy of classifying posttraumatic stress disorder using heart rate variability measures. Physiol. Meas. (2017).

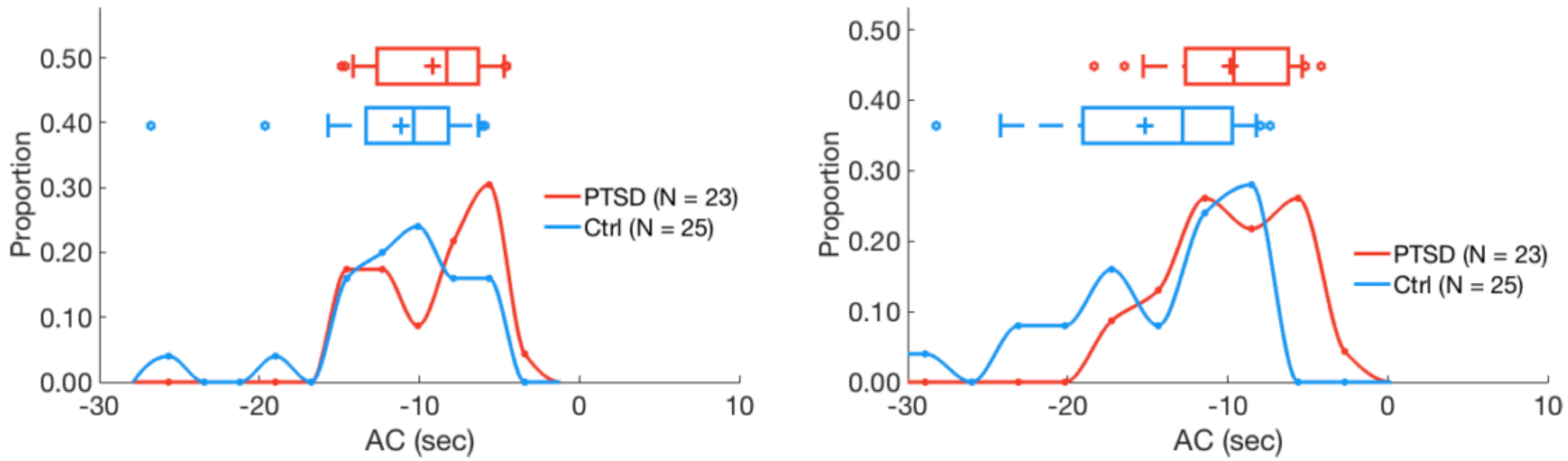

(a) 24 hours of data (b) Quiescent segments

Figure 3: Acceleration capacity (AC) does not differ by PTSD status for 24 hours of RR intervals (a; $P = 0.18$) but is higher in subjects with PTSD for quiescent segments (b; $P < 0.05$).

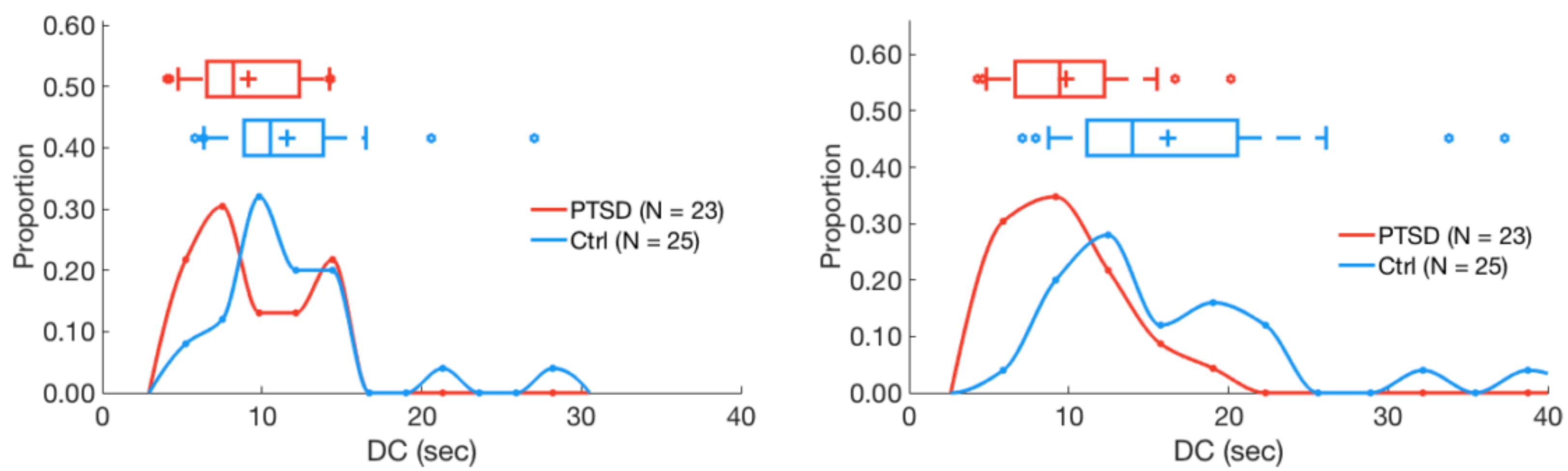

(a) 24 hours of data (b) Quiescent segments

Figure 4: Deceleration capacity (DC) does not differ by PTSD status for 24 hours of RR intervals (a; $P = 0.09$) but is lower in subjects with PTSD for quiescent segments (b; $P < 0.05$).

Reinertsen, E. et al. Heart rate-based window segmentation improves accuracy of classifying posttraumatic stress disorder using heart rate variability measures. Physiol. Meas. (2017).

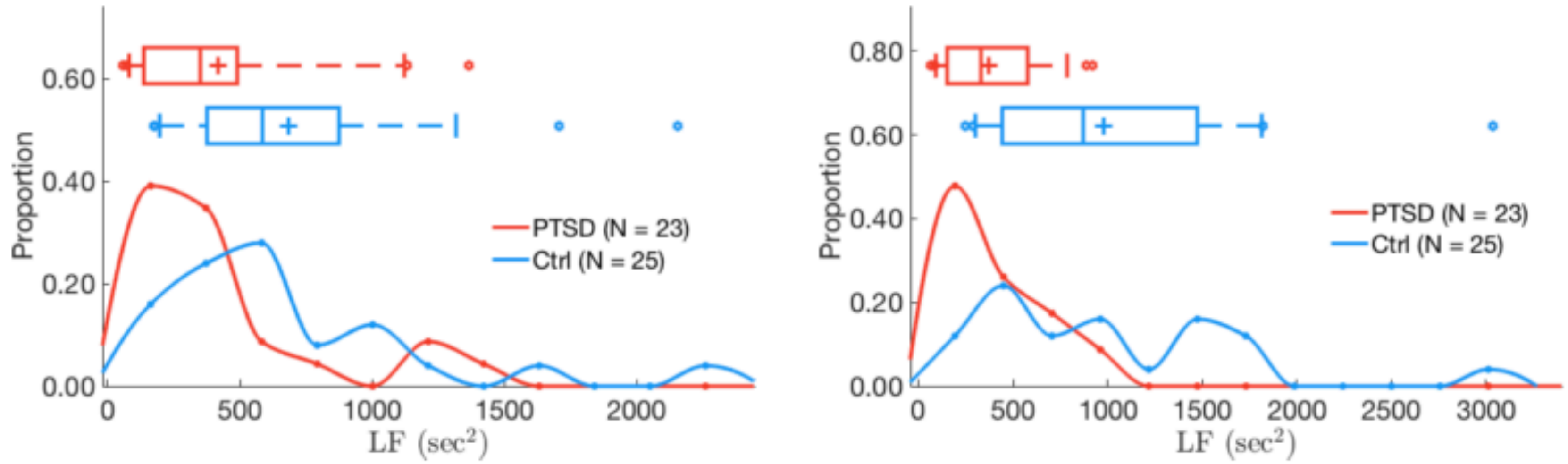

(a) 24 hours of data **(b)** Quiescent segments

Figure 5: Low frequency (LF) power differs by PTSD status for both 24 hours of RR intervals (a; $P < 0.05$) and quiescent segments (b; $P < 0.05$).

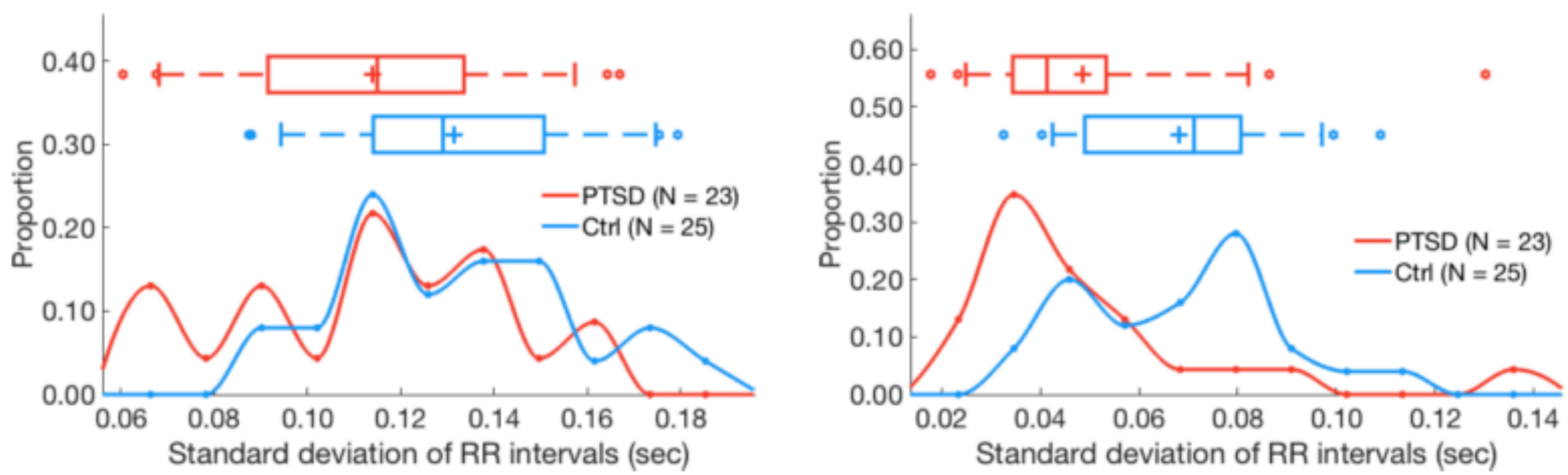

(a) 24 hours of data **(b)** Quiescent segments

Figure 6: σ_{rr} (standard deviation of RR intervals) does not differ by PTSD status for 24 hours of RR intervals (a; $P = 0.25$) but but is higher in control subjects for quiescent segments (b; $P < 0.05$).

Reinertsen, E. et al. Heart rate-based window segmentation improves accuracy of classifying posttraumatic stress disorder using heart rate variability measures. Physiol. Meas. (2017).

AUCs of L1L2 regularized logistic regression models using **a)** all or **b)** most predictive four HR and HRV features extracted from RR intervals

	Train AUC		Test AUC	
	No RR cleaning	RR cleaning	No RR cleaning	RR cleaning
24 hours	0.77 [0.75 0.82]	0.75 [0.70 0.78]	0.54 [0.46 0.64]	0.58 [0.46 0.64]
Random segments	0.76 [0.73 0.80]	0.78 [0.77 0.80]	0.50 [0.45 0.57]	0.56 [0.50 0.71]
Quiescent segments	0.89 [0.87 0.91]	0.87 [0.83 0.89]	0.73 [0.70 0.80]	0.75 [0.71 0.82]

	Train AUC		Test AUC	
	No RR cleaning	RR cleaning	No RR cleaning	RR cleaning
24 hours	0.74 [0.73 0.78]	0.73 [0.69 0.74]	0.66 [0.45 0.66]	0.67 [0.62 0.71]
Random segments	0.70 [0.66 0.76]	0.76 [0.72 0.77]	0.61 [0.50 0.64]	0.72 [0.62 0.77]
Quiescent segments	0.85 [0.84 0.88]	0.85 [0.83 0.88]	0.81 [0.70 0.84]	0.86 [0.75 0.88]

Reinertsen, E. et al. Heart rate-based window segmentation improves accuracy of classifying posttraumatic stress disorder using heart rate variability measures. Physiol. Meas. (2017).

Table 3: Features extracted from 24 hours of of RR intervals, shown as medians and IQR bounds in brackets. CTRL refers to the control group. Test AUC reports performance of univariate classifier trained solely on one feature.

	PTSD status		
Feature	PTSD	CTRL	Test AUC
AC (sec)	−8.28 [−1.27e1 −6.31]	−1.04e1 [−1.33e1 −8.18]	0.54 [0.52 0.68]
DC (sec)	8.19 [6.55 1.23e1]	1.05e1 [8.89 1.38e1]	0.58 [0.54 0.73]
LF power (sec^2)†,*	3.51e2 [1.37e2 4.91e2]	5.86e2 [3.76e2 8.76e2]	0.71 [0.64 0.80]
σ_{rr} (sec)*	1.15e−1 [9.15e−2 1.34e−1]	1.29e−1 [1.14e−1 1.51e−1]	0.65 [0.59 0.73]
$\mathrm{IQR}_{\mathrm{rr}}$ (sec)*	1.76e−1 [1.26e−1 2.11e−1]	2.08e−1 [1.52e−1 2.34e−1]	0.63 [0.59 0.67]
SDNN (sec)*	3.89e1 [2.97e1 5.42e1]	5.07e1 [4.09e1 6.32e1]	0.61 [0.55 0.75]

†: $P < 0.05$ comparing feature values from PTSD vs. control subjects via two-sided Kolmogorov-Smirnov test.

⋆: Feature among combination that maximizes training set AUC.

Table 4: Features extracted from quiescent segments of of RR intervals, shown as medians and IQR bounds in brackets. CTRL refers to the control group. Test AUC reports performance of univariate classifier trained solely on one feature.

	PTSD status		
Feature	PTSD	CTRL	Test AUC
AC (sec)†,*	−9.62 [−1.26e1 −6.22]	−1.28e1 [−1.91e1 −9.72]	0.77 [0.73 0.82]
DC (sec)†,*	9.43 [6.64 1.22e1]	1.40e1 [1.11e1 2.06e1]	0.82 [0.73 0.84]
LF power (sec^2)†,*	3.31e2 [1.52e2 5.78e2]	8.71e2 [4.44e2 1.47e3]	0.81 [0.75 0.88]
σ_{rr} (sec)†	4.14e−2 [3.44e−2 5.34e−2]	7.12e−2 [4.9e−2 8.06e−2]	0.82 [0.73 0.84]
$\mathrm{IQR}_{\mathrm{rr}}$ (sec)†	5.40e−2 [3.55e−2 5.60e−2]	7.20e−2 [5.50e−2 9.38e−2]	0.78 [0.71 0.81]
SDNN (sec)†,*	4.68e1 [3.16e1 5.97e1]	6.47e1 [4.32e1 7.70e1]	0.75 [0.57 0.86]

†: $P < 0.05$ comparing feature values from PTSD vs. control subjects via two-sided Kolmogorov-Smirnov test.

⋆: Feature among combination that maximizes training set AUC.

Reinertsen, E. et al. Heart rate-based window segmentation improves accuracy of classifying posttraumatic stress disorder using heart rate variability measures. Physiol. Meas. (2017).

PDFs of classifier output, P(schizophrenia), is highly separable using features from (a) two-day and (b) eight-day analysis windows

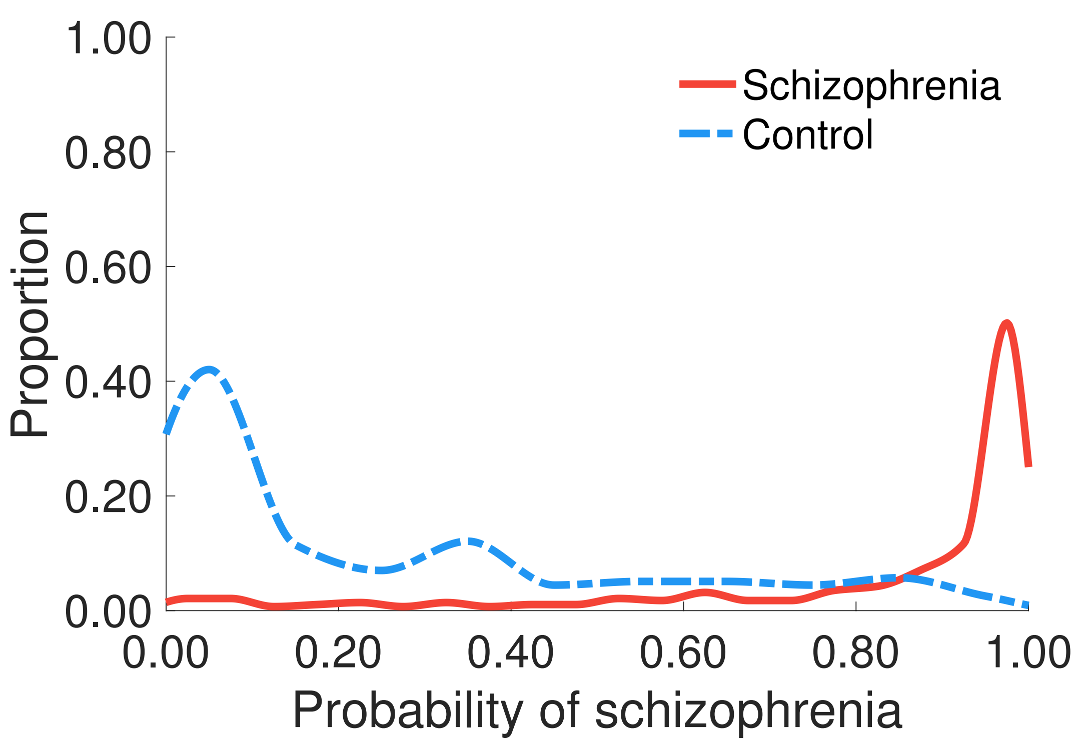

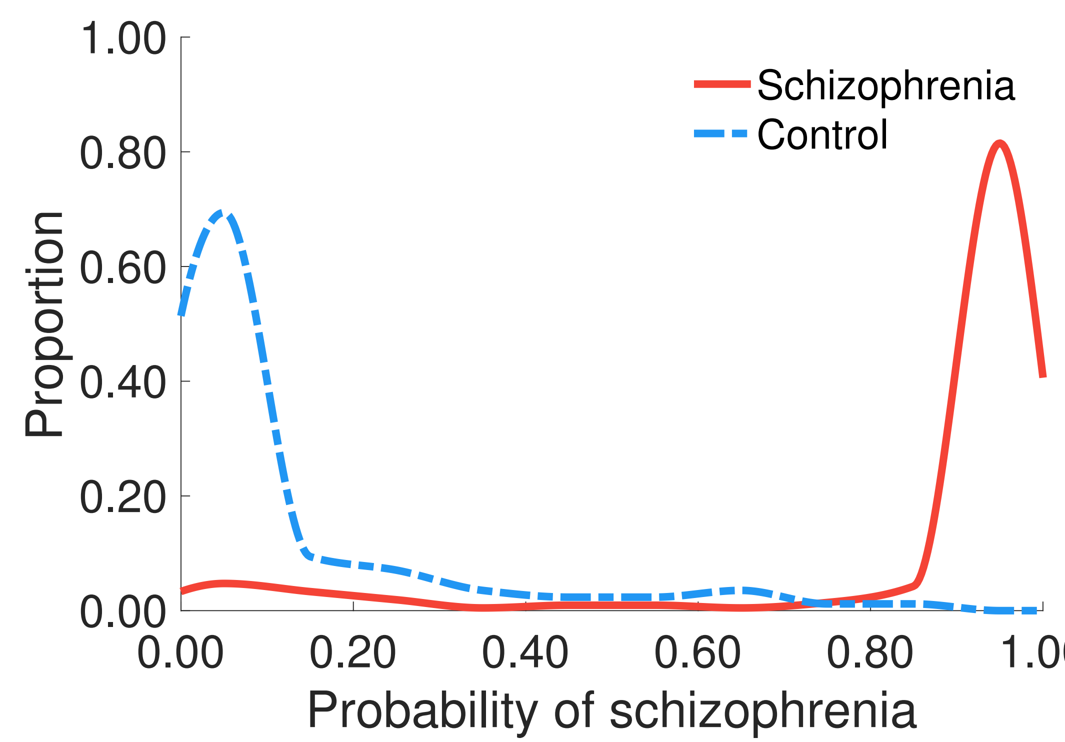

Reinertsen, E. et al. Continuous assessment of schizophrenia using heart rate and accelerometer data. Under review.

TE from activity to HR (and vice-versa) differs in schizophrenia for all time scales and lags

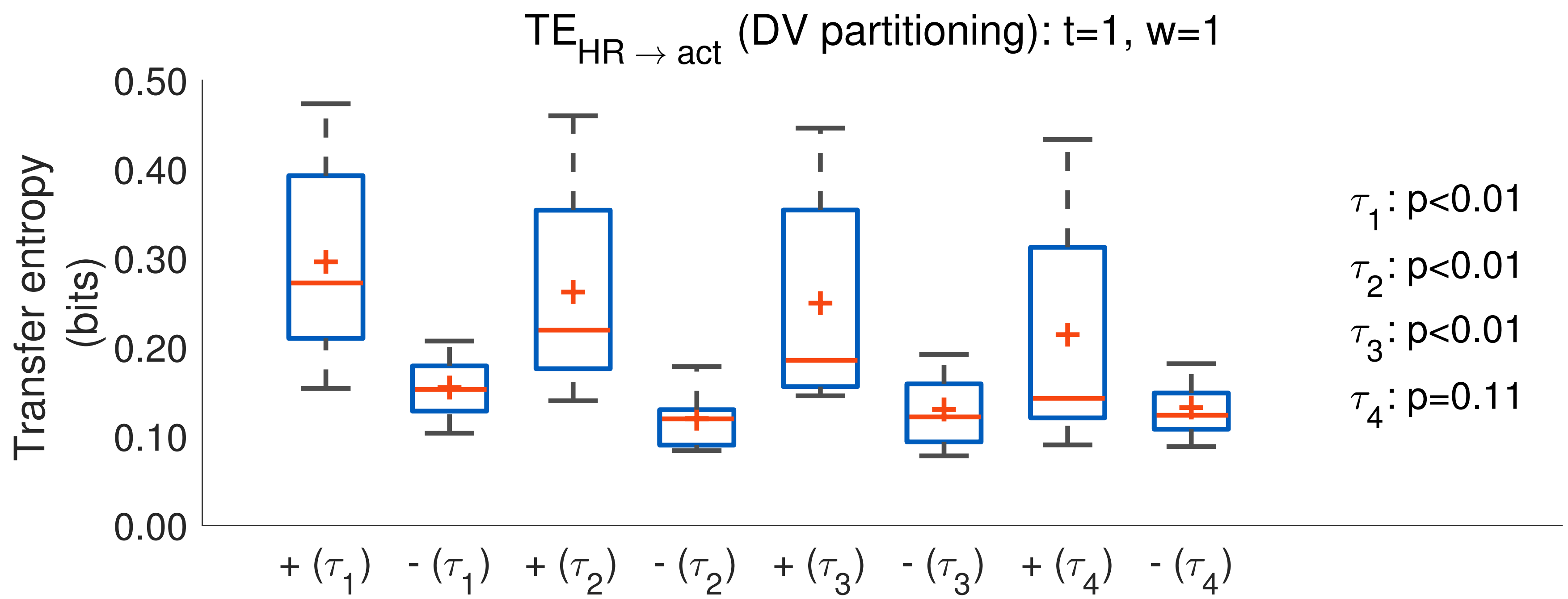

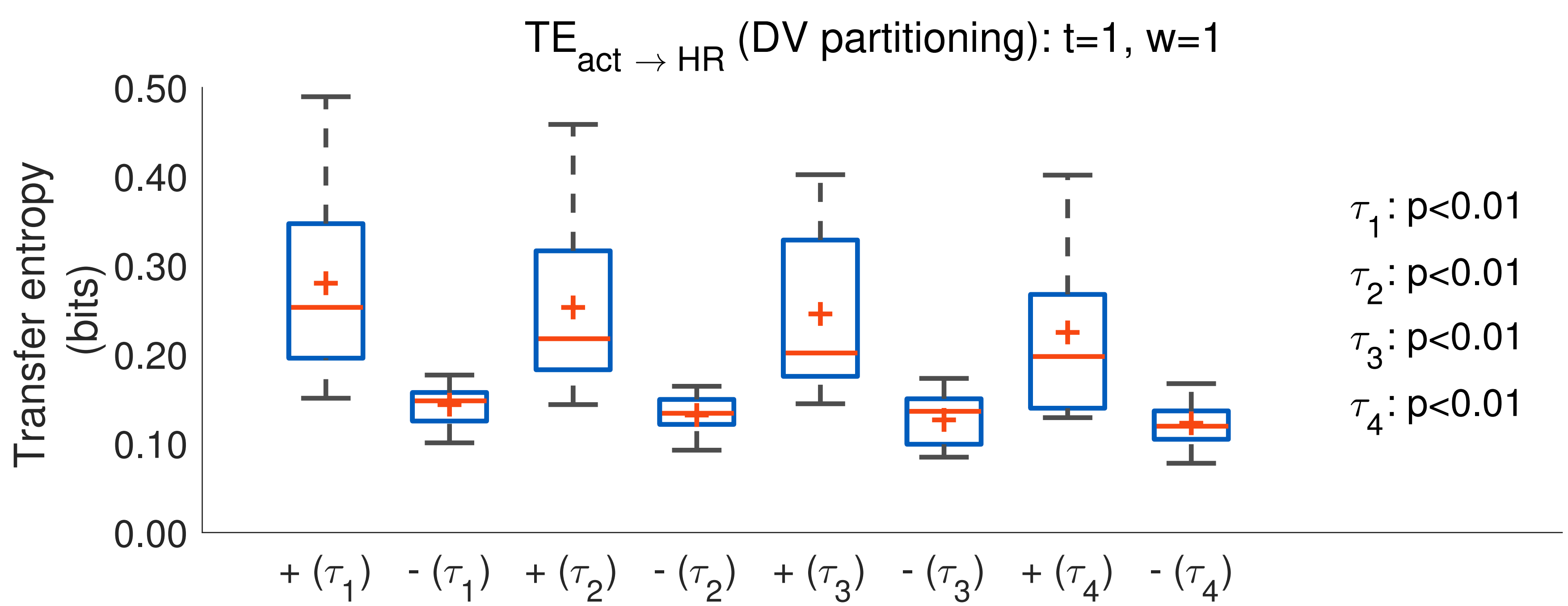

P-value calculated via two-sided Wilcoxon rank sum test.

TE from HR to activity differs by AF class for all time scales and lags

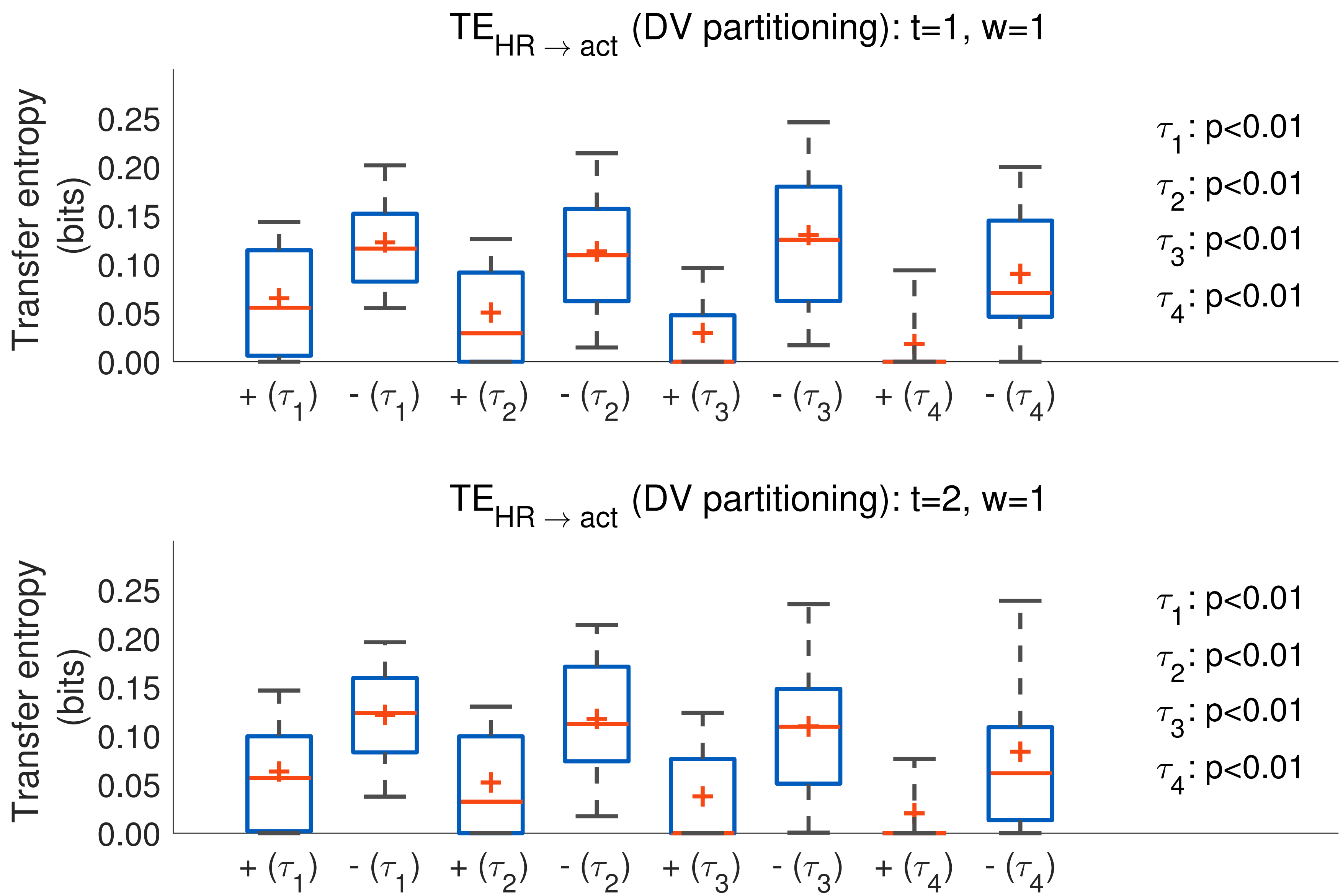

P-value calculated via two-sided Wilcoxon rank sum test.

TE from activity to HR differs by AF class for all time scales and lags

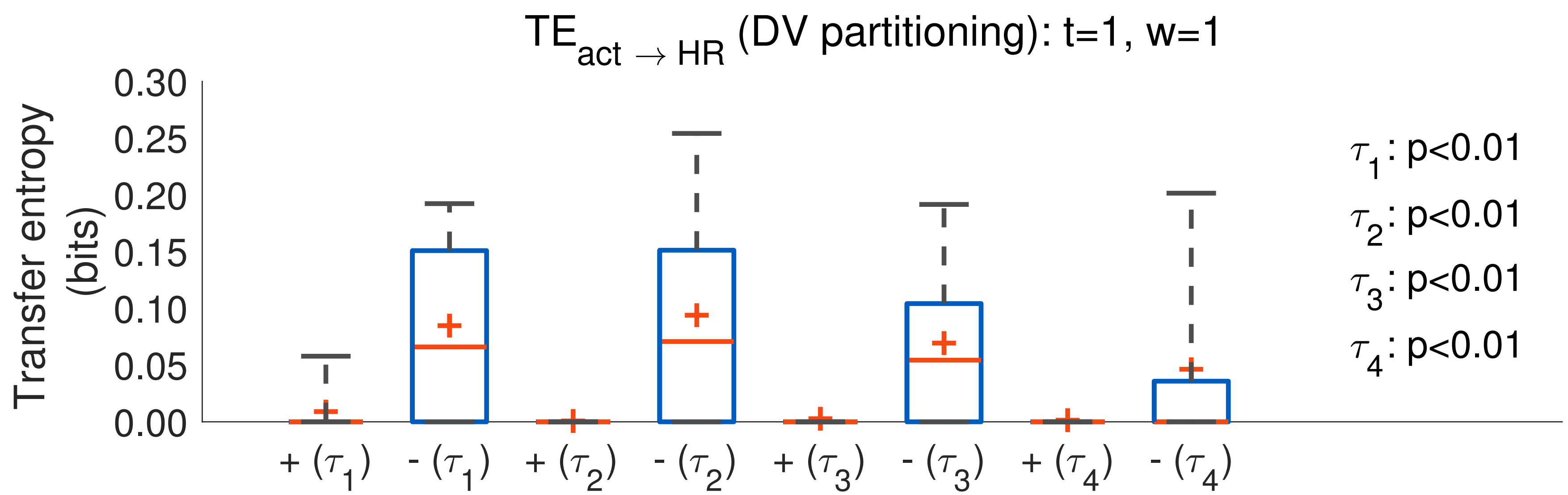

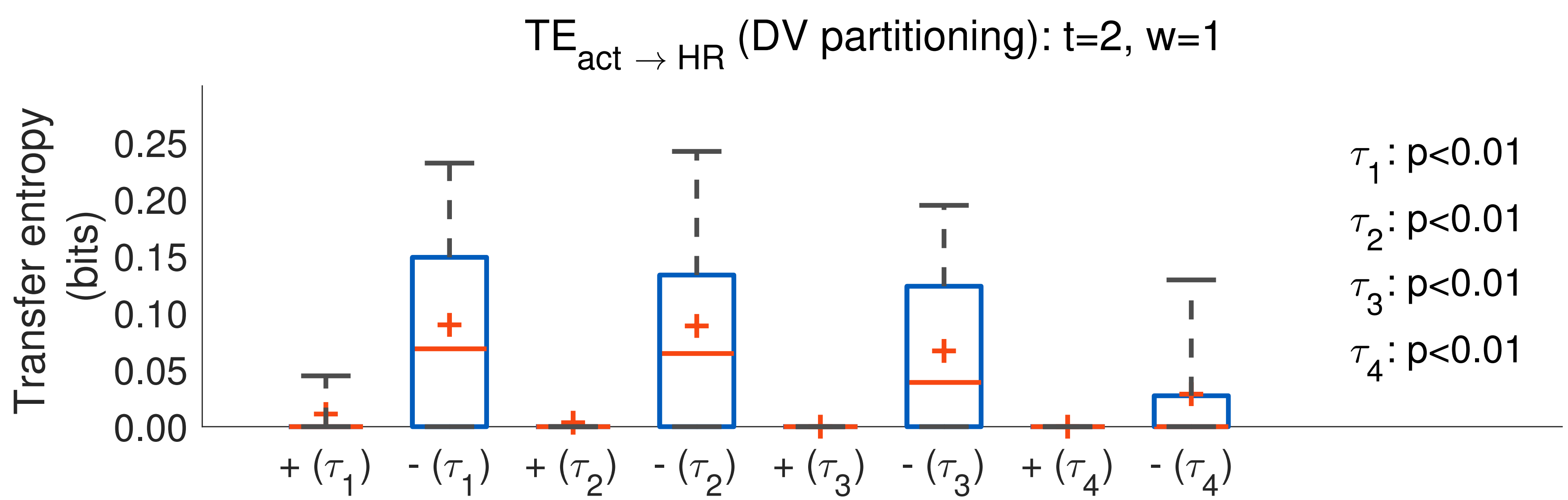

P-value calculated via two-sided Wilcoxon rank sum test.

TE from schizophrenia patients and controls differs from randomized surrogate data

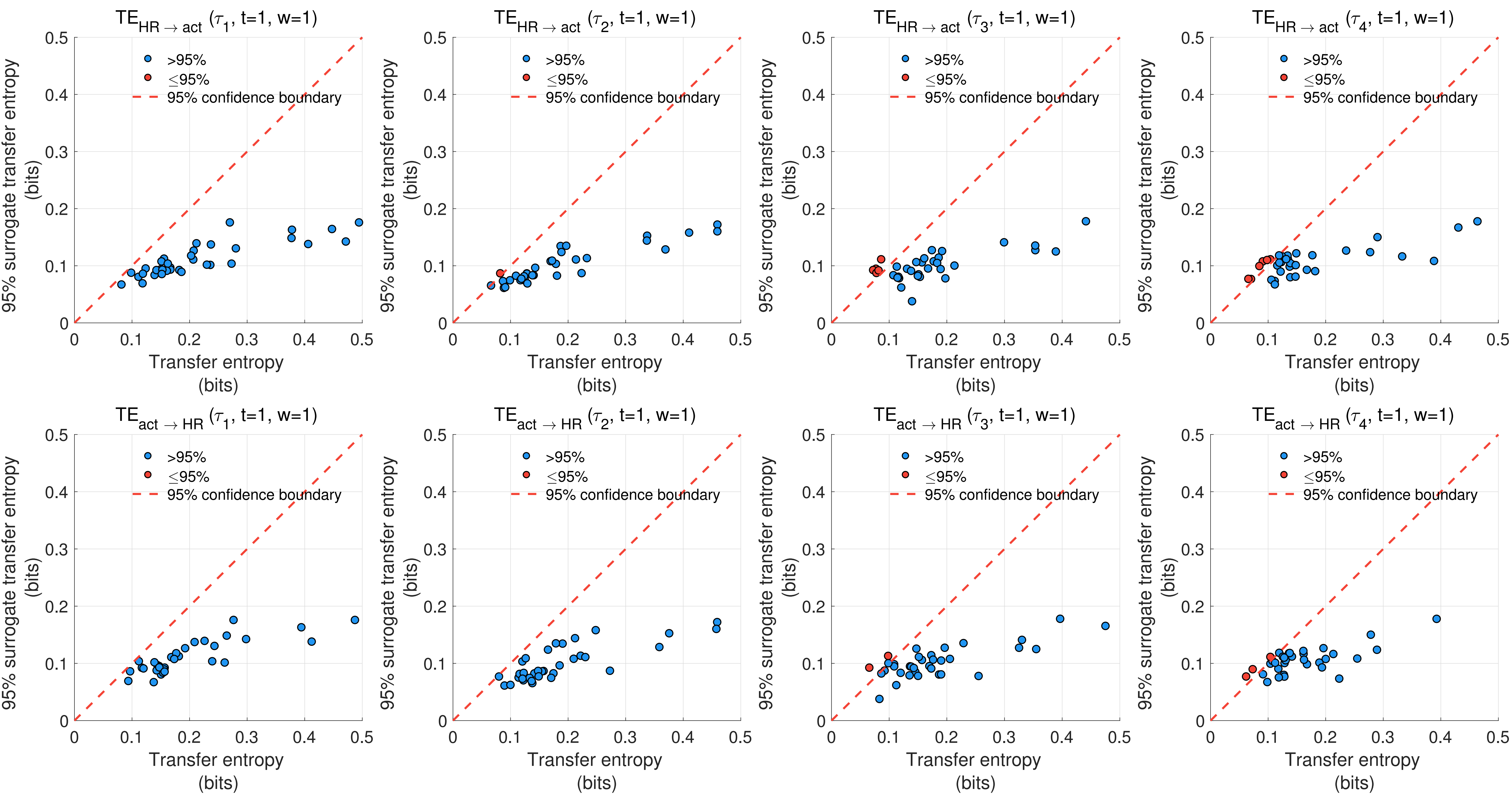

TE from AF patients and controls does not differ from randomized surrogate data

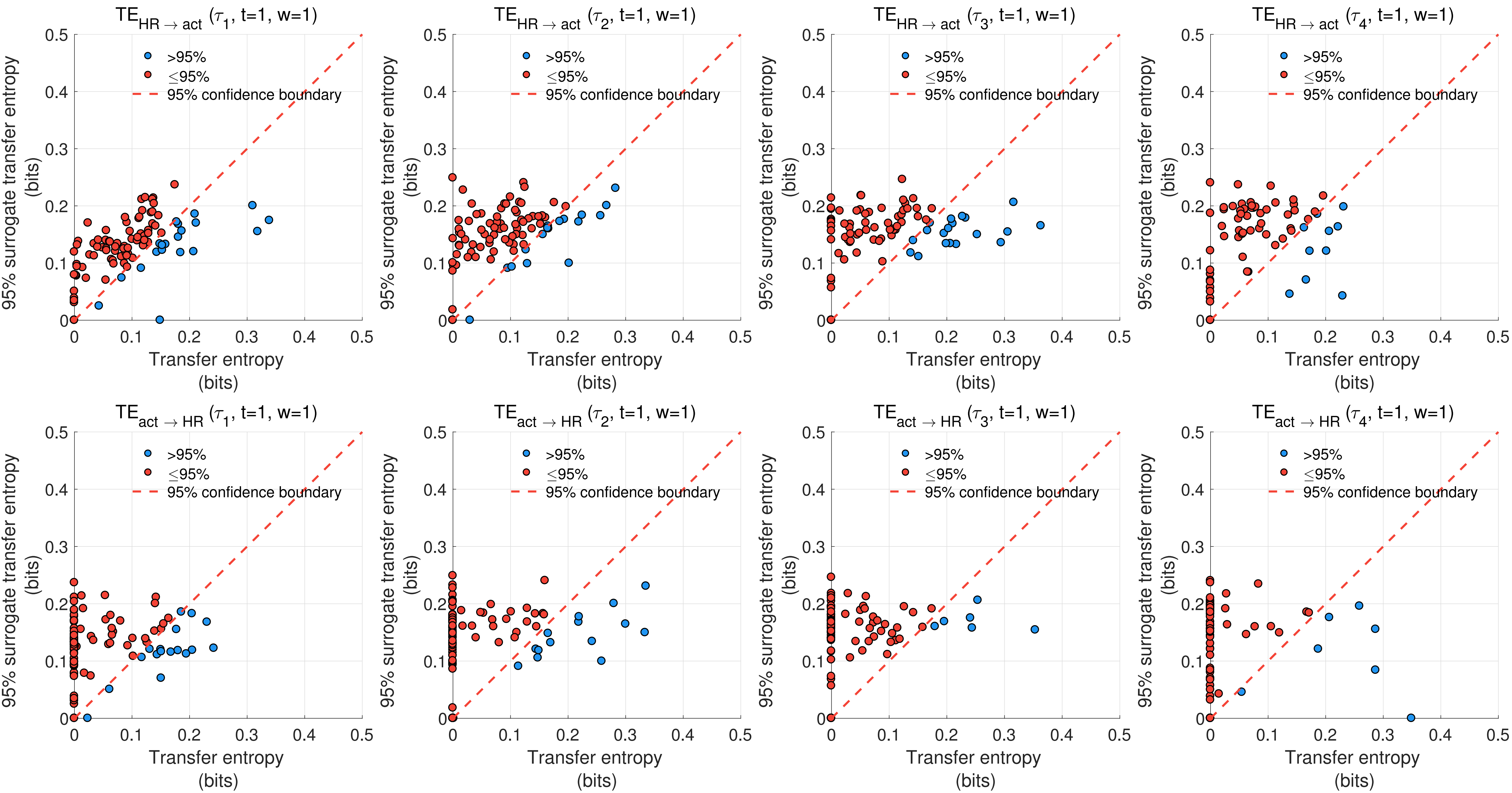

TVI seeks solutions that

- Apply tech to a relevant pharma business problem.
- Have founders with domain expertise in tech and pharma.
- Pragmatically focus on implementation (vs. tech development).

Three investment categories

Digital Biology

- Genetics: geno/ pheno integration to identify and prosecute targets
- Chemistry: AI to accelerate lead generation
- Imaging: cellular and phenotype extraction

Re-imagined clinical evidence generation

- Siteless trials using smart phones
- Leveraging RWE from EHR, claims, combo
- Digital phenotypes

Patient Engagement – Beyond The Pill

- Tech-enabled services to guide patients thru rx
- Adjunctive digital therapeutics
- Patient-empowerment tools & platforms

Science 37

Smartphone-enabled clinical trials

In March 2018, Novartis announced major collaboration with Science37, anticipating the launch of 10 studies this year in dermatology, oncology, and neuroscience.

RECURSION
pharmaceuticals

FILTER BY: **THERAPEUTIC AREA** **STAGE**

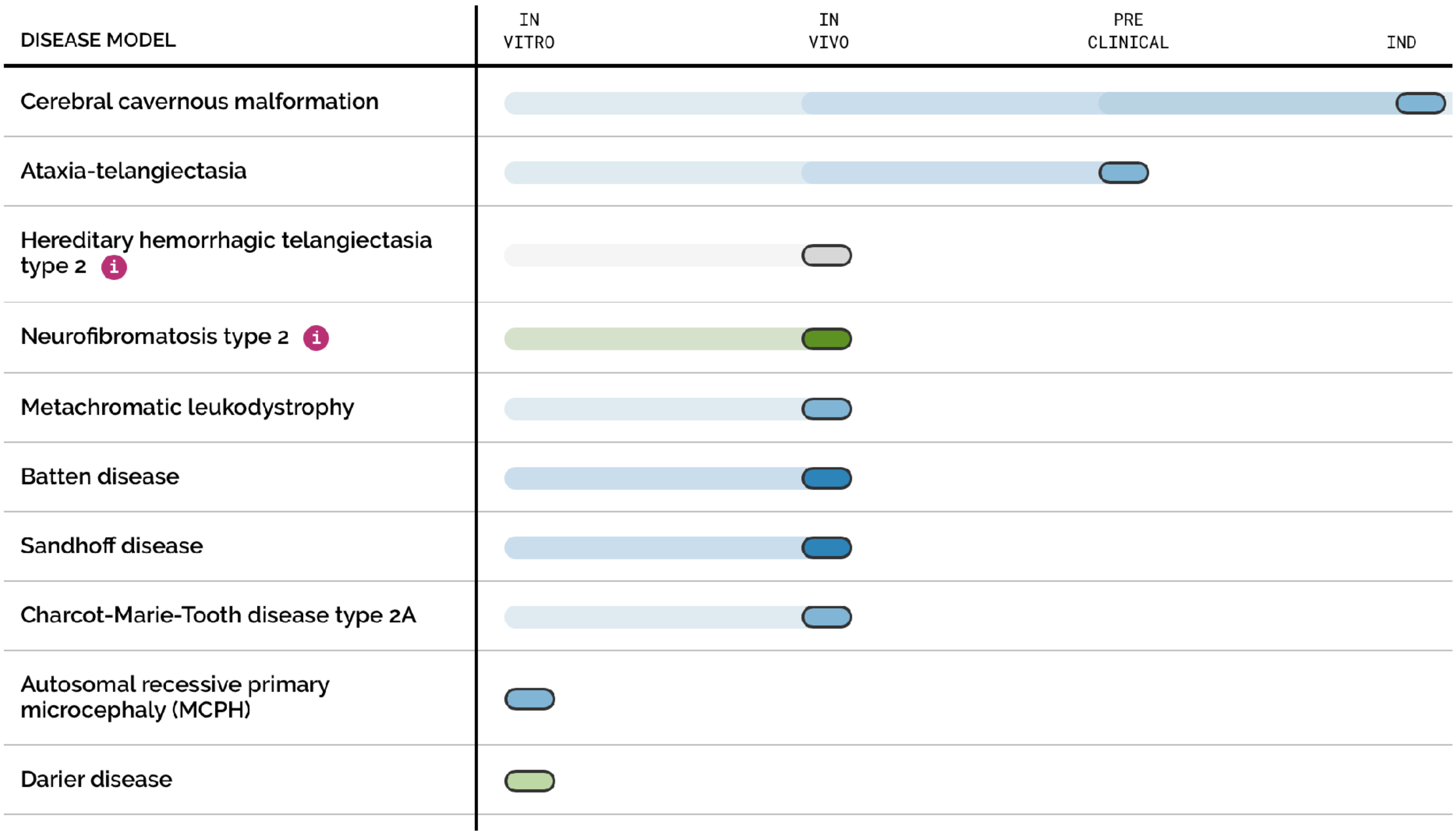

flatiron

Organize cancer data to improve care and drive research

Secret sauce: Tech-enabled data abstraction of oncology-focused EHR data performed by carefully trained and supervised people.

Acquired by Roche in 2018 for $2.2B

npj | Digital Medicine

Review Article | OPEN | Published: 15 January 2018

Impact of remote patient monitoring on clinical outcomes: an updated meta-analysis of randomized controlled trials

Benjamin Noah, Michelle S. Keller, Sasan Mosadeghi, Libby Stein, Sunny Johl, Sean Delshad, Vartan C. Tashjian, Daniel Lew, James T. Kwan, Alma Jusufagic & Brennan M. R. Spiegel

npj Digital Medicine **1**, Article number: 20172 (2018) | Download Citation

estimates. Difference-in-difference point estimation revealed no statistically significant impact of remote patient monitoring on any of six reported clinical outcomes, including body mass index (−0.73; 95% CI: −1.84, 0.38), weight (−1.29; −3.06, 0.48), waist circumference (−2.41; −5.16, 0.34), body fat percentage (0.11; −1.56, 1.34), systolic blood pressure (−2.62; −5.31, 0.06), and diastolic blood pressure (−0.99; −2.73, 0.74). Studies were highly heterogeneous in their design, device type,